**Forschungszentrum Karlsruhe**
Technik und Umwelt

**Wissenschaftliche Berichte**
FZKA 5626

# Characterization and Assessment of Ferritic/Martensitic Steels

**K. Ehrlich, D. R. Harries, A. Möslang**

**Institut für Materialforschung**
**Projekt Kernfusion**
**Association Forschungszentrum Karlsruhe/EURATOM**

**Februar 1997**

Forschungszentrum Karlsruhe

Technik und Umwelt

Wissenschaftliche Berichte
FZKA 5626

# Characterization and Assessment of Ferritic/Martensitic Steels

K. Ehrlich, D.R. Harries, A. Möslang (Editors)

Institut für Materialforschung
Projekt Kernfusion
Association Forschungszentrum Karlsruhe / EURATOM

Forschungszentrum Karlsruhe GmbH, Karlsruhe
1997

Als Manuskript gedruckt


Forschungszentrum Karlsruhe GmbH
Postfach 3640, 76021 Karlsruhe

ISSN 0947-8620

## Abstract

Ferritic/martensitic steels are candidate structural materials for a DEMO fusion reactor and are investigated intensively within the frame of the European Long Term Fusion Technology Programme. This report summarizes general features of ferritic/martensitic steels and gives a broad overview on the available data of the 9-12% CrMoVNb steels MANET I and II. The data include informations on the physical metallurgy, the transformation and hardening/tempering behaviour as well as results on tensile, creep, creep-rupture, isothermal and thermal fatigue, charpy impact and fracture toughness properties. Other topics are corrosion tests of helium or high pressure water coolants, compatibility with breeding and neutron multiplier materials, advanced welding techniques, and a short review on fabrication and technology of these steels. In the relevant temperature region from ambient temperatures to 450°C a widespread field of results on pre-, postirradiation and in-situ mechanical properties is available up to a few dpa and up to 500 appm helium.

Special emphasis has been put on the recent world-wide optimization of these steels. New 7-10% CrWVTa steels have been developed with significantly improved impact and fracture toughness properties. Initial results from unirradiated and neutron irradiated charpy specimens from various heats are favourable and showed a general improvement of the fracture toughness properties. These ferritic/martensitic steels also satisfy the criteria of reduced long-term activation. The potential for fusion applications is discussed together with some guidelines for required R&D.

## Zusammenfassung

### Kenntnisstand zur Entwicklung ferritisch/martensitischer Stähle für die Fusion

Ferritisch/martensitische Stähle sind aufgrund einer Reihe attraktiver Eigenschaften potentielle Kandidaten für die Erste Wand und Strukturkomponenten von Brutblankets in zukünftigen Fusionsanlagen. Sie werden im Rahmen des Europäischen Fusionstechnologieprogramms eingehend untersucht. Der vorliegende Bericht faßt die derzeit vorliegenden Ergebnisse an den für die Fusion entwickelten 9-12% CrMoVNb-Stählen MANET I und II zusammen. Die Daten umfassen Informationen zur physikalischen Metallkunde, dem Umwandlungs-, Härtungs- und Anlaßverhalten sowie zu den mechanischen Eigenschaften wie Zugfestigkeit, Kriech- und Zeitstandfestigkeit, isothermes und thermisches Ermüden sowie Kerbschlag- und Bruchzähigkeit. Weitere Daten betreffen das Korrosionsverhalten mit Druckwasser bzw. Helium als Kühlmittel, die Kompatibilität mit Brutstoffen und Materialien zur Neutronenmultiplikation sowie Informationen zum Schweißverhalten mit fortgeschrittenen Schweißmethoden. Ein kurzer Abriß über die Fabrikationstechnologie dieser Werkstoffgruppe wird ebenfalls gegeben. Schließlich werden umfangreiche Daten zum mechanischen Werkstoffverhalten nach und unter Bestrahlung mit Neutronen und Ionen bis zu 15 dpa und 500 appm Helium in dem für die Anwendung relevanten Temperaturbereich RT bis 450°C zusammengestellt.

Auf die Entwicklung niedrig-aktivierender Legierung auf der Basis von 7-11% CrWVTa wird ebenfalls eingegangen. Diese Legierungen können die Kriterien für niedrige Langzeitaktivierbarkeit nach hoher Bestrahlungsdosis unter der Voraussetzung erfüllen, daß unerwünschte Verunreinigungen unterhalb der maximal zulässigen Konzentration gehalten werden können. Dies stellt hohe Anforderungen an die Stahlherstellung. Die ersten vorläufigen Ergebnisse an diesen Legierungen zeigen bei ansonsten mit den konventionellen 9-12% Cr-Stählen vergleichbaren Eigenschaften deutlich verbesserte Kerbschlag- und Bruchzähigkeitsdaten. Erste Bestrahlungsergebnisse ergeben tendenziell eine geringere bestrahlungsinduzierte Härtung und dementsprechend eine weniger ausgeprägte Verschiebung der Sprödbruchübergangstemperatur an diesen Legierungen, so daß diese Entwicklungsrichtung insgesamt erfolgversprechend ist. Schließlich werden in diesem Bericht die notwendigen weiteren F&E-Arbeiten benannt, die notwendig sind, um noch offene Fragen zu klären.

This report contains contributions from:

A. Alamo
H.U. Borgstedt
A. Donato
K. Ehrlich,
G. Filacchioni
W. Hendrix
M.T. Hernández
P. Jung
R. Källström
S. Kelzenberg
R. Lindau
V. Massaut
P. Marmy
E. Materna-Morris
A. Möslang
A.C. Nystrand
C. Petersen
L. Pilloni
Ch. De Readt
D.H. Röhrig
M. Rieth
O. Romer
L. Schäfer
M. Schirra
R. Schmitt
J.L. Seran
H. Ullmaier
W. Vandermeulen
J. Van de Velde
M. Victoria
M.I. de Vries
F. Wolter

Contents

# 1. Introduction

Martensitic steels containing 9 - 12% Cr and about 1% Mo, with and without additions of V and Nb, have been developed and used successfully as core component materials to high fuel burn-ups in sodium cooled fast breeder reactors in France, Germany and the U.K. These steels have relatively high strengths at temperatures up to about 550°C and are resistant to thermal stress development, irradiation - induced void swelling, high temperature grain boundary (helium) embrittlement and irradiation creep. Consequently, a 11% CrMoVNb steel, based on the German 1.4914 and British FV448 steel specifications and termed "MANET" (Martensitic steel for NET), was selected in 1984 as an alternative first wall and breeder structural material for the Next European Torus (NET) [1][2].

The high Cr martensitic steels offer many advantages over other potential fusion reactor structural materials such as austenitic steels and vanadium alloys [2][3] and the MANET steel has therefore been chosen as the reference structural material for the DEMO fusion power reactor - relevant tritium breeding blanket concepts (solid ceramic cooled with helium and liquid LiPb self - or water - cooled) being developed as part of the European Long Term Fusion Technology Programme [4]. The operating temperature range and target fluence for the steel structure in the blanket sectors in DEMO are envisaged to be about 200 - 550°C and 5 MWy/m$^2$; the latter corresponds to a displaced atom production of approximately 70 dpa and helium and hydrogen gas generations by (n,$\alpha$) and (n,p) reactions of 700 and 3,500 appm respectively in the MANET steel.

The development of reduced activation high (7-10%) Cr martensitic steels for fusion reactor structural applications has also been pursued in Europe as well as in the U.S.A., Japan and Russia. The principal approach adopted in this development has involved elemental tailoring; that is, the substitution of elements such as W, V, Mn, Ta and Ti, which have an equivalent influence on the constitution and structure but a lower radiological impact, for some of the principal alloying elements such as Mo, Nb and Ni in the conventional steels.

The progress made in the tasks on the ferritic/martensitic steels in general [5,6], the MANET steel [6] and low activation materials [7], also undertaken as part of the European Long Term Fusion Technology Programme, has been surveyed periodically. The current status of the technological development of the high Cr martensitic steels is reviewed and assessed, their potential for fusion reactor applications reappraised and the research and development required to resolve some of the critical issues and clarify remaining uncertainties are considered in this report.

*References*

1. D.R. Harries, J.M. Dupouy and C.H. Wu, J. Nucl. Mater., 133 and 134 (1985) 25.
2. D.R. Harries, Radiat. Eff., 101 (1986) 3.
3. K. Ehrlich and K. Anderko, J. Nucl. Mater., 171 (1990) 139.
4. M. Dalle Donne et al, ibid, 212 - 215 (1994) 69.
5. R.L. Klueh, K. Ehrlich and F. Abe, J. Nucl. Mater. 191-194 (1992) 116.
6. I. Curbishley, W. Dietz, D. Lehmann, A.A. Tavassoli, and J. Wareing, CEC Study Contract RAI-0199 UK, 1994.
7. D.R. Harries, FTSC-P(90) P4.2, July 1990; FTSC (I) 9/4.3.1, July 1992.
8. D.R. Harries, FTSC-P(90) P4.3, June 1990; FTSC (I) 9/4.3.4, September 1992.

# 2. 9 - 12% Cr-MoVNb Steels (MANET type)

## 2.1 Characterisation and optimisation

A 1 ton reference heat of the high Cr martensitic steel (MANET I) was produced by vacuum induction melting (VIM) followed by vacuum arc refinining (VAR) by SAARSTAHL GmbH; the analysis of the steel is given in Table I. Structural examinations, investigations of the continuous cooling time - temperature - transformation (TTT) behaviour and evaluations of the mechanical (tensile, impact and stress - rupture) properties of the wrought steel, together with studies aimed at optimising the initial austenitising and tempering treatments, were carried out and the results reported [1].

The steel was fully martensitic and the properties were generally comparable to those of the standard 1.4914 grade. However, the fracture appearance ductile brittle transition temperature (DBTT) was relatively high ( +27 and +16°C in the austenitised at 1075°C/0.5 h and tempered for 2 h at 720 and 750°C conditions respectively). Additional research on the 1.4914 and MANET I steels was directed towards establishing the effect of δ-ferrite in the structures on the impact properties [2], the influence of substituting nitrogen for carbon [3] and the cause of the often observed creep instabilities (significant increases in the continuously measured creep rates after 1 - 2 x 10 h at 600°C, a few hundred hours at 650°C and about 10 h at 700°C) [4]; the latter behaviour was associated with a high (hyper - stoichiometric) Al : N ratio in the steels.

These findings led to the specification of a second reference martensitic steel, designated MANET II and procurement from SAARSTAHL GmbH; six heats, yielding 7 tons of steel, were produced by the VIM + VAR route and hot forged to

**Table I: Analyses (wt.%) of MANET I and II Steels (SAARSTAHL)**

| Element | MANET I | MANET II |
|---|---|---|
| C | 0,13 | 0.10 - 0.11 |
| Si | 0,37 | 0.14 - 0.28 |
| Mn | 0,82 | 0.75 - 0.96 |
| S | 0,004 | 0.004 - 0.005 |
| P | 0,005 | 0.003 - 0.007 |
| Cr | 10,6 | 10.3 - 10.37 |
| Ni | 0,87 | 0.62 - 0.68 |
| Mo | 0,77 | 0.56 - 0.61 |
| V | 0,22 | 0.19 - 0.21 |
| Nb | 0,16 | 0.14 - 0.16 |
| Al | 0,054 | 0.004 - 0.012 |
| B | 0,0085 | 0.0072 - 0.0089 |
| N | 0,02 | 0.027 - 0.032 |
| Co | 0,01 | 0.005 - 0.010 |
| Cu | 0,015 | 0.007 - 0.015 |
| Zr | 0,053 | 0.007 - 0.028 |
| As | | 0.008 - 0.010 |
| Sb | | 0.0002 - 0.0004 |
| Sn | | 0.001 |

rods ranging in diameter from 95 to 6 mm or rolled to 30 to 4 mm thick plates [5]. The analysed compositional ranges for the MANET II steel heats are included in Table I.

The characterisation of the MANET II steel has been completed [5] and the principal studies and observations may be summarised as follows:

(i) Determination of the continuous cooling time - temperature - transformation (TTT) curves showed that the MANET II steel had an improved hardenability compared to MANET I and is similar to that of the commercially available 9 - 12% Cr martensitic steels such as Types 1.4922 and T91 [6]. The transformation temperatures of the MANET I and II steels are given in Table II and Fig. 1.

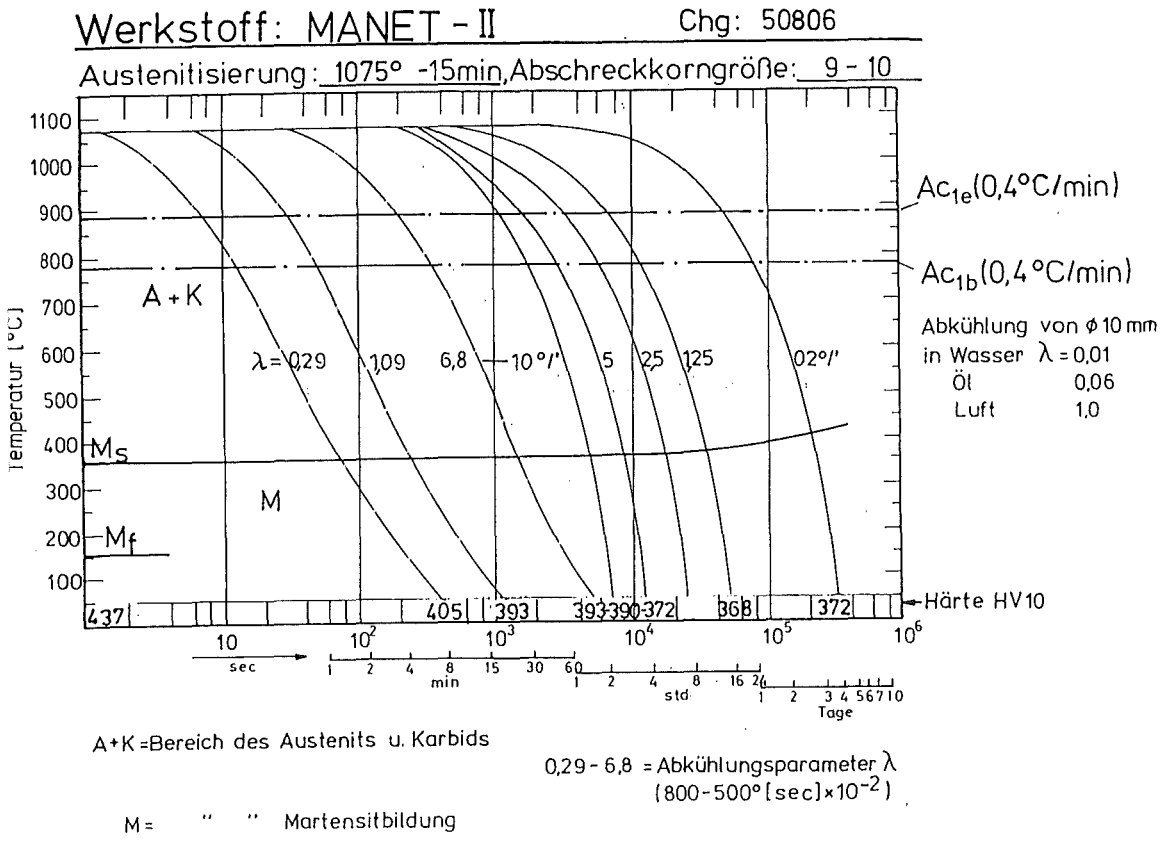


Fig. 1: Continuous cooling time-temperature-transformation (TTT) behaviour of MANET II [5].

**Table II: Transformation Temperatures (°C) for MANET I and II Steels**

| Steel | $Ac_{1b}$ | $Ac_{1e}$ | $M_s$ | $M_f$ |
|---|---|---|---|---|
| MANET I | 790 | 870 | 310 | 155 |
| MANET II | 775 - 780 | 890 - 900 | 340 - 357 | 155 - 161 |

(ii) The following reference heat treatment for the MANET II steel, aimed at achieving an optimum balance of good impact (fracture toughness) properties and high creep strength, was derived from the results of investigations of the hardening (quenching from temperatures in the range 850 - 1150°C) and tempering (200 - 800°C) behaviour [5]:

Austenitised at 1075°C for 0.5 h, air cooled, tempered at 750°C for 2 h and air cooled.

(iii) The tensile strengths of the lower carbon content MANET II steel were slightly inferior to those of the MANET I at 550°C but the strengths were comparable at temperatures in the 550 to 750°C range [5][7].

(iv) The creep - rupture properties of the different heats of the MANET II steel at temperatures ranging from 450 - 700°C and times of 10 h showed little scatter and were, due to their hypo - stoichiometric Al : N ratios, superior to those of the MANET I steel in not exhibiting instabilities in the creep deformation rates [5].

(v) The DBTTs and upper shelf energies (USEs) of the MANET II steel, as evidenced in Charpy V - notch impact tests, were significantly better (lower DBTT of +3°C and higher USEs) than those of the MANET I (both steels in the reference heat treatment condition) and only slightly inferior to those of the modified 9% Cr - 1 Mo (T91) steel (Fig. 2) [5]. The improved toughness characteristics of the MANET II steel has been attributed to its lower Zr content compared to that of the MANET I [8]; large Zr(C,N) primary particles influenced the fracture behaviour of the MANET I steel but the smaller Zr(C,N) precipitates in the MANET II steel appeared to be innocuous in this respect.

An additional reduction in the DBTT combined with an increase in the tensile proof stress can be effected by further optimisation of the austenitisation and tempering temperatures for the MANET II steel [7]; thus, as shown in Fig. 3, a high 0.2% tensile proof stress at 500°C (518 MPa) and a low DBTT ( - 30°C at 90 J) may be achieved by austenitisation at 900°C and tempering at 700°C.

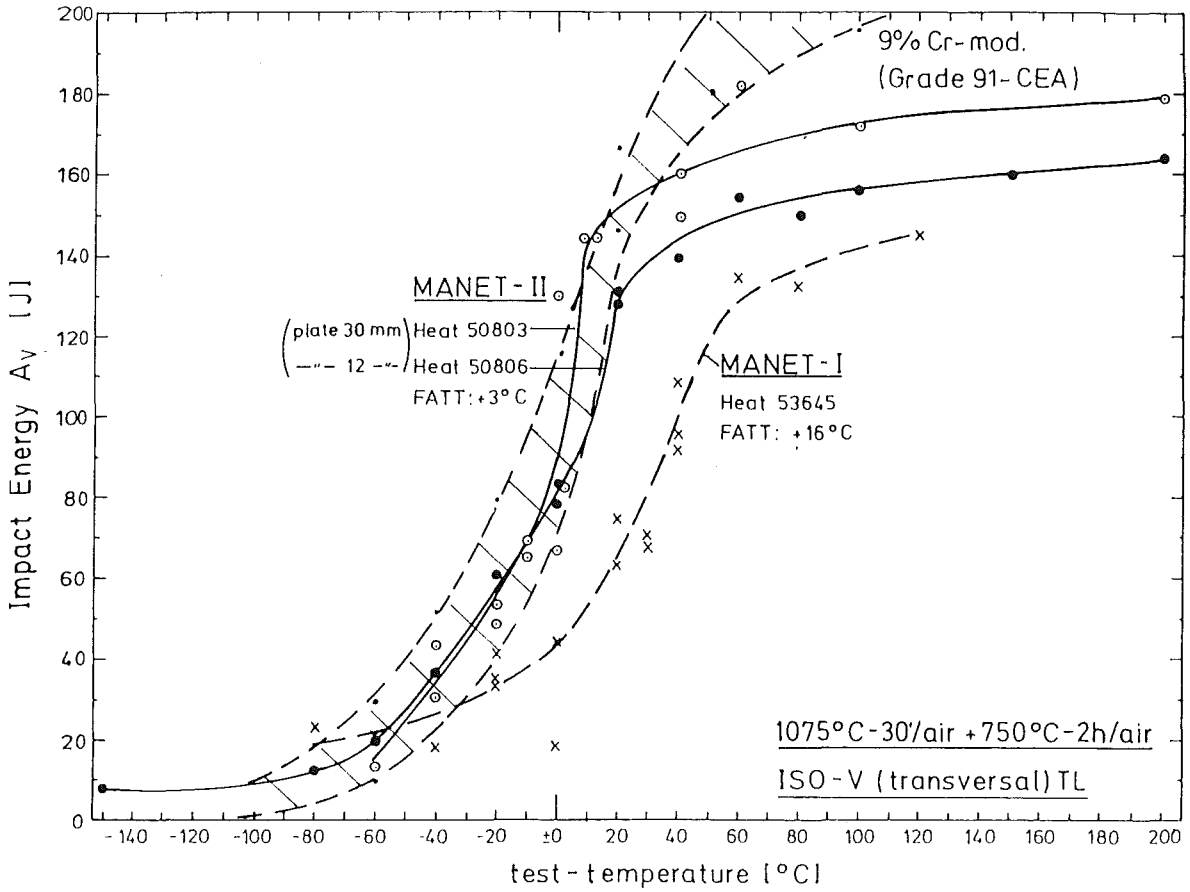


Fig. 2: Charpy V - notch impact transition curves for the MANET I and II and modified 9% Cr - 1Mo steels.

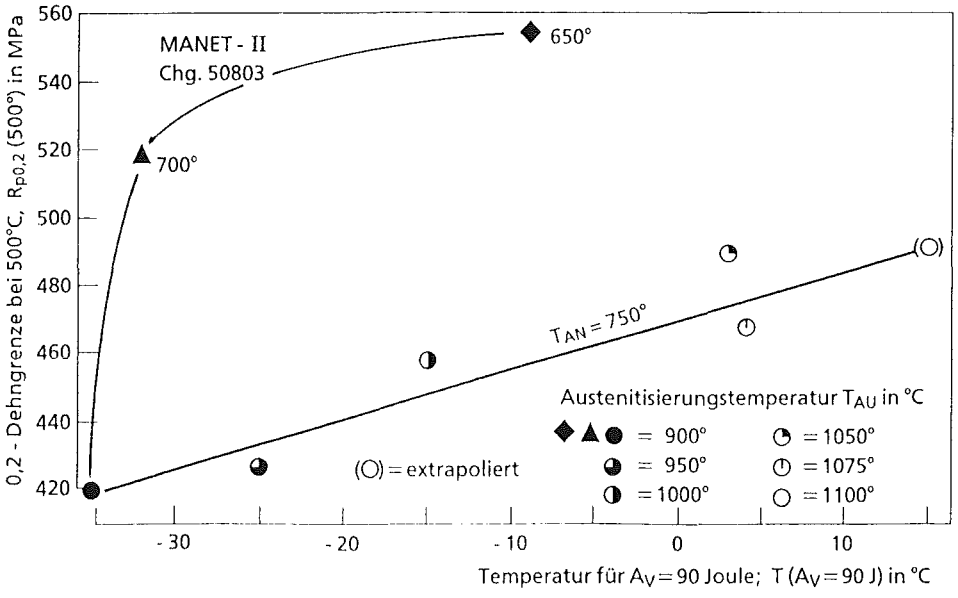


Fig. 3: Effect of austenitisation and tempering temperatures on the DBTT (90 J) and 0.2% tensile proof stress at 500°C of the MANET II steel.

*References*

1. M. Schirra et al, KfK Report 4561, June 1989.

2. K. Anderko, L. Schäfer and E. Materna-Morris, J. Nucl. Mater., 179 - 181 (1991) 492.

3. K. Ehrlich and M. Schirra, Vortragsveranstaltung der Arbeitsgemeinschaften für warmfeste Stähle und Hochtemperaturwerkstoffe, Düsseldorf, November 1992, p. 64.

4. M. Schirra and K. Anderko, Steel Research No. 6 (1990) 242.

5. M. Schirra et al, KfK Report 5177, May 1993.

6. Commission of the European Communities, "The Manufacture and Properties of Steel 91 for the Power Plant and Process Industries", ECSC - Information Day, November 5th. 1992, VDEh - Dusseldorf.

7. L. Schäfer et al, KfK Report 5245, October 1993.

8. E. Materna-Morris, M. Schirra, K. Ehrlich; Das Bruchverhalten von Kerbschlagproben an Varianten des X 18 CrMoVNb 12 1.
13. Vortragsveranstaltung des Arbeitskreises "Rastermikroskopie in der Materialprüfung", München, 18.-20. April 1988. Berlin: DVM, 1988, S. 323-332.

## 2.2 Melting, fabrication and welding

There is a well established industrial capability for the melting and primary fabrication of high chromium martensitic steels but relatively little technical information has been published due primarily to the proprietary nature of the commercial processes involved. Nevertheless, a review of the available information concluded that [1]:

(i) A wide range of air and vacuum melting and refining techniques could be applied depending on the required steel specifications.

(ii) Hot working by forging, extrusion and rolling did not pose any unsurmountable problems but there were no systematic data on the factors which affected the hot workability; these included primary carbides, δ-ferrite and eutectic phases which could promote liquidation cracking and hot shortness in the high temperature austenite phase.

(iii) Cold workability during rolling, drawing and reducing was enhanced if the steels were first fully softened and appropriate intermediate annealing treatments applied.

(iv) The steels had good machineability without the necessity for free - cutting elemental additions.

Secondary fabrication has posed some problems in that the high chromium steels always have to be heat treated to temper the brittle martensite structure formed during cooling from high temperatures. The welding of the martensitic steels, particularly in thick sections, may be facilitated by balancing the steel wire composition so as to avoid the formation of δ-ferrite, controlling the pre-heating, maintaining appropriate interpass temperatures and applying post-weld heat treatments [1]. It has been demonstrated that TIG welds in the MANET type steels were very resistant to reheat cracking whilst the sensitivity to hydrogen cracking was comparable to that of other hardenable steels and could be minimised by pre-heating to about 200°C [2]; however, the 10 - 11% Cr MANET steel was more prone to solidification cracking than martensitic steels containing ~9% Cr, the fractures being associated with regions of high chromium and other alloying element segregation and which were potential sites for the formation of embrittling α′ (Cr-rich ferrite) and carbide phases.

Experience of non-nuclear plant operation has shown that weldments in low and high alloy ferritic steels were susceptible to Type IV [heat affected zone (HAZ) / parent steel] cracking during service, particularly in the range 500 - 565°C; laboratory work has suggested that it may also be a problem in 9% Cr - 1Mo and 9% Cr -

1 MoVNb martensitic steels. A review of the literature [3] has concluded that Type IV cracking was a high temperature creep failure mode and arose as a consequence of the combined effects of the low creep strength of the intercritically deformed structure of the HAZ adjacent to the base steel and high stresses across the weldments due to poor design or operation of the plant. However, it is not clear at present if the MANET and other high chromium martensitic steels will be prone to Type IV weld cracking under the temperature and loading conditions appropriate to the first wall and breeder blanket structural components in a fusion reactor.

Investigations of advanced autogenous welding techniques (laser and electron beam), in which the heat is concentrated in narrow zones, and of solid state diffusion bonding of the MANET I and/or II steels have been pursued in an attempt to develop processes which can be readily applied to the joining of fusion reactor structural components with minimal distortion and produce weld or bond structures and properties comparable or superior to those made by the more conventional techniques.

(i) Laser welding

Preliminary welding trials with a 5 kW $CO_2$ laser were performed on 3.5 mm thick plates of the MANET I steel which were initially austenitised at 950°C/2 h and 1075°C/0.5 h and tempered at 750°C/ 2 h [4]. Sound welds were produced and the widths of the fusion and heat- affected zones were approximately 2 and 0.4 mm respectively. Metallographic examinations showed that the weld structures consisted of martensite with a small number of δ-ferrite islands; however, the HAZs and base steel were fully martensitic but contained regions rich in precipitates and/or non-metallic inclusions of ZrC or Zr(CN). The maximum hardness of 400-460 $HV_2$ was produced in the weld and in the regions of the HAZ immediately adjacent to the fusion zone; the hardness of the base steel was 171 $HV_2$.

The 5 and 6 kW $CO_2$ laser welding parameters were optimised using 3 and 5 mm thick plates of quenched and tempered T91 (9% Cr : 1% Mo) and 1.4914 martensitic steels because of limited availability of the MANET I steel [4][5]. However, 4 and 6 mm thick plates of the MANET II steel have now been welded using the 5 kW $CO_2$ laser and the welds characterised by radiographic and metallographic examinations and hardness, tensile and sub-size Charpy V-notch impact tests [6]. The welds were free from defects and their hardness values were comparable to those of the base plates after tempering at 760°C/1 h; however, the tensile strengths of the tempered welds in the 6 mm thick plate were approximately 100 and 75 MPa lower at ambient temperature and 400°C respectively

whilst the DBTT was reduced and the USEs increased relative to those of the parent steel.

More recently, welding trials on the 4 and 6 mm thick plates of the MANET steel have been conducted using a pulsed 1.2 kW YAG laser and the welding parameters defined [7]. Metallographic examinations showed that the widths of the fusion and heat affected zones were slightly greater than those produced by the $CO_2$ laser process but the hardness, tensile and toughness properties of the respective fusion zones were comparable.

(ii) Electron beam welding

Electron beam weldments have been produced in 8, 15 and 20 mm (nominal) thick plates of the MANET I steel, non-destructively tested and heat treated; tensile, creep, fatigue, standard and sub-size Charpy V-notch impact and compact tension fracture toughness specimens were then machined from the welded plates.

Microstructural examinations of the MANET steel and electron beam welded samples of the 20 mm thick plate were performed by transmission and extraction replica electron microscope techniques [8][9]; the plate had been austenitised at 1075°C, tempered at 750°C and re-tempered at 750°C after welding. The weld and parent steel exhibited similar microstructures in terms of dislocation density and grain size. $M_{23}C_6$ type precipitates in the welds were smaller and more finely distributed than in the HAZs, with some of the precipitates being located at the prior austenite grain boundaries in both regions. There were small precipitates in the parent steel but none at the grain boundaries. These micro-structural differences could be attributed to the parent steel having been tempered twice whilst the welds and HAZs were only tempered once.

The results of tensile tests at temperatures in the range ambient to 625°C showed that the yield and ultimate tensile strengths of the welds were about 50 MPa lower but the elongations to fracture were similar to those of the parent steel [10][11]. The tensile properties of the parent steel depended on the plate thickness, with the strengths of the 8 mm thick plate being higher than those of the thicker plates; however, the weld strengths were independent of the plate thickness.

The Charpy V - notch impact DBTTs of the electron beam welds and the steel plate were comparable and below room temperature but the the USEs of the welds were considerably higher than those for the steel plate [11]; all fractures occurred in the welds and not in the HAZs. The fractures produced in creep - rupture tests

at 525°C generally occurred in the steel plate and not in the welds and HAZs; the rupture elongations and reductions of area were 20 % and 70 % respectively [11][12]. Fatigue crack propagation tests at 250 and 450°C showed comparable growth rates for the plate and welds [12].

It may be concluded from the observations summarised here that the electron beam welding produced a fine microstructure and mechanical properties comparable to or only slightly inferior to those of the wrought MANET steel.

(iii) Diffusion bonding

An investigation has been performed to evaluate the feasibility of diffusion bonding MANET steel plates for the highly loaded blanket structures in a DEMO fusion reactor [13]. The technique essentially involves pressing together two plates with parallel faces in vacuum at temperatures up to about 1050°C so as to facilitate inter-diffusion and thereby promote strong bonding. The bonding tests were carried out on behalf of FZK by the Forschungsinstitut für Kerntechnik und Energiewandlung, Stuttgart, using a facility in which the parts were heated in high vacuum by medium frequency radiation and the mechanical pressure imposed by hydraulic displacement of plungers and pressure plates.

The optimum temperature and pressure bonding conditions were first established in tests on small (80 mm diameter) MANET II steel plate specimens provided with coolant and inspection channels; the effects of initial surface condition (rolled, milled and ground surfaces) and intermediate electrodeposited nickel layers were also studied. The bonded samples were subsequently heat treated, helium leak tested, metallographically examined and bend tested. The optimum bonding conditions were as follows:

(a) Plates with finely ground surfaces (roughness $\leq 3$ µm), 980°C, pressurised at 30 MPa for 1h and subsequently at 7 MPa for 1h.

(b) Samples with 20 µm thick nickel surface layers, 1050°C, pressurised at 18 MPa for 1 h and then at 7 MPa for 1 h.

The plates bonded under these conditions were leak tight and the bond bend strengths were almost equivalent to those of the base steel.

Three specimen plates, 320 mm thickness and with a typical first wall coolant geometry, were bonded using the optimised parameters; helium leak tests showed that the tightness conformed to the detection limit of the instrument.

*References*

1. P. Buttol et al, ENEA NUC-RIN Report CT. WCH. 00017, February 1993.
2. R. Boler et al, NNC, Engineering Development Centre Report 92/114, Issues A, September 1992.
3. C.K. Bullough, AEA FUS 145, September 1991.
4. C. Charissoux and A. Richard, CEA Report STA/LMS/89-NT620, November 1989.
5. C.Charissoux and A. Richard, CEA Report STA/LMS/92-NT658, May 1992.
6. A. Richard, CEA Report STA/LMS/93-NT730, December 1993.
7. A. Richard and J. Schildknecht, CEA Report STA/LMS/94-NT753, November 1994.
8. P. Groot and F.A. van der Berg, ECN Report 1-90-045, November 1990.
9. P. Groot and F.A. van der Berg, ECN Report 1-91-066, October 1991.
10. B. van der Schaaf and M.I. de Vries, Proc. 16th. Symp. on Fusion Technology, London, September 1990, Vol. 1, p.954.
11. H. Th. Klippel (Ed.), Progress Report 1990 on Fusion Technology Tasks, ECN Report C-91-035, June 1991.
12. H. Th. Klippel (Ed.), Progress Report 1991 on Fusion Technology Tasks, ECN Report C-92-049, July 1992.
13. G. Haufer, KE-Report Forschungsinstitut f. Kerntechnik und Energieumwandlung, Stuttgart 1994.

## 2.3 Pre- and post (reactor)- irradiation mechanical properties and structure

### 2.3.1 Radiation hardening and embrittlement

(i) FZK

Tensile and impact properties of the MANET I steel in the reference heat treatment were determined for the unirradiated and irradiated material [1-4]. The irradiation was performed in the HFR-reactor in Petten and included fluence levels ranging from 5 to 15 dpa at nominal temperatures of 300, 400 and 475°C.

The observed radiation hardening defined as the difference in yield strength (0,2% YS) and ultimate tensile strength (UTS) of the irradiated to the unirradiated thermal control specimen is shown in Fig. 1. Significant hardening occurs at the irradiation/test temperature of 300°C. Radiation hardening is accompanied by a reduction in uniform and total elongation and also a reduction of area after fracture. The fracture mode is, however, not affected by irradiation and is always ductile and transgranular, with dimples mostly nucleated at Zr(C,N) inclusions. The data also indicate an early saturation of radiation hardening at displacement doses below 5 dpa.

The irradiation also produces major changes in the impact properties of this material [2-4]. Fig. 2 shows the influence of irradiation on the impact energy after a neutron exposure of 10 dpa. At the lowest irradiation temperature of 290/300°C a large shift in the ductile to brittle transition temperature (DBTT) and a strong decrease in the upper shelf energy (USE) is observed. Similar to the observed radiation hardening, the influence of irradiation on the impact properties is less with increasing irradiation temperature and negligible for a reactor exposure at 475°C (Figs. 3 and 4). Also the saturation of the shift in DBTT and in the USE at a relatively low dpa level of 5 dpa parallels the course of the radiation-induced increase in yield strength. Thus tentatively a correlation of radiation hardening and observed shift in DBTT can be expected.

For 300°C the following linear relation between $\Delta$DBTT and $\Delta\sigma_y$ can be found:

$$\Delta DBTT = (0.50 - 0.55)\,\Delta\sigma_y$$

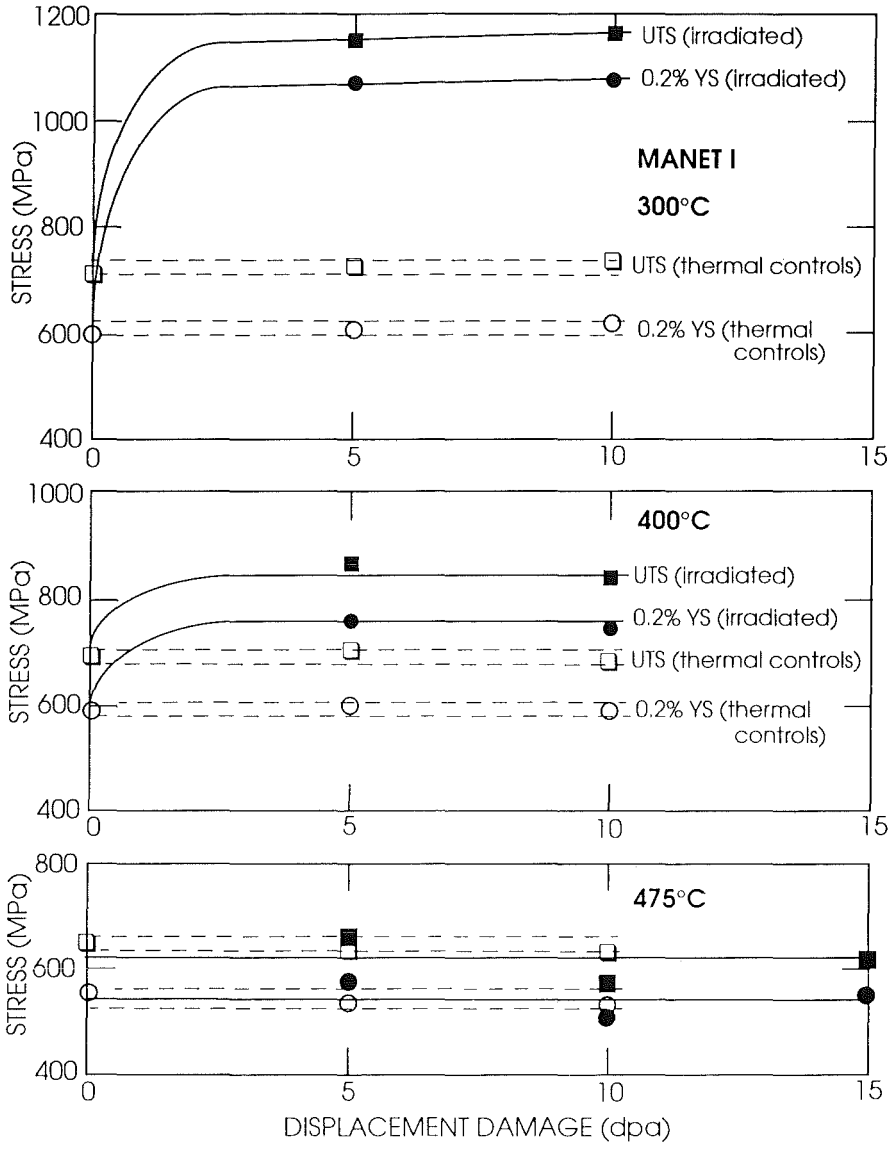


Fig. 1: Effect of displacement dose on the radiation hardening of the MANET I steel at 300, 400 and 475°C [1].

The correlation factor decreased from 0.55 to (0.35 - 0.42) for the irradiation temperature of 400°C.

Initial investigations on the effect of tempering treatment on the impact properties had shown that the DBTT decreases linearly and the USE increases exponentially with increasing tempering temperature in the range 600 to 780°C. However, the ΔDBTT and -ΔUSE induced by irradiation to 5 or 10 dpa at 290, 390 and 470°C were not significantly dependent on the initial tempering treatment [2-4]. Hence a remarkable improvement of impact properties after irradiation through a proper tempering treatment before irradiation seems not to be successful.

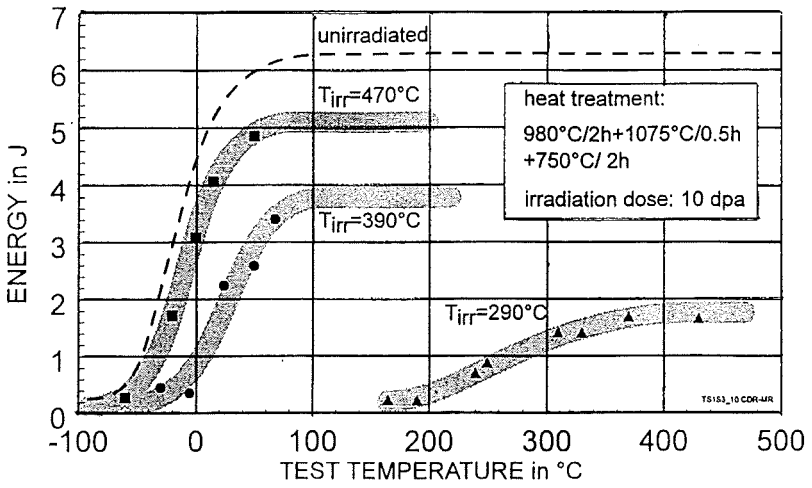


Fig. 2: Influence of irradiation temperature and displacement dose on the notched impact properties of MANET I[2].

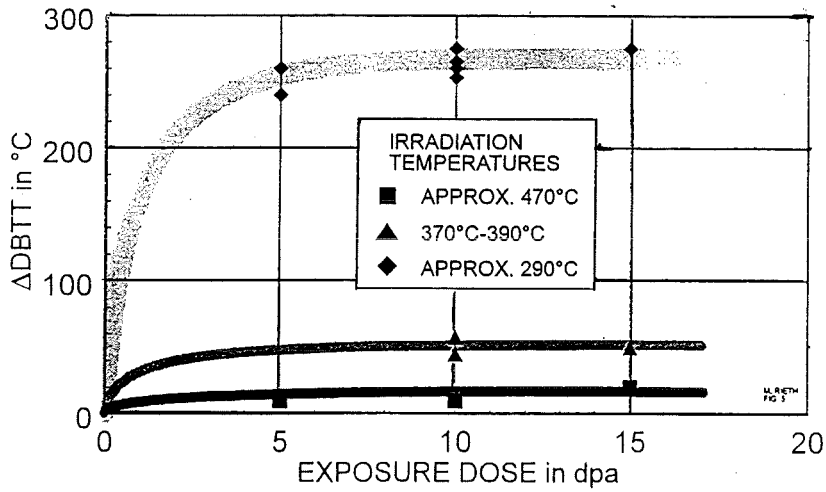


Fig. 3: Effect of displacement dose and irradiation temperature on the radiation-induced shift in DBTT [3] [4].

The microstructure of the MANET I steel in the reference heat treatment irradiated at about 300°C, as examined by high resolution transmission electron microscopy, consisted of tempered lath martensite with small $M_{23}C_6$ particles at the prior austenite grain boundaries, of a high density ($7x10^{15}cm^{-3}$) of planar dislocation loops, dislocation networks, small precipitates and of small, approx. 2.5 nm diameter helium bubbles homogeneously distributed within the martensite laths

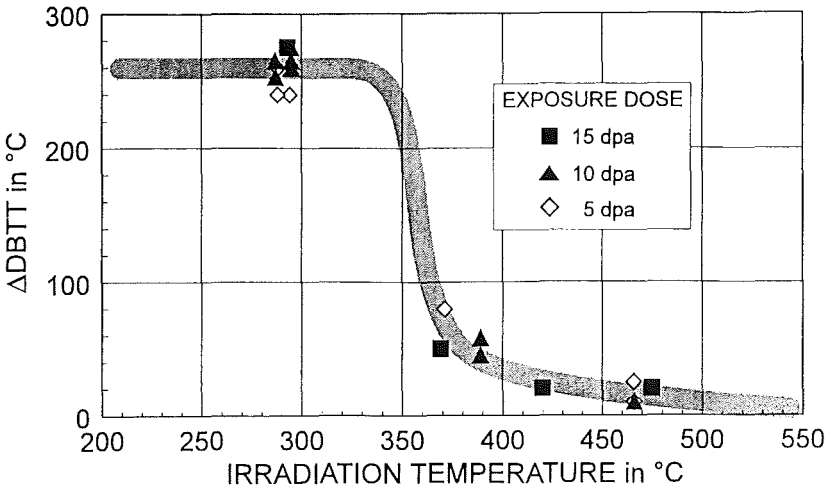


Fig. 4: Effect of irradiation temperature on the radiation-induced shift in DBTT [3][4].

[1]. Major contribution to the observed radiation hardening stems from the immobile dislocation loops. The lath and dislocation structure progressively recovered with increasing irradiation temperature, and fine, coherent α′ (chromium - rich ferrite) precipitates were formed during irradiation at 400°C; furthermore, coarser $M_{23}C_6$ particles were precipitated on the lath boundaries and larger helium bubbles were nucleated on the dislocations at the higher irradiation temperatures.

*References*

1. E. Materna - Morris and O. Romer, Proc. 18th. Symposium on Fusion Technology, Karlsruhe, Germany, August 1994, Vol. II, 1281, 1995.
2. C. Wassilew and K. Ehrlich, J. Nucl. Mater., 191 - 194 (1992) 850.
3. M. Rieth, B. Dafferner and C. Wassilew, KfK Report 5243, June 1993.
4. M. Rieth, B. Dafferner, H.D. Röhrig and C. Wassilew, Fusion Engineering and Design 29 (1995) 365.

(ii) ECN

Tensile

Thermal exposure for times of 15,000 h at temperatures up to 450°C had little or no effect on the tensile properties of the MANET I steel, but irradiation in HFR at 250 and 350°C to displacement doses in the range 0.5 to 10 dpa produced severe

radiation hardening as evidenced by the increases in 0.2% yield and ultimate tensile strengths in tests at the irradiation temperatures [1][2]; the irradiation - induced increases in yield strengths were 370 and 430 MPa following exposure to 5 dpa at 250°C and 10 dpa at 350°C respectively [Fig. 1]. The radiation hardening increased rapidly with neutron exposure up to about 1.5 dpa but there was little further irradiation - induced increase in yield strength beyond this displacement dose; it was apparent therefore that the radiation hardening of the steel had saturated at a displacement dose of $\leq 5$ dpa at these temperatures. The uniform and total elongations were also reduced following the irradiation at 350°C to 10 dpa but the steel still retained some work hardening capability and ~2% uniform elongation [Fig. 2]; exposures to doses up to 5 dpa at 250°C had relatively little effect on the ductility values. Irradiation to 10 dpa and testing at 450°C resulted in relatively small increases in yield strength (~45 MPa) and negligible changes in ductility.

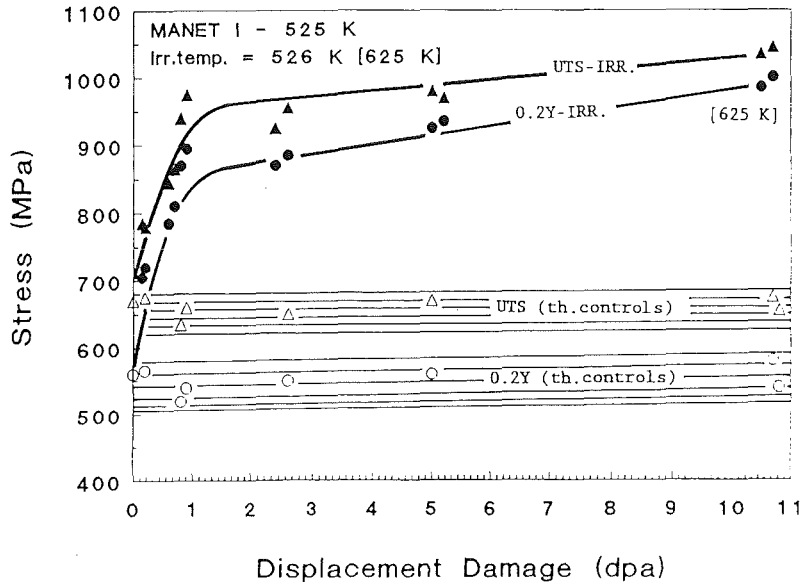


Fig. 1: Effects of irradiation to $\leq 5$ dpa at 250°C and 10 dpa at 350°C on the yield and ultimate tensile strengths of the MANET I steel at 250°C.

The magnitudes of the radiation hardening of the MANET II steel were comparable to those of the MANET I steel; thus, irradiation of the former to about 1.5 dpa at 75 and 300°C in HFR produced increases in the 0.2% yield strengths of about 300 MPa but there was a large scatter in the 75°C data, due probably to the strong dependence of the hardening on the displacement dose at this lower temperature.

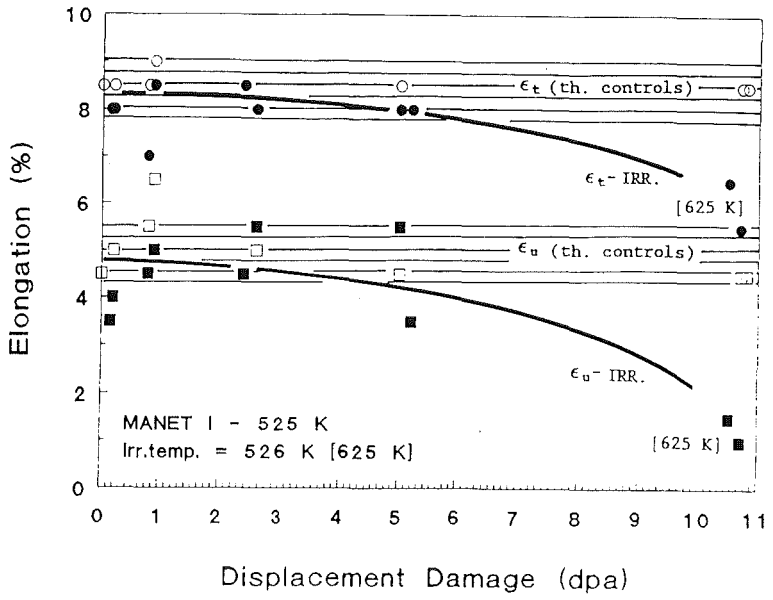


Fig. 2: Effects of irradiation to ≤5 dpa at 250°C and 10 dpa at 350°C on the uniform and total tensile elongations of the MANET I steel tested at 250°C.

Post - irradiation annealing treatments of 2 and 4 h at 500°C, 1.5 h at 525°C and 15 min. at 550°C produced complete recovery of the radiation hardening of the MANET steel as evidenced by the results of Vickers hardness measurements. TEM examinations also showed that the microstructures of the irradiated and annealed samples were comparable to those of the unirradiated steel.

The effects of irradiation to 0.5 dpa in HFR on the tensile properties of MANET I steel electron beam welds at temperatures in the range 25 to 575°C have also been investigated [3]. The yield and ultimate tensile strengths were increased by the irradiation but the magnitudes of the changes decreased with increasing test temperature such that the changes were negligible at 525 to 575°C; the total elongations to fracture were reduced at test temperatures of ≤425°C from 15-20 % before to 10-15 % after irradiation, primarily as a result of decrease in the uniform elongations.

Fracture toughness

Fracture mechanics tests, in which the load, displacement and electrical potential were simultaneously recorded [4], were performed on thermal control and irradiated (<5 dpa at 250°C; 10 dpa at 350°C) 10 mm thick compact tension specimens of the MANET I steel in the linear elastic, transition and fully elastic-plastic regimes. These tests enabled the fracture toughness behaviour from lower to upper shelf in the ductile - brittle transition curves to be determined. In addition, the results of tests which were apparently conducted in the transition regime were corrected for size effects on the K toughness distribution. The $K_{1c}$- values, as calculated from the $J_{1c}$ - values, were amended using the following empirical relationships to determine the fracture toughness $K_{1c}$ from measurements of the elastic - plastic slow crack extension preceeding unstable fracture:

$$K_{1c} = K_{Jc}\,[\beta_{1c} / \beta_c]$$

where $\beta_c$ is a dimensionless strength ratio parameter.

$$\beta_c = \frac{1}{B}(K_{Jc} / \sigma_{ys})$$

and

$$\beta_{Jc} = f(\beta_c)$$

The "as - measured" $K_{1c}$ and $K_{Jc}$ data are presented in Fig. 3. Irradiation to low displacement doses of around 1 dpa at 250°C in HFR produced large increases in DBTT so that the samples failed in a brittle manner with a minimum $K_{1c}$ value of 20 MPa $\sqrt{m}$ when tested at ambient temperature [1][5]. The $K_{Jc}$ - values, calculated from the J-values, ranged between 70 and 120 MPa at test temperatures of 250 to 450°C. Some of the 250°C irradiated samples also failed in an unstable (brittle) manner when tested at 250 and 350°C [5]; the "as - derived" $K_{1c}$-values ranged from 40 to 80 MPa $\sqrt{m}$. The conservative value of the stress intensity factor of 40 MPa $\sqrt{m}$ at 250°C was in agreement with the fatigue crack growth data at this temperature, showing unstable growth at equivalent $\Delta K$ values. The fracture toughness was also decreased at the test temperature of 450°C after the irradiations at 250 and 350°C (Fig. 3); the initiation toughness $J_{0.2}$ and the crack growth resistance dJ/da were similarly dependent on the test temperature and were significantly reduced in tests at 250, 350 and 450°C after irradiation (Figs. 4 and 5).

Fractographic examinations showed a broad range of features, ranging from classical cleavage facets to ductile dimple fractures, with the irradiated specimens generally exhibiting mixed fracture modes.

An independent analysis of the normal operational behaviour of a martensitic steel first wall in a fusion reactor has yielded critical stress intensity factors of about 50 MPa $\sqrt{m}$ for 3 to 5 mm deep surface defects [6]. This observation and the available experimental data suggest that, for safety reasons, the lower limit of the temperature window for the application of the MANET steel as the first wall in a fusion system will have to exceed 250°C for displacement doses of $\geq 1$ dpa.

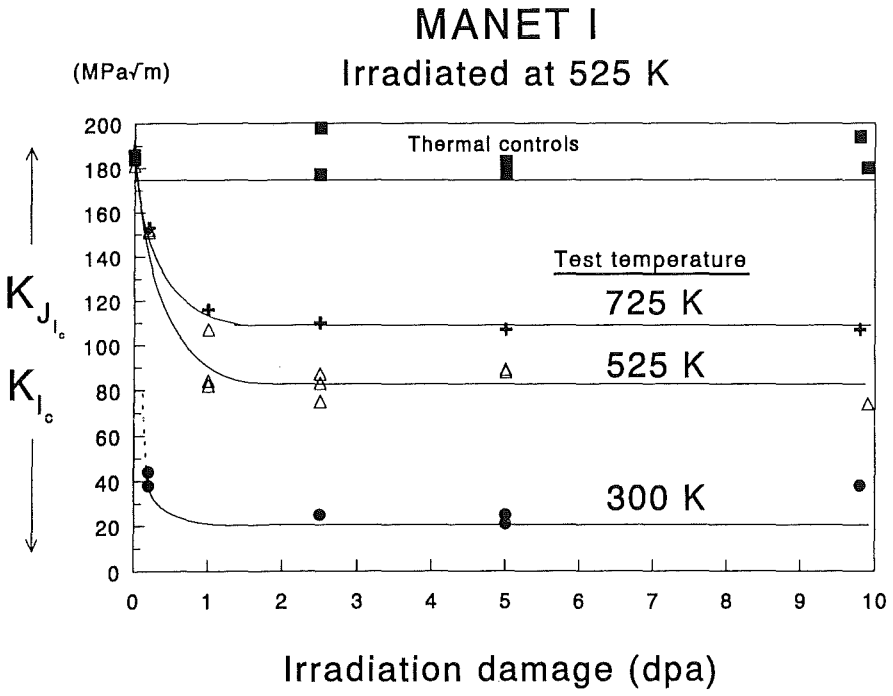


Fig. 3: Effects of irradiation on the fracture toughness parameters for the MANET I steel tested at ambient temperature, 250 and 450°C together with thermal control data at 450°C.

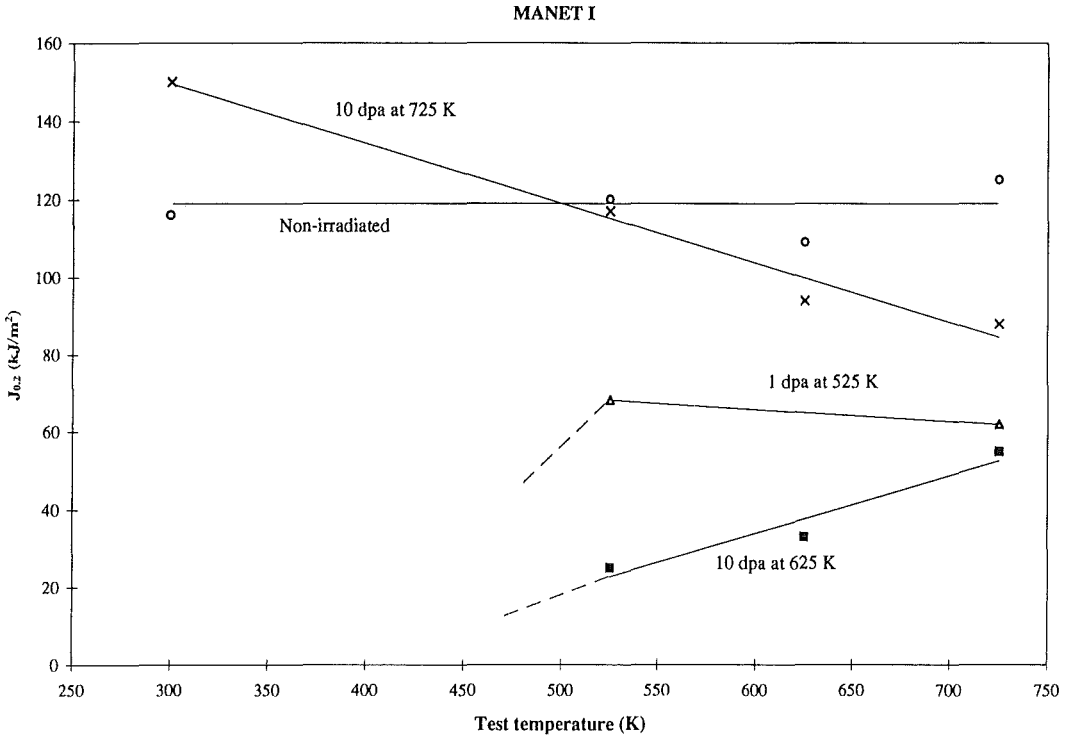


Fig. 4: Test temperature dependency of the initiation toughness J for the irradiated and unirradiated MANET I steel.

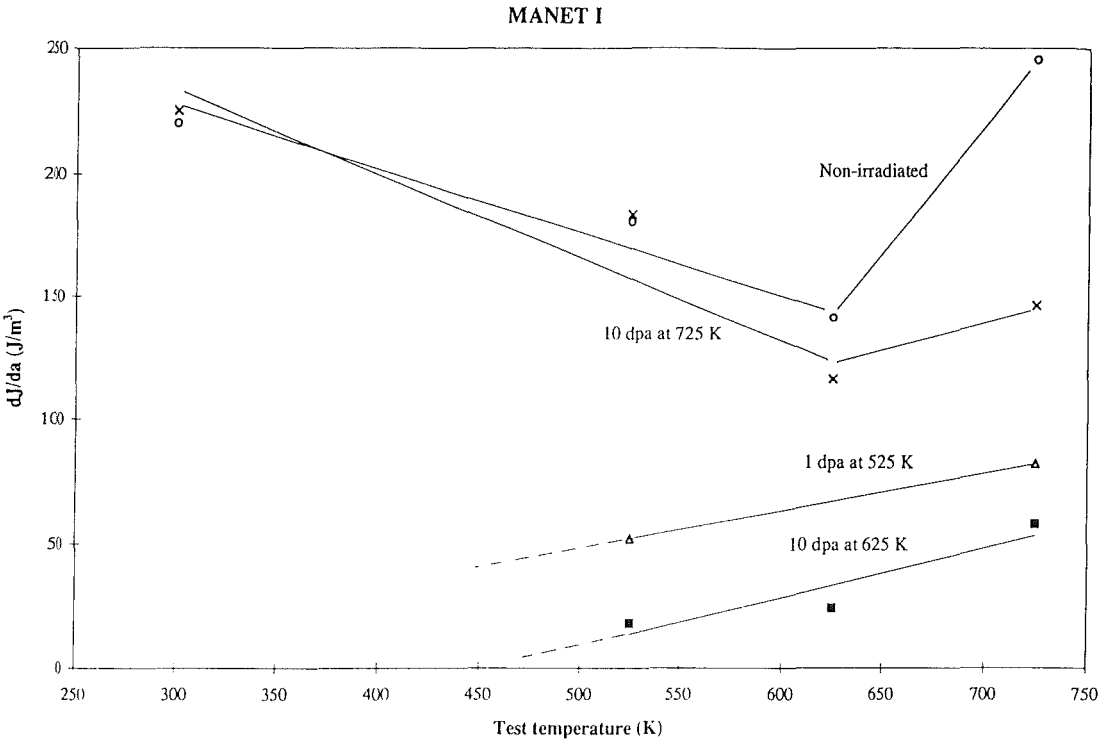


Fig. 5: Effects of test temperature on the crack growth resistance dJ/da of the irradiated and unirradiated MANET I steel.

### *References*

1. M.I. de Vries, ASTM Special Tech. Pubn. No. 1175, 1993, p.558.
2. H. Th. Klippel, Ed.. Progress Report on Fusion Technology Tasks, ECN Report C - 94 - 041, September 1994.
3. B. van der Schaaf and M.I. de Vries, Proc. 16th. Symp. on Fusion Technology, London, September 1990, Vol. 1, p. 954.
4. H.Th. Klippel (Ed.), Progress Report 1990 on Fusion Technology Tasks, ECN Report C-91-035, June 1991.
5. H.Th. Klippel (Ed.), Progress Report 1991 on Fusion Technology Tasks, ECN Report C-92-049, July 1992.
6. E. Diegele, ERB 5000 CT 9100 7, NET, KfK, IMF II, June 1992.

(iii) SCK / CEN

The tensile properties of the MANET I steel, initially heat - treated at 970°C / 2 h + 1075°C / 0.5 h + 750°C / 2 h, have also been determined after irradiation to approximately 5 and 10 dpa at 250 and 400°C in the BR2 reactor at Mol [1]; the tests were carried out at the same temperatures as the irradiations at initial strain rates of about $2.8 \times 10^{-3}$ and $2.8 \times 10^{-2}$ $s^{-1}$. The 0.2 % proof and ultimate stresses are plotted as a function of displacement dose in Fig. 1.

The strengths increased more or less linearly with the displacement dose at 250°C. However, the irradiation - induced increases in strengths saturated at 5 dpa at an initial strain rate of $2.8 \times 10^{-3}$ $s^{-1}$ at 400°C but saturation had not been achieved after 10 dpa at the higher strain rate of $2.8 \times 10^{-2}$ $s^{-1}$. Furthermore, the magnitudes of the strength increases were generally greater at a given dose at 400°C, particularly at the higher strain rate, than at 250°C. It should be noted, that these data are not in accordance with the other observations on these steels. The radiation hardening at 400°C was accompanied by reductions in total elongations but the ductility changes at 250°C were small.

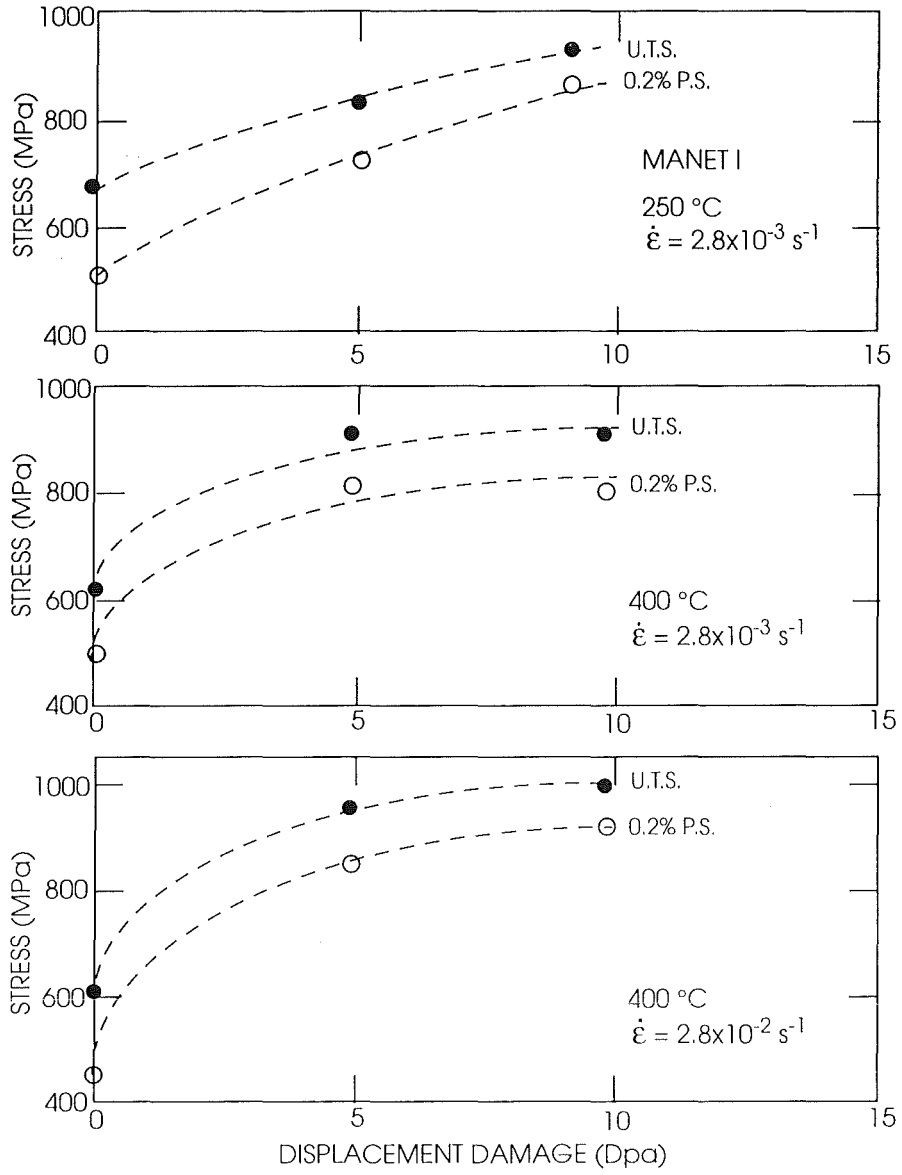


Fig. 1: Effects of irradiation at 250 and 400°C in the BR2 reactor on the proof and ultimate tensile strengths of the MANET I steel [1].

***Reference***

1. W. Vandermeulen et al, Report FT / Mol / 92 - 05, December 1992.

(iv) CEA

Tensile and sub - size Charpy V - notch impact specimens of the EM10 fully martensitic base steel (0.1% C, 8,76% Cr, 1.05% Mo) and of autogenous TIG and electron beam welds of the steel have been irradiated to about 65 dpa at 459°C (tensile) and at 450 and 474°C (impact) in the PHENIX reactor [1][2]. The tensile strengths and elongations of the weld specimens, in both the "as - welded" and " post - weld heat treated" conditions, were generally comparable to those of the base steel in tests at ambient temperature, 180, 275 and 450°C after irradiation, the only exception being the "as - welded" TIG samples which exhibited higher strengths and lower ductilities. The impact properties of the welds were also similar to those of the base steel at test temperatures of 20, 180 and 450°C and their fracture resistances were not significantly impaired after these elevated temperature irradiations.

*References*

1. J.L. Séran et al, J. Nucl. Mater., 212 - 215 (1994) 588.

2. A. Alamo et al, Proc. 17th. ASTM Symp. on Effects of Irradiation on Materials, Sun Valley, Idaho, June 1994, ASTMSTP 1270 (1996), p. 761.

(v) Comparison of the radiation hardening data for MANET

The data on the effect of irradiation in BR2 [1] and HFR [2][3] on the proof and ultimate tensile strengths of the MANET I steel are presented in Table 1. Comparison of the results shows that:

(i) The 0.2 % proof and ultimate tensile strengths of the unirradiated steel determined in the tests at Mol [1] and ECN [2] were comparable and significantly lower than those of the steel tested at KfK [3].

(ii) The radiation hardening at 250°C / 5 dpa measured in the Mol tests [1] was significantly smaller than that determined by ECN [2] and much lower than that in the KfK tests at 300°C [3]. This conclusion was also applicable in the case of the Mol and KfK data after a dose of about 10 dpa.

(iii) The radiation hardening measured at 400°C after exposure to 5 and 10 dpa was much greater in the Mol [1] than in the KfK [3] tests. This was a consequence of the radiation hardening increasing with irradiation / test temperature in the Mol tests and decreasing in the KfK investigations.

(iv) These differences in behaviour may be associated with the differences in the prior history of the steel products tested, minor compositional variations, and differences in the heat treatments of the steels, in the initial tensile strain rates or a combination of these effects.

**Table 1: Effects of Neutron Irradiation on the Tensile Strengths of the MANET I Steel**

| Test Temp. °C | Irrad. Temp.°C | Strain Rate $s^{-1}$ | dpa | 0.2% PS MPa | ΔPS MPa | UTS MPa | ΔUTS MPa | Ref. |
|---|---|---|---|---|---|---|---|---|
| 250 | - | $2.7 \cdot 10^{-3}$ | - | 525 | - | 685 | - | [1] |
| 250 | - | $3 \cdot 10^{-4}$ | - | 560 | - | 670 | - | [2] |
| 300 | - | $1.7 \cdot 10^{-4}$ | - | 600 | - | 715 | - | [3] |
| 250 | 250 | $2.8 \cdot 10^{-3}$ | 5.1 | 725 | 200 | 840 | 155 | [1] |
| 250 | 250 | $2.8 \cdot 10^{-2}$ | 5.1 | 740 | | 845 | | [1] |
| 250 | 250 | $3 \cdot 10^{-4}$ | 5 | 930 | 370 | 980 | 310 | [2] |
| 300 | 300 | $1.7 \cdot 10^{-4}$ | 5 | 1.060 | 460 | 1.145 | 430 | [3] |
| 250 | 250 | $2.8 \cdot 10^{-3}$ | 9.3 | 870 | 345 | 940 | 255 | [1] |
| 250 | 250 | $2.8 \cdot 10^{-2}$ | 9.3 | 880 | | 950 | | [1] |
| 300 | 300 | $1.7 \cdot 10^{-4}$ | 10 | 1.075 | 475 | 1.152 | 437 | [3] |
| 400 | - | $2.7 \cdot 10^{-3}$ | - | 450 | - | 615 | - | [1] |
| 400 | - | $2.7 \cdot 10^{-2}$ | - | 445 | - | 605 | - | [1] |
| 400 | - | $1.7 \cdot 10^{-4}$ | - | 590 | - | 690 | - | [3] |
| 350 | - | $3 \cdot 10^{-4}$ | - | 540 | - | 625 | - | [2] |
| 450 | - | $3 \cdot 10^{-4}$ | - | 435 | - | 465 | - | [2] |
| 400 | 400 | $2.8 \cdot 10^{-3}$ | 4.9 | 820 | 370 | 915 | 300 | [1] |
| 400 | 400 | $2.8 \cdot 10^{-2}$ | 4.9 | 865 | 420 | 945 | 340 | [1] |
| 400 | 400 | $1.7 \cdot 10^{-4}$ | 5 | 750 | 160 | 855 | 165 | [3] |
| 400 | 400 | $2.8 \cdot 10^{-3}$ | 9.7 | 805 | 355 | 920 | 305 | [1] |
| 400 | 400 | $2.8 \cdot 10^{-2}$ | 9.7 | 930 | 485 | 1.000 | 395 | [1] |
| 400 | 400 | $1.7 \cdot 10^{-4}$ | 10 | 730 | 140 | 825 | 135 | [3] |
| 350 | 350 | $3 \cdot 10^{-4}$ | 10 | 970 | 430 | 1.010 | 385 | [2] |
| 450 | 450 | $3 \cdot 10^{-4}$ | 10 | 480 | 45 | 515 | 50 | [2] |

*References*

[1] W, Vandermeulen et al, Report FT / Mol / 92 - 05, December 1992.

[2] M.I. de Vries, ASTM Special Tech. Pubn. No. 1175, 1993, p.558.

[3] E. Materna - Morris and O. Romer, Proc. 18th. Symp. on Fusion Technology, Karlsruhe, Germany, August 1994, Vol. II, 1281, 1995.

## 2.3.2 Fatigue

### 2.3.2.1 Isothermal

(i) FZK

Strain controlled, low cycle fatigue tests have been conducted on solid hourglass shaped specimens of the quenched and tempered MANET I steel at temperatures in the range ambient to 650 C and total strain ranges ($\Delta\varepsilon_t$) of 0.4 - 1.0% , zero mean strain and strain rates of $3 \times 10^{-3}$ to $3 \times 10^{-5}$/s [1-3]. The endurances at high strain amplitudes ($\Delta\varepsilon_t = 1.5\%$) decreased by a factor of $\leq 2$ when increasing the test temperature from ambient to 650°C (Fig. 1); however, the effect of temperature was more pronounced at the lower strain ranges, the fatigue life for $\Delta\varepsilon_t = 0.6\%$ being about 1/3 at 650°C of the value at room temperature.

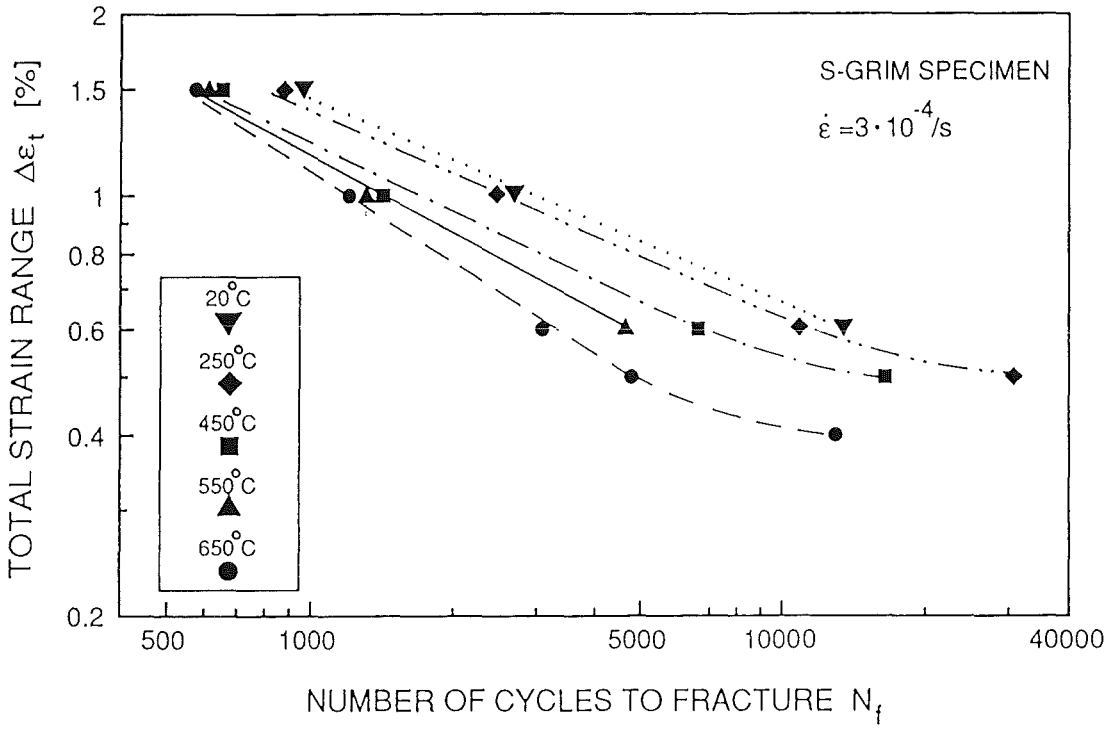


Fig. 1: Influence of test temperature on the low cycle fatigue endurance of the MANET I steel.

The fatigue endurances at 450°C were only slightly reduced on decreasing the strain rate from $3 \times 10^{-3}$ to $3 \times 10^{-4}$ and $3 \times 10^{-5}$ $s^{-1}$, thereby demonstrating that fatigue damage controlled the failure at this temperature; a reduction in the number of cycles to failure with decreasing strain rate was more evident in the tests at 650°C, particularly for 0.6%.

Experiments were also performed with hold times in tension or compression or in both phases of the cycles so as to ascertain the most damaging loading procedure [4][5]. The introduction of hold times of 1 to 30 minutes in the tension phase of the cycles in tests at 450 and 550°C and at a strain rate of 3 x $10^{-3}$ $s^{-1}$ had a negligible or only a small effect on the endurances for $\Delta\varepsilon_t$ = 0.6 and 1.0% . However, larger reductions in the number of cycles to failure, especially at the higher temperature of 550°C and the lower strain amplitude of 0.6%, were produced in the tests with the hold times in compression. But the lowest endurances were obtained with hold times in both tension and compression phases. This behaviour is exemplified by the results of the tests at 450°C in Fig. 2. Metallographic examinations of the fractured specimens tested at 550°C with the hold periods in tension showed characteristic fatigue striations whereas the compression hold time samples exhibited dimple type fractures.

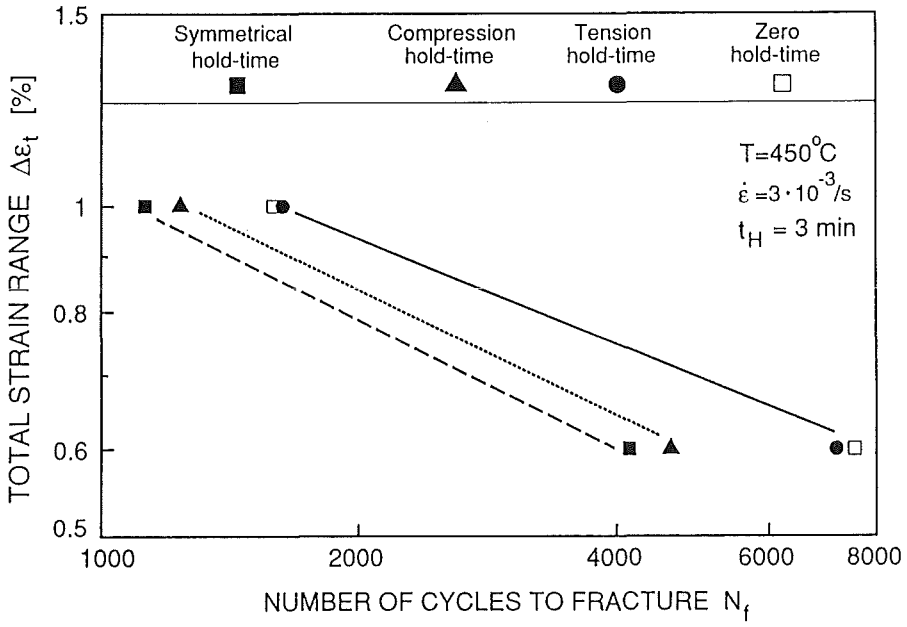


Fig. 2: Effect of hold periods on the number of cycles to failure of the MANET I steel at 450°C.

These test results have confirmed earlier observations [6][7] that hold times in compression were more damaging than in tension in the fatigue of high chromium martensitic steels. This behaviour contrasts with that of austenitic steels and has been attributed [7] to the fact that creep cracks or cavities are not

formed in ferritic / martensitic steels during either tensile or compressive holds and to the development of increasingly detrimental tensile mean stresses for the cycles following relaxation by thermal creep during the compressive holds. Systematic studies of the isothermal low cycle fatigue behaviour of the tempered 1.4914 steel in a broad temperature range and parallel investigations of microstructural changes allowed a comprehensive correlation between both properties [8]. This steel shows in the tempered condition a cycling softening under LCF conditions. This softening is caused by a transformation from the typical martensitic lath structure to a cellular dislocation arrangement, the size of cells being dependent on test temperature and plastic strain amplitude. REM investigations are revealing the onset of transcrystalline crack formation at slip bands of the specimen surfaces. Finally, also the effect of a dynamic strain ageing on the LCF behaviour of this material was shown.

(ii) SCK / CEN

Electropolished specimens of the MANET I steel in the 1075°C / 0.5 h + 750°C / 2 h reference heat treatment condition were irradiated at 250 and 400°C to 10 dpa (max.) in the BR2 reactor and subsequently tested in strain or load controlled fatigue at the irradiation temperature [9].

The endurances of the unirradiated and irradiated steels were marginally lower at 400°C than at 250°C, possibly due to the slightly smaller displacement doses (8.8-9.7 dpa) at 400°C compared to 250°C (9 - 10 dpa). For both irradiation / test temperatures, there was no detectable effect of the irradiation on the numbers of cycles to failure at the higher strain amplitudes (0.6 and 1.0 %) but the endurances at the lower strains (~0.4 %) were greater after irradiation. Irradiation at 250 and 400°C produced considerable hardening; however, significant softening occurred during the fatigue of the unirradiated and irradiated steels at the strain amplitude of ~1.0 % at 250 and 400°C but there was no measurable softening in the tests at lower strain ranges.

*References*

1. W. Baumgärtner et al, KfK, unpublished Report, December 1990.

2. W. Scheibe and R. Schmitt, Jahrestagung Kerntechnik, Nürnberg, May 1990, p. 597.

3. W. Baumgärtner, KfK, unpublished Report, June 1992.

4. Annual Report of the Association KfK / EURATOM, Oct. 91 - Sept. 92, KfK 5099, EUR 14795 EN, October 1992.

5. Annual Report of the Association KfK / EURATOM, Oct. 92 - Sept. 93, Kfk 5288, EUR 15466 EN, December 1993.

6. L. Lundberg and R. Sandstrom, Scand. J. of Metallurgy, 11 (1982) 85.

7. D.R. Harries, Rad. Effects, 101 (1987) 3.

8. R. Gersinska, Strukturuntersuchungen zum Ermüdungsverhalten des 12% Cr-Stahls 1.4914. KfK-Report 5069, Oktober 1992.

9. W. Vandermeulen et al, Report FT / Mol / 92 - 05, December 1992.

2.3.2.2 Thermal

The technique developed for investigating the effects of thermal cycling on the fatigue lives of the MANET I and II steels has been described elsewhere [1]. It consists essentially of a rigidly clamped and ohmically heated hollow specimen in which the longitudinal thermal elongation is converted into elastic or inelastic deformation and the alternating thermal stresses are generated by cycling between low ($T_L$) and high ($T_H$) temperatures [2]. The test conditions employed were: $T_L$ = 200°C (constant), $T_H$ = variable in the range 550 - 700°C, heating and cooling rates = 5.8 °C/s, total mechanical strain range = 0.2 - 0.8%.

Fig. 1 shows the thermal fatigue endurance, $N_f$, plotted as a function of the total mechanical strain range for the MANET I and II steel specimens tested at $T_H$ = 500, 600, 650 and 700°C and compared with the isothermal fatigue data generated in various European Fusion Association Laboratories. The $N_f$ values at the mean temperatures of the thermal fatigue (375 - 450°C) were more than an order of magnitude lower than those of the specimens tested in isothermal fatigue at approximately the same temperatures [3-5]; however, the number of thermal fatigue cycles to failure at a given strain range were only a factor of about two lower than the isothermal fatigue endurances at 650 - 700°C.

In addition, constant hold periods of 100 s were imposed at $T_H$ (HTH), at $T_L$ (HTL) or at both $T_H$ and $T_L$ (HTHL) during thermal fatigue tests on the MANET II steel [6]. The introduction of the hold times reduced the endurances, the magnitudes of the reductions increasing in the sequence HTL, HTH and HTHL as illustrated in Fig. 2 [7].

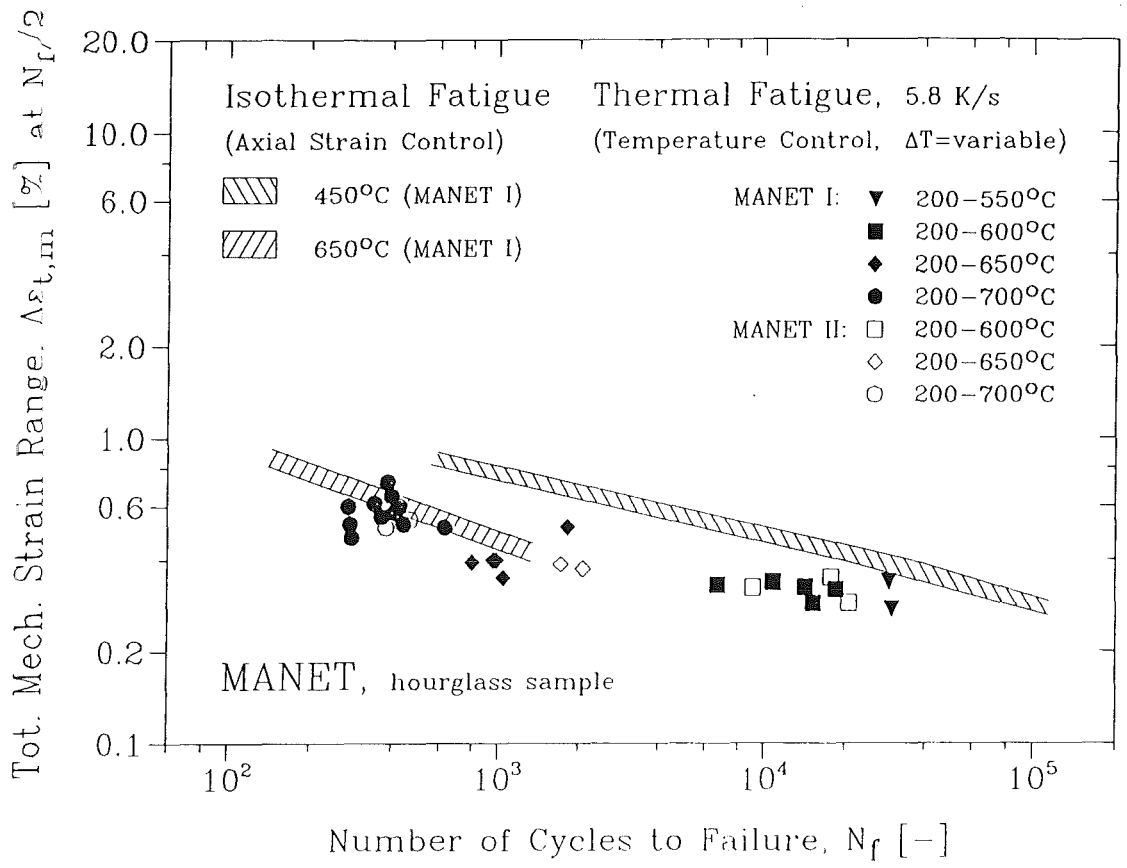


Fig. 1: Total mechanical strain versus number of cycles to failure of thermal fatigue tested MANET I and II steels and comparison with isothermal fatigue data.

The thermal fatigue tested MANET steel showed continuous softening after an initial stable period whose duration depended on $T_H$-$T_L$ and the nature of the temperature hold period imposed. Accelerated softening, due to enhanced recovery of the martensite lath dislocation structure and leading to lower endurances, was produced by increasing the magnitudes of the temperature cycles and by the introduction of the hold periods [8-11].

*References*

1. C. Petersen and G.H. Rubiolo, J. Nucl. Mater., 179 - 181 (1991) 488.

2. C. Petersen and I. Alvarez-Armas, Proc. 18th. Int. Symp. on Creep - Resistant Metallic Materials, Czechoslovak Sci. and Tech. Soc., (Ceske Budejovice), 1991, p. 245.

3. F. Wolter and C. Petersen, Proc. 12th. Int. Conf. on Structural Mechanics in Reactor Technology, Stuttgart, August 1993, Paper L01/2.

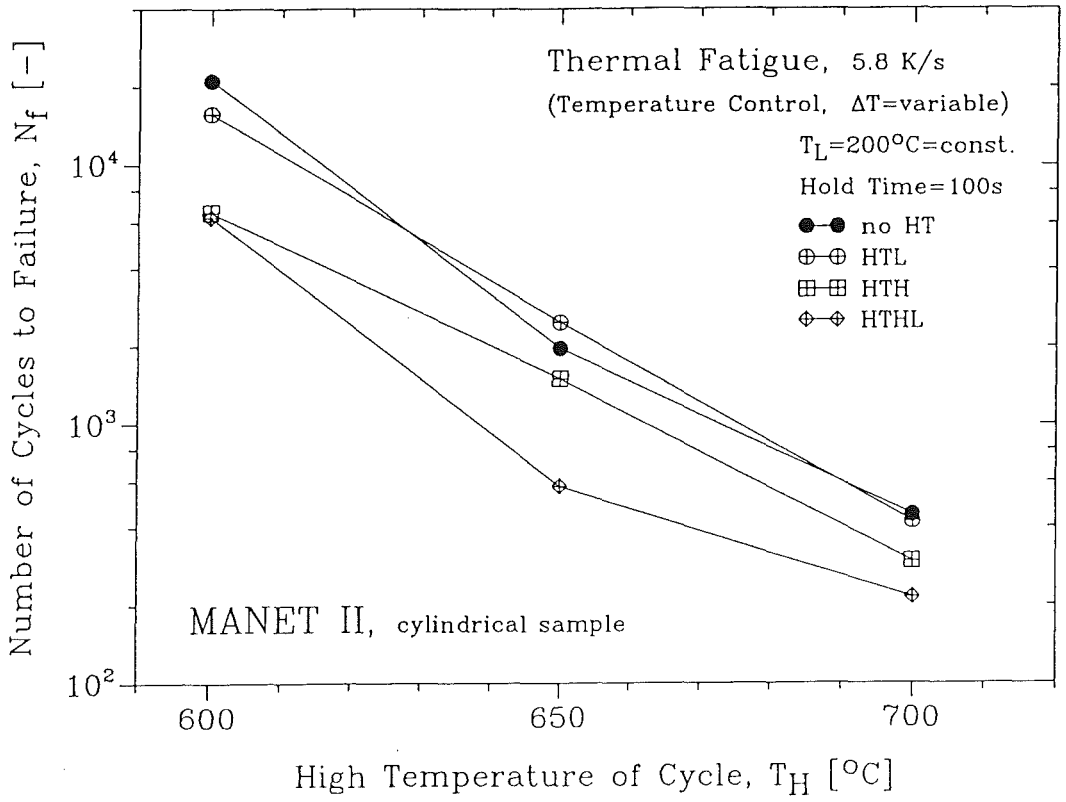


Fig. 2: Comparison of thermal fatigue data with and without hold periods for the MANET II steel.


4. C. Petersen and F. Wolter, Proc. MATEC 93, Paris - Marne la Vallee, December 1993, p. 157-162.

5. F. Wolter and C. Petersen, Proc. Annual Meeting on Nucl. Tech. '94, Stuttgart, May 1994, p. 493.

6. A.F. Armas, I. Alvarez-Armas and C. Petersen, Proc. 3rd. Int. Conf. on Low Cycle Fatigue and Elasto-Plastic Behaviour of Materials, Berlin, Sept. 1992, p. 275-280.

7. C. Petersen, J. Nucl. Mater., 212 - 215 (1994) 584.

8. I. Alvarez-Armas, A.F. Armas and C. Petersen, ibid, 191 - 194 (1992) 841.

9. I. Alvarez-Armas, A.F. Armas and C. Petersen, Proc. FATIGUE 93, Montreal, May 1993, J.-P. Bailon and J.I. Dickson, Eds., 1993, p. 903.

10. F. Wolter and C. Petersen, Proc. Annual Meeting on Nucl. Tech. '93, Cologne, May 1993, p. 401.

11. I. Alvarez-Armas, A.F. Armas and C. Petersen, Fatigue Fract. Engng. Struct., 17 (1994) 671.

### 2.3.3 Fatigue crack growth

Standard CR-1 compact tension specimens with a thickness of 50 mm and a width of 25 mm have been used to measure fatigue crack growth rates of the tempered ferritic/martensitic steel DIN 1.4914. Fig. 1 shows [1] the fatigue crack propagation rate at room temperature for the sub-critical (Paris) region II. This analysis also confirmed more recent investigations in various other materials, that the crack growth behaviour below about $10^{-5}$ mm/cycle (often defined as region I) is strongly correlated with microstructural details and cannot be described by a continuum mechanics approach which might be valid in the stable crack growth regime II. Investigations on CT-1 specimens made of the tempered MANET I steel showed under the same conditions very similar crack growth rates in the Paris region at room temperature and somewhat higher ones at 300°C [2].

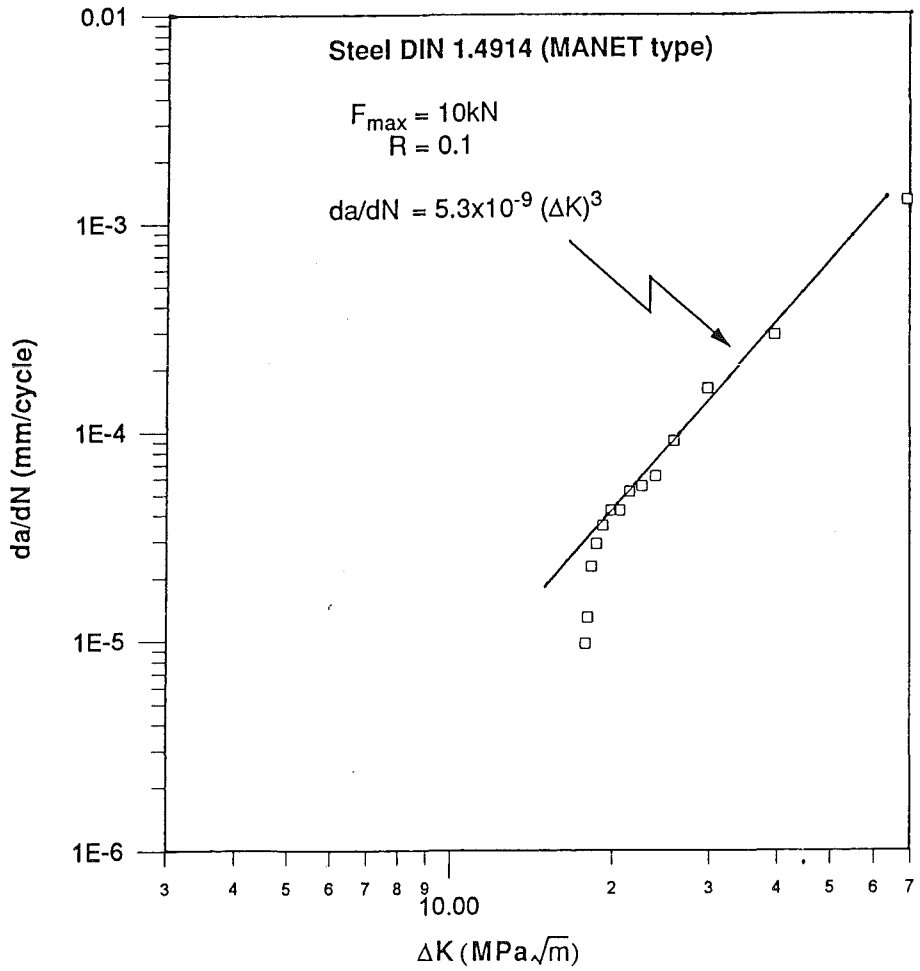


Fig. 1: Crack growth rate for the DIN 1.4914 steel in the sub-critical Paris region II at room temperature.

Small (W $\leq$24 mm) compact tension specimens of the quenched and tempered MANET I steel were irradiated to 0.5 - 10 dpa at 250°C and 10 dpa at 350 and 450°C in HFR. The crack propagation rates in both the unirradiated and irradiated steels were measured as a function of the stress intensity factor range (K) in the sub - critical (Paris) region II [3- 5].

The crack growth rates for the unirradiated steel specimens machined from plates ranging in thickness from 8 to 12 mm and tested at a frequency of 10 Hz at room temperature, 250 and 450°C and with R values of 0.05 - 0.3 increased markedly with test temperature but were not significantly affected by thermal ageing or dependent on the steel plate thickness [6].

The irradiated specimens could not be tested at ambient temperature because the large reduction in fracture toughness induced by the irradiation resulted in the fatigue crack growth curves exhibiting only regions I and III (that is, direct transition from threshold behaviour to critical crack growth) [6][7]. The crack propagation rates of the irradiated specimens at 250 and 450°C were only marginally different from those of the unirradiated thermal control samples (no more than a factor 2 - 3); thus, there was a small increase in the crack growth rate due to the irradiation at 250°C (Fig. 2) and a small reduction at high $\Delta K$ in the 450°C irradiated and tested samples [6][7]. However, there were large reductions of the Paris region (reduction of $\Delta K_{max}$) due to the strong decrease of fracture toughness at 250°C; this implies a reduction of the allowable fatigue loading and, even more so, a decrease in the permitted crack extension by fatigue ($\Delta K_{max} \leq 40$ MPa $\sqrt{m}$ ).

Most of the samples exhibited ductile failures but some brittle regions were often evident on the fracture surfaces of the 250°C irradiated and tested specimens.

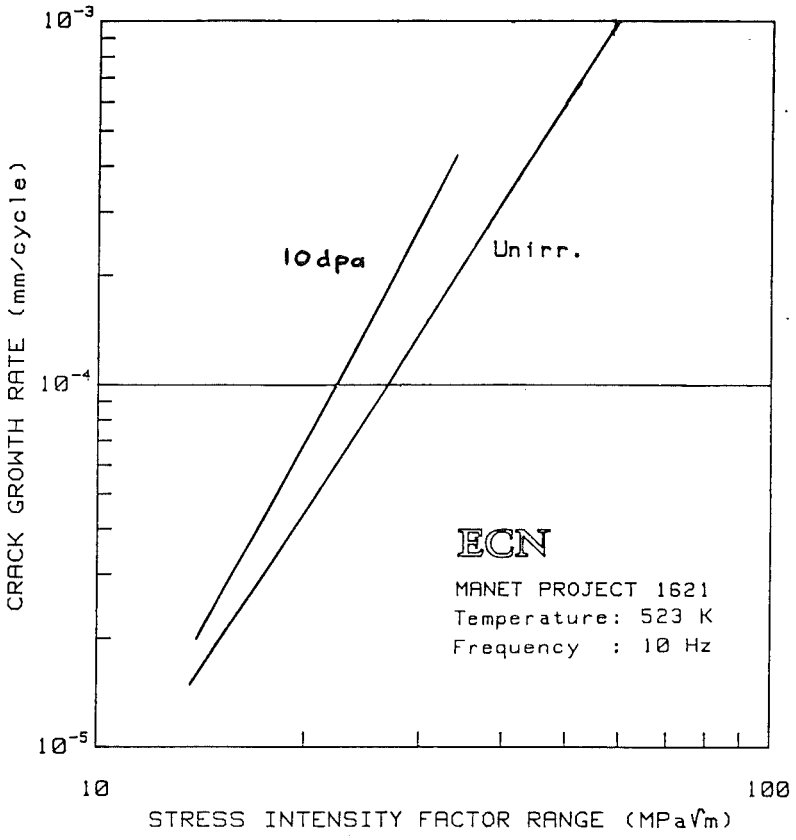


Fig. 2: Crack growth rate as a function of stress intensity factor range for the MANET I steel before and after irradiation to 10 dpa at 250°C.

*References*

1. F. Müller, Diploma thesis at University Karlsruhe, May 1994; "Experimentelle Ermittlung des Rißausbreitungsverhaltens verschiedener Werkstoffe mit Methoden der Bruchmechanik".

2. S. Müller, KfK Report 5334 (March 1994), P. 6.

3. H. Th. Klippel (Ed.), Progress Report 1990 on Fusion Technology Tasks, ECN Report C-91-035, June 1991.

4. H. Th. Klippel (Ed.), Progress Report 1991 on Fusion Technology Tasks, ECN Report C-92-049, June 1992.

5. N. van der Kleij (Ed.), Progress Report 1989 on Fusion Technology Tasks, ECN Report C-90-041, August 1990.

6. M.I. de Vries, Workshop on "Fatigue of Fusion Reactor Materials", Vevey, Switzerland, October 1991.

7. M.I. de Vries, ASTM Special Tech. Pubn. No. 1175, 1993, p. 558.

## 2.4 Pre-, in-situ and post irradiation mechanical properties and structure under ion beam irradiation

### 2.4.1 Tensile

The tensile properties of quenched and tempered 1.4914 and/or the MANET I steel, initially in the reference heat treated condition, have been extensively studied after irradiation using: (i) A light ion simulation technique at KFA, in which 0.1 mm thick specimens were homoeneously implanted with helium by 28 MeV α-particle bombardment, (ii) The Dual Beam facility at KfK [1] in which 0.2 mm thick specimens have been bombarded with degraded 104 MeV α-particle and 30 MeV proton beams to vary the helium and hydrogen generation rates and enable helium to displacement per atom ratios in the range 10 to 2,000 appm He per dpa to be achieved, and (iii) The PIREX facility at PSI [2] which utilises a 590 MeV proton beam; protons of this energy produce displacement damage and helium and hydrogen isotopes by spallation reactions, resulting in a ratio of ~130 appm He per dpa in 0.3 mm thick tensile specimens.

Tests at ambient and elevated temperatures ( 20 - 700°C [3][4] and 300 - 720°C [5] ) following α-particle bombardment to 100 appm helium in the KFA and Dual Beam facilities respectively did not show any significant changes in the tensile strengths and ductilities compared to the non - implanted samples, the fractures being ductile and transgranular.

Specimens were also homogeneously implanted in the Dual Beam facility with up to 500 appm helium and/or 500 appm hydrogen at temperatures between 80 and 500°C and then tensile tested to establish the temperature dependency and the individual and combined influences of the displacement damage and implanted helium and hydrogen on the radiation hardening (increases in tensile yield and ultimate strengths) and embrittlement (reductions in uniform and total elongations to failure) [5-7]. The yield stresses and total elongations are plotted as a function of the irradiation / test temperature in Figs. 1 and 2 respectively. These results illustrate that:

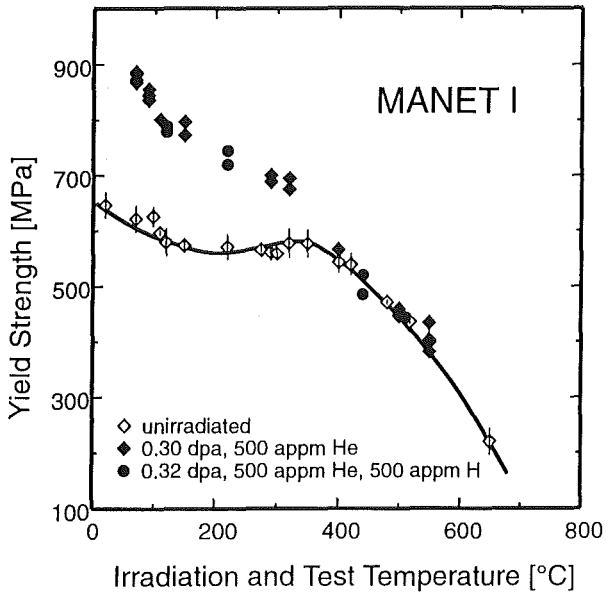


Fig. 1:
Temperature dependence of the yield stress of the MANET I steel in the range 20 to 620°C before and after irradiation in the Dual Beam facility, showing the effects of helium, hydrogen and displacement damage.

(a) Significant radiation hardening occurred below ≤400°C; both the unirradiated and implanted samples showed marked softening and little or no effect of the implantation on the tensile strengths at higher temperatures. The yield and ultimate tensile strengths were similar to those produced by neutron irradiation of the steel to comparable displacement doses / temperatures in HFR (see section 2.3.1.); the helium concentrations produced in the steel in the HFR irradiations were relatively low and the implantation - induced increases in tensile strengths were therefore attributed to displacement damage rather than helium effects.

(b) The reductions in both the uniform and total elongations at irradiation / test temperatures of ≤400°C were modest except at temperatures of 250 - 350°C. Serrations in the stress - strain curves, indicative for dynamic strain ageing (DSA), were evident on testing at these latter temperatures; the yield stresses were increased to values approaching the ultimate tensile strengths after irradiation, with the uniform and total elongations to failure being reduced to ≤0.3 and 2 - 3 % respectively. However, the fractures of the helium and hydrogen implanted

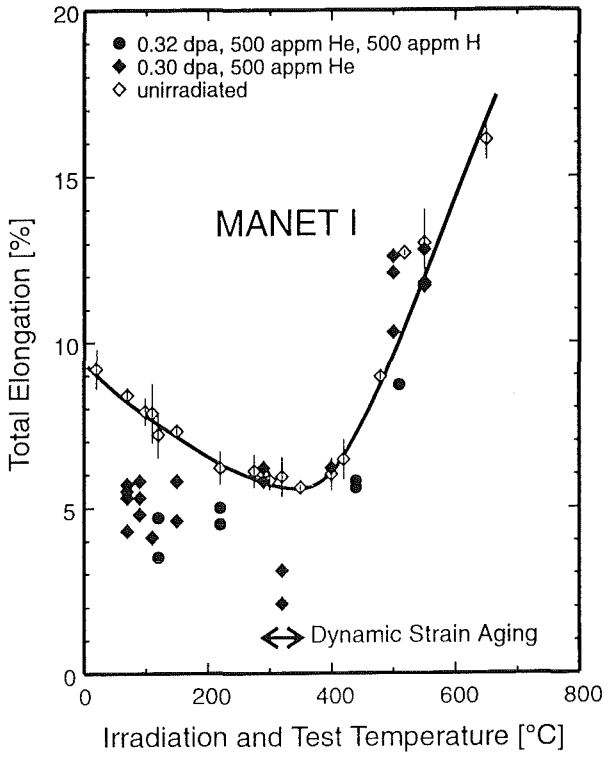


Fig. 2:
Influence of helium, hydrogen and displacement damage produced by irradiation in the Dual Beam facility on the total elongations of the MANET I steel at temperatures in the range 20 to 620°C.

specimens remained ductile and transgranular under all irradiation / test conditions. Comparison of these data with the results obtained on the steel samples irradiated to similar displacement doses in HFR suggested that the tensile ductilities were dependent, at least partially, on the implanted helium concentrations.

(c) Implantation with $\leq$500 appm hydrogen had little or no effect on the tensile strengths and ductilities at temperatures above 100°C, due possibly to the rapid loss of hydrogen by diffusion from the test pieces.

The steel also showed radiation hardening at ambient temperature following proton irradiation at 170°C in PIREX (Fig. 3) [8][9]; the magnitudes of the hardening decreased at higher irradiation / test temperatures, but there was some remnant hardening even after exposure at 420°C. The yield stress values were comparable to those measured following irradiation to similar displacement doses (0.3 - 0.4 dpa) but to a higher helium concentration of 500 appm in the Dual Beam

facility and also after the relevant reactor exposure. These results again imply that the displacement damage determined the strength properties whilst the helium appeared to be effective in reducing the ductilities at temperatures of 400°C.

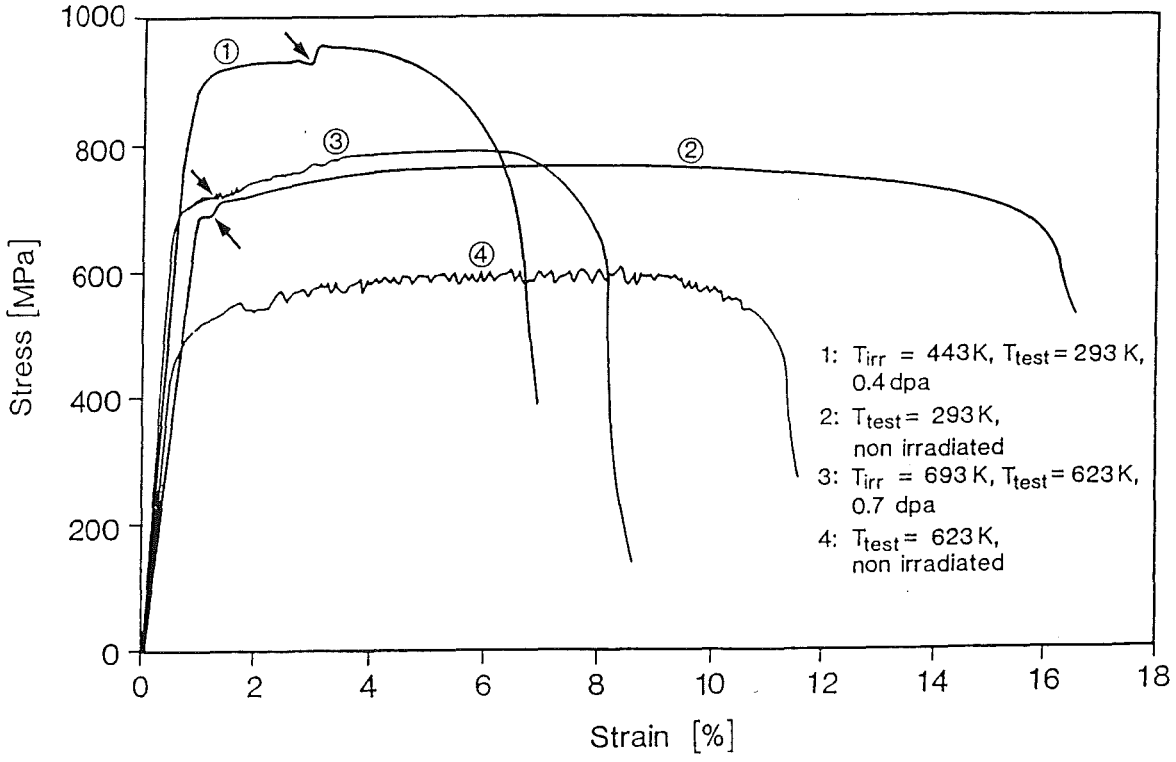


Fig. 3: Temperature dependence of the tensile stress - strain curves of the unirradiated and PIREX irradiated MANET I steel under several test conditions.

Serrations in the stress - strain curves and other characteristics of the DSA have been found under various test conditions [6][10][11]. The serrated yielding was less prounced after irradiation than in the unirradiated steel [6][9][10] but the strain rate sensitivity was still negative [9]. Furthermore, the measured thermal activation parameters suggested that the mechanism of the DSA was not modified by the displacement damage or helium implantation [11].

*References*

1. A. Möslang, S. Cierjacks and R. Lindau, Proc, 12th Int. Conf. on Cyclotrons and their Applications, May 1989, Berlin, B. Martin and K. Ziegler, Eds., World Scientific, London, 1991, p.545.
2. P. Marmy et al, Nucl. Instr. and Methods in Phys. Res., B47 (1989) 37.
3. U. Stamm and H. Schroeder, J. Nucl. Mater., 155 - 157 (1988) 1059.
4. H. Schroeder, KfA Report Jul - 2454, March 1991.
5. A. Möslang and D. Preininger, J. Nucl. Mater., 155 - 157 (1988) 1064.
6. K.K. Bae, K. Ehrlich and A. Möslang, ibid, 191 - 194 (1992) 905.
7. K.K. Bae, K. Ehrlich and A. Möslang, KfK, unpublished Report, 1990.
8. P. Marmy and M. Victoria, J. Nucl. Mater., 191 - 194 (1992) 862.
9. P. Marmy and M. Victoria, Proc. ICSMA - 9, D.G. Brandon, R. Chaim and A. Rosen, Eds., 1991, p.841.
10. P. Marmy, Y. Ruan and M. Victoria, J. Nucl Mater., 179 - 181 (1991) 697.
11. P. Marmy, J.L. Martin and M. Victoria, Stress Relaxation Tests of a Ferritic/Martensitic Steel before and after Irradiation, Plasma Devices and Operations, 1994, Vol. 3, pp. 49-63.

### 2.4.2 Creep and creep rupture properties

High temperature thermal creep - rupture tests at 600 and 700°C were conducted on the high chromium martensitic steels before and after helium implantation at the same temperatures to concentrations of 100 to 1000 appm by 28 MeV α-particle bombardment in the Jülich compact cyclotron [1]; in addition, "in - beam" creep - rupture tests at 600 and 700°C were performed with homogeneous implantation of up to 3000 appm helium [1 - 3].

High temperature implantation of 100 appm helium had no influence on the post - implantation creep - rupture properties of the MANET I steel at 600 and 700 C. However, higher helium concentrations of up to 1000 appm led to markedly reduced creep rates, indicative of hardening by the implantation, and to reduced rupture elongations, particularly at 700°C; nevertheless, the rupture times were increased relative to those of the unirradiated controls. Broadly similar observations were made in the "in - beam" tests, that is, no major detrimental influence of the implanted helium on the rupture lives and ductilities; the fractures were

ductile and transgranular and only with 3000 appm implanted helium there was any indication of cracking along the prior austenite grain boundaries.

Analysis of these creep rupture data and associated TEM observations [4], together with a comparison of the results with those for austenitic steels and model alloys, have indicated the reason for the excellent resistance of the high chromium martensitic steels to high temperature grain boundary (helium) embrittlement [5]. The helium bubble sizes and densities in the matrix and grain boundaries of the MANET steel were comparable to those in the irradiated austenitic steels, which show significant embrittlement at high temperatures following irradiation. However, in contrast to the austenitic steels, the relatively weak matrix of the MANET steel at the higher temperatures does not allow high stresses to be developed at the prior austenite grain boundaries. The critical radius ($r_c$) for catastrophic growth of the intergranular helium bubbles, leading to premature grain boundary fracture, is inversely proportional to the applied tensile stress ($\sigma$) and is large in this material; a very high helium concentration and/or long times would therefore be required to reach it. Consequently, no large helium effects were observable in the MANET steel, at least in the parameter ranges investigated [3].

The creep rates of the 1.4914 and MANET I martensitic steels under 6.2 MeV proton irradiation at displacement damage rates of $\leq 4 \times 10^{-6}$ dpa s, temperatures in the range 400 to 540°C and tensile stresses of up to 480 MPa have also been determined in the Jülich compact cyclotron and showed no enhancement compared to thermal creep [6]. The 1.4914 and MANET I steels differed slightly in composition (mainly in the nitrogen contents, 0.012 and 0.034 % respectively) and the former showed significantly higher creep rates with and without irradiation. Pulsed irradiation did not influence the deformation [7] but stress changes during the "in - beam" tests resulted in prolonged transients as observed in thermal creep; this implies that the apparent stress dependence of the creep under non - stationary conditions may be significantly lower than at constant stress [8]. A contraction against the applied uniaxial load at low doses and a linear decrease in the electrical resistivity were also observed in tests at a low stress of 50 MPa at 520°C under irradiation but not during thermal creep [9]; these effects may be attributed to the irradiation - induced micro - chemical and - structural changes revealed by analytical electron microscopy with, for example, enrichment by factors of up to seven in the Si, P and Mn contents of existing $M_{23}C_6$ particles being found [10].

*References*

1. U. Stamm, KFA Report Jul 2225, August 1988.
2. U. Stamm and H. Schroeder, J. Nucl. Mater., 155 - 157 (1988) 1059.
3. H. Schroeder and H. Ullmaier, ibid, 179 - 181 (1991) 118.
4. H. Schroeder, KfA Report Jul 2454, March 1991.
5. H. Ullmaier and H. Trinkaus, Mater. Sci. Forum, 97 - 99 (1992) 451.
6. P. Jung and N.M. Afify, J. Nucl. Mater., 155 - 157 (1988) 1019.
7. P. Jung and H. Klein, ibid, 202 (1993) 222.
8. P. Jung, KfA Report Jul - Spez - 468 (1988) ISSN 0343 - 7639.
9. P. Jung, J. Nucl. Mater., 179 - 181 (1991) 745.
10. P. Jung and H. Klein, ibid, 182 (1991) 1.

### 2.4.3 Fatigue and creep - fatigue

The fatigue and creep - fatigue properties and behaviour of the MANET I and / or II steels in high vacuum and under various push - pull conditions have been investigated before, during and / or after irradiation with plasma particles in the TEXTOR tokamak at KFA [1] and with light ions in the facilities at KfK [2] and PSI [3]. These studies were carried out in support of the reactor irradiation experiments, the primary objectives being to establish: (i) The individual and combined influence of displacement damage and implanted helium and hydrogen on the fatigue, and (ii) The effects of stress relaxation by irradiation creep or irradiation modified thermal creep on the cyclic endurance.

Surface modifications produced by plasma discharges (about 1500 shots each of approximately 3 s duration at temperatures of 150 - 300°C) in the TEXTOR Tokamak had no significant effect on the post - exposure fatigue endurance of the MANET II steel in load controlled tests at 250 and 450°C [1]; this contrasted with the behaviour of Type 316L austenitic steel which showed a factor of eight reduction in the numbers of cycles to failure under the same experimental conditions [4].

The KfK Dual Beam irradiations for the post - irradiation fatigue tests on the MANET I steel were performed at temperatures in the range 300 to 600°C to displacement damage levels and helium concentrations of $\leq$1.2 dpa and $\leq$200 appm respectively and with helium to dpa ratios of 10 - 250; the strain-controlled push

pull tests were carried out in air at the same temperature as the irradiation, at a strain rate of 5 x $10^{-4}$ $s^{-1}$, total strain range of 1.2% and with and without hold times of 120 s in the tension or compression phase. The principal observations were as follows [5][6]:

(a) All the samples tested showed continuous cyclic softening, due to the recovery of the lath dislocations and the formation of distinct cell structures, with the slopes of the stress amplitudes being similar for both the unirradiated and irradiated specimens; the stress amplitudes were increased by irradiation / testing at 300°C, were unaffected at 450 C and reduced slightly at 520 and 600°C. The helium to dpa ratio had only a small effect on the endurance at 450°C.

(b) The introduction of hold times at peak tensile and compressive strains resulted in stress relaxation of 70 - 80 MPa and decreases in the endurance of the unirradiated steel by 35 - 40 and 15 - 20 % respectively at 450°C. The influence of the implanted helium and displacement damage on the fatigue endurance at all temperatures in the range 300 - 600°C was small ($\leq$30 %), even when the hold times were introduced.

Continuous, strain controlled push-pull (R = - 1) fatigue tests were also performed in the Dual Beam facility at 420°C and at total strain ranges of 0.5 - 1.0 % [7][8]. The fatigue lives were comparable to those of the unirradiated reference specimens at high strain amplitudes ($\Delta\varepsilon_t > 0.6$ %). However, at $\Delta\varepsilon_t = 0.5$ % the mean endurance for the unirradiated reference samples was about 80 x $10^3$, whereas the number of cycles to failure "in beam" was 42 x $10^3$ with an accumulated helium concentration and displacement damage of 400 appm and 1.6 dpa respectively; the latter was a factor of seven higher than that of the corresponding post - irradiation tested sample (6 x $10^3$ cycles) with equivalent helium and damage levels (Fig. 1). It may be concluded from these data that the endurance was determined by the time evolution of the irradiation - induced hardening and that the post - irradiation test results provided a conservative approach to "in situ" conditions. The introduction of the 120 s hold periods in tension and compression produced no significant effect, again demonstrating that the endurance was determined by fatigue and not creep damage.

The rupture mode remained ductile and transcrystalline for all irradiation / test conditions.

The low cycle fatigue endurance was likewise reduced following the proton irradiation in PIREX, particularly in the temperature range of DSA between 280 and 380°C [9]; thus, there was a reduction by a factor of 7.5 in the endurance at 350°C after irradiation to a displacement dose of 0.55 dpa and a helium concentration

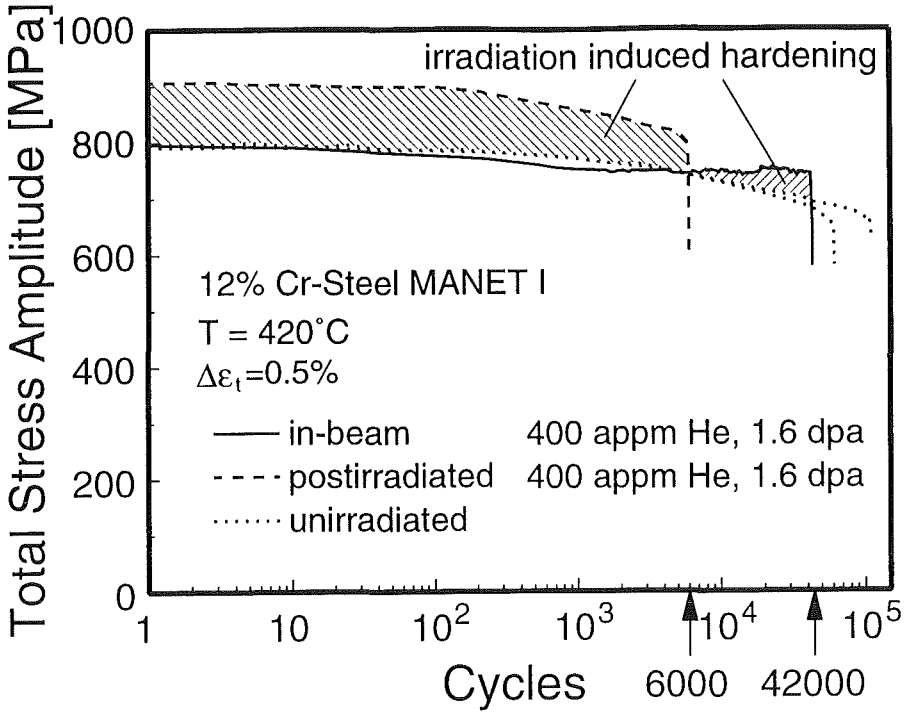


Fig. 1: Development of the total stress amplitude during the strain controlled in - beam, postirradiation and unirradiated fatigue testing; Dual - Beam facility, test and irradiation temperature = 420°C, MANET I steel.

of about 72 appm at 370°C [9][10]. Fatigue softening was observed under all test conditions, with the irradiated steel exhibiting a faster softening rate and approaching that of the unirradiated steel at the end of life.

"In - beam" strain controlled fatigue tests have also been conducted on the MANET II steel under 590 MeV proton bombardment in the PIREX facility with an imposed total strain amplitude of 0.7 % and at test temperatures of 35 - 40, 250 and 300°C [11][12].

The endurance of the "in - beam" specimen tested at 300 C was 4660 cycles with an end - of - life displacement dose of 0.17 dpa; this endurance was about forty per cent lower than that for unirradiated specimens (mean $N_f$ = 8,400 cycles) but a factor of approximately three greater than for the corresponding post - irradiation tested samples (mean $N_f$ = 1,460) [Fig. 2]. Significant radiation hardening was produced in the post - irradiation (0.26 dpa) tested specimens but not during the in - beam testing; fatigue softening occurred at a comparable rate in the unirradiated and in - beam tests, but the rate of softening was considerably faster in the post - irradiation tested specimens. Preliminary microstructural observa-

tions have confirmed that a relatively high dislocation density was maintained during the in - beam testing as the martensite lath dislocations did not recover to form a cell structure as rapidly as in the post - irradiation tests.

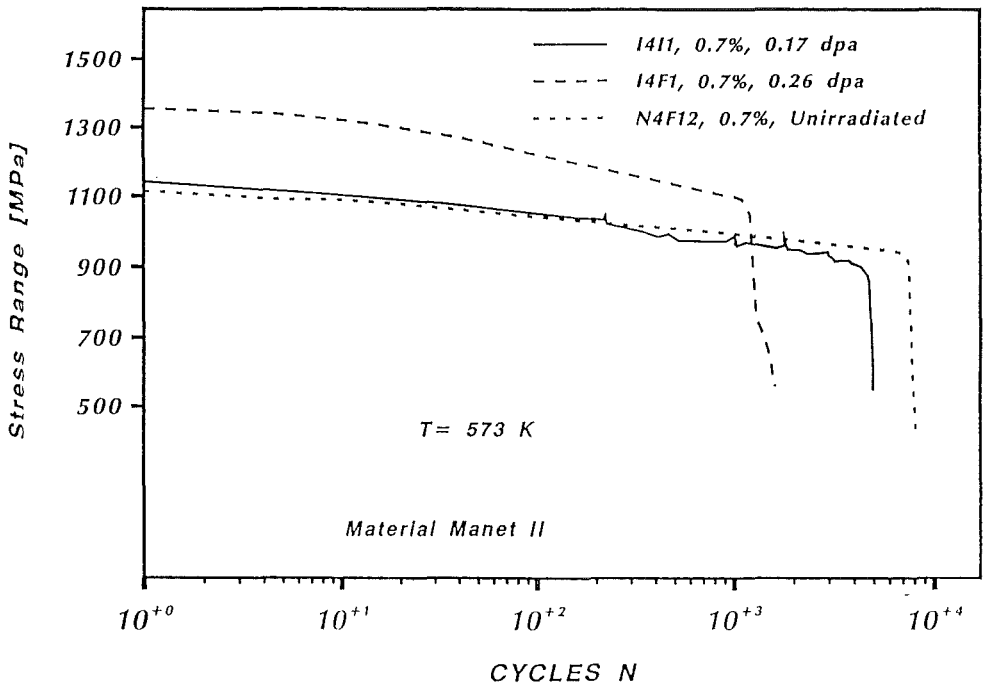


Fig. 2: Stress range as a function of the number of fatigue cycles for the in - beam (0,17 dpa), post - irradiation and unirradiated conditions; PIREX facility, test and irradiation temperature = 300°C, MANET II steel.

The endurances of the in - beam specimens were decreased on reducing the test temperature from 300°C (4,660 cycles) to 250°C (1,500) and to 35 - 40°C (1,100) [Fig. 3]; the maximum radiation hardening was produced in the lowest temperature test.

Stress relaxation tests performed during the in - beam and post - irradiation fatigue testing at 35 - 40°C showed a logarithmic recovery with time, implying that the deformation was controlled by a thermally activated dislocation glide process for which an activation volume could be defined. The available data suggested that the glide mechanism was not modified during the in - beam tests.

These post - irradiation and in - beam fatigue data and observations confirm that radiation hardening was principally responsible for controlling the endurances.

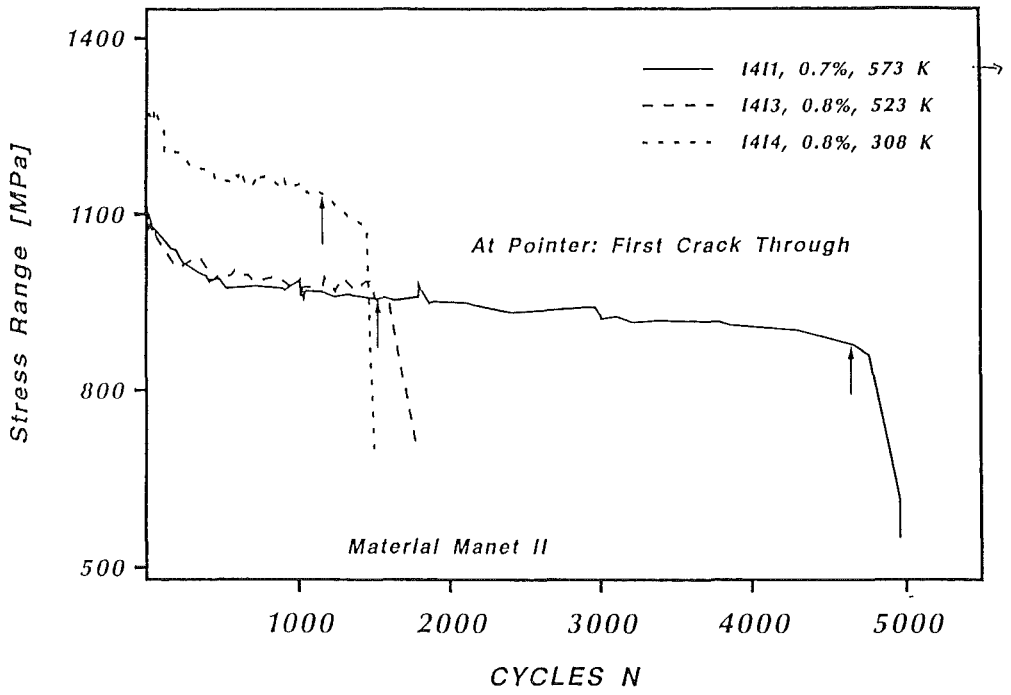


Fig. 3: Effect of test temperature on the in - beam stress development and fatigue endurance of the MANET II steel; PIREX facility.

***References***

1. J.I. Shakib et al, J. Nucl. Mater., 191 - 194 (1992) 1404.
2. A. Möslang, S. Cierjacks and R. Lindau, Proc. 12th. Int. Conf. on Cyclotrons and Their Applications, Berlin, May 1989, B. Martin and K. Ziegler, Eds., World Scientific, London, 1991, p.545.
3. P. Marmy et al, Nucl. Instr. and Methods in Phys. Res., B47 (1989) 37.
4. H. Ullmaier and N. Schmitz, J. Nucl. Mater., 169 (1989) 233.
5. R. Lindau and A. Möslang, ibid, 179 - 181 (1991) 753.
6. R. Lindau and A. Möslang, ibid, 191 - 194 (1992) 915.
7. A. Möslang et al, Proc. 17th. Symp. on Fusion Tech., C. Ferro, M. Gasparotto and H. Knoepfel, Eds., North - Holland, 1993, p.1439.
8. R. Lindau and A. Möslang, J. Nucl. Mater., 212 - 215 (1994) 599.

9. P. Marmy and M. Victoria, Proc. ICSMA - 9, D.G. Brandon, R. Chaim and A. Rosen, Eds., 1991, p.841.

10. P. Marmy and M. Victoria, J. Nucl. Mater., 191 - 194 (1992) 862.

11. P. Marmy, ibid, 212 - 215 (1994) 594.

12. P. Marmy, In-Beam Fatigue of a Ferritic/Martensitic Steel, Plasma Devices and Operations, 1996, Vol. 4, pp. 211-219.

## 2.5 Microchemical and microstructural stability

### 2.5.1 Structural stability

The individual and combined effects of the displacement damage and helium produced by 14 MeV neutrons have been simulated by charged particle irradiation at elevated temperatures in single - and dual - beam accelerator facilities and the effects on the microstructures and void swelling of the MANET steel and laser and electron beam welds examined by TEM [1 - 4] and atom probe field ion microscopy (APFIM) [3][4].

The observations have confirmed that the base steel, welds and heat - affected - zones were resistant to void swelling when irradiated with 500 keV $Fe^+$ and 20 keV $He^+$ ions to produce 100 dpa and 1000 appm helium at temperatures in the range 400 to 550°C [2]. Also, small, roughly spherical cavities, approximately 2.7 nm diameter and in concentrations of about $4 \times 10^{22}$ $m^{-3}$, resulting in swelling of 0.04 % , were resolved in the MANET steel after simultaneous irradiation with 300 keV $Fe^+$ and 15 keV $He^+$ ions to 50 dpa and 1200 appm helium at 500°C [3]. Inter- and intra - granular $M_{23}C_6$ type precipitates were resolved by TEM and regions rich in Cr, Mo and C, identified by APFIM in both the as - quenched and tempered and irradiated MANET steel [3]; regions rich in Cr, N and Si were also detected by APFIM in the irradiated steel [4].

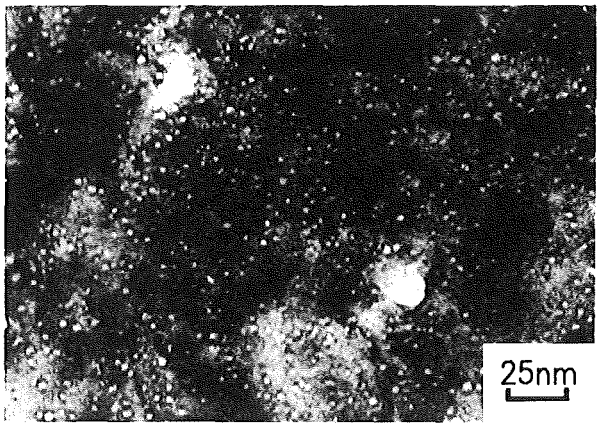


Fig. 1:
Transmission electron micrograph of MANET steel simultaneously irradiated with 300 keV Fe- and 15 keV He-ions to 50 dpa and 1200 appm helium [3].

*References*

1. M.D. Wiggins, Studsvik Report NS-88/347, July 1988.

2. D. Gilbon and C. Rivera, CEA Report N.T. SRMA 90.1822, April 1990.

3. P. Dauben, R.P. Wahi and H. Wollenberger, J. Nucl. Mater., 133-134 (1985) 619.

4. N. Wanderka and R.P. Wahi. App. Surf. Sci., 76/77 (1994) 272.

### 2.5.2 Interfacial segregation

Interfacial elemental segregation in metals and alloys can occur by several processes:

(i) Equilibrium segregation to free surfaces and grain boundaries, the driving force being the minimisation of the free energy of the system when misfitting atoms diffuse from the matrix to the more accommodating sites at the interfaces.

(ii) Stress - driven segregation, resulting from the interaction between the stress field of a loaded crack and solute atoms in the matrix. This interaction imposes a drift flow of under- and oversized solutes which determines their migration in the vicinity of the crack tip; thus, enhanced segregation to the crack as well as to the grain boundary ahead of the crack may occur. A kinetic model of this process

[1] has provided a satisfactory explanation of the stress - relief cracking within the heat - affected - zones of low alloy steel welds at 300 - 650°C due to the stress - driven segregation of sulphur [2][3].

(iii) Non - equilibrium segregation resulting from the formation of solute atom - thermal vacancy complexes at high temperatures and the diffusion of these mobile clusters during cooling to the free surfaces and grain boundaries, where the vacancies are annihilated [4][5]. Thus, strong segregation of silicon near the martensite lath boundaries in a 1.4914 (10.5% Cr - MoVNb) steel after quenching from 1075°C has been detected by field emission gun scanning transmission electron microscopy (FEG - STEM), the maximum segregation being produced at a cooling rate of 50°C/s [6].

Non - equilibrium segregation, termed Radiation - Induced Segregation (RIS), may also be produced during irradiation. It has been postulated to occur because some solutes interact strongly with the (vacancy) point defects generated during irradiation, resulting in coupled transport of the solute atoms by the point defect fluxes to and away from sinks such as grain boundaries, void surfaces, etc. Other (substitutional) solutes may segregate by the Inverse Kirkendall Effect, whereby the faster diffusing species exchange more often with the vacancies migrating to sinks than slow diffusing species; the fast diffusing solutes are therefore depleted at sinks whilst the concentrations of the slowest diffusing species increase. The RIS has been modelled by several authors (see, for example, [7 - 9]) and the theoretical work and experimental observations reviewed [10 - 12, 17].

The early work on RIS was carried out almost exclusively on face - centred - cubic alloy systems such as austenitic steels and it was established that extensive local changes in chemical composition could occur leading to microstructural instability. However, increasing attention has recently been devoted to the body - centred - cubic iron and steels; thus, experimental observations and quantitative analyses of the segregation at the prior austenite grain and martensite lath boundaries in neutron irradiated HT-9 (12% Cr - MoVW) [13] and FV448 (11% Cr - MoVNb) [14][15] martensitic steels (see, for example, Fig. 1), matrix/precipitate interfaces in ion irradiated 1.4914 steel [16], and grain boundaries in 1 MeV electron and heavy ion irradiated Fe - 12% Cr - X alloys [17] have now been made by Auger Electron Spectroscopy (AES) or FEG - STEM techniques. Whilst the observations on the ferritic / martensitic steels were not completely unambiguous, it has been concluded [12] that the RIS was markedly dependent on the displacement dose and the irradiation temperature in the approximate range 300 to 625°C and that: (a) Cr was generally depleted from interfaces, (b) Ni, Si and P were always

enriched at sinks, and (c) Mo and Mn may either be enriched or depleted at sinks. It is believed that Si and Ni segregated by the first of the mechanisms referred to above, whilst Cr and Fe were depleted at interfaces as a result of the Inverse Kirkendall Effect [18].

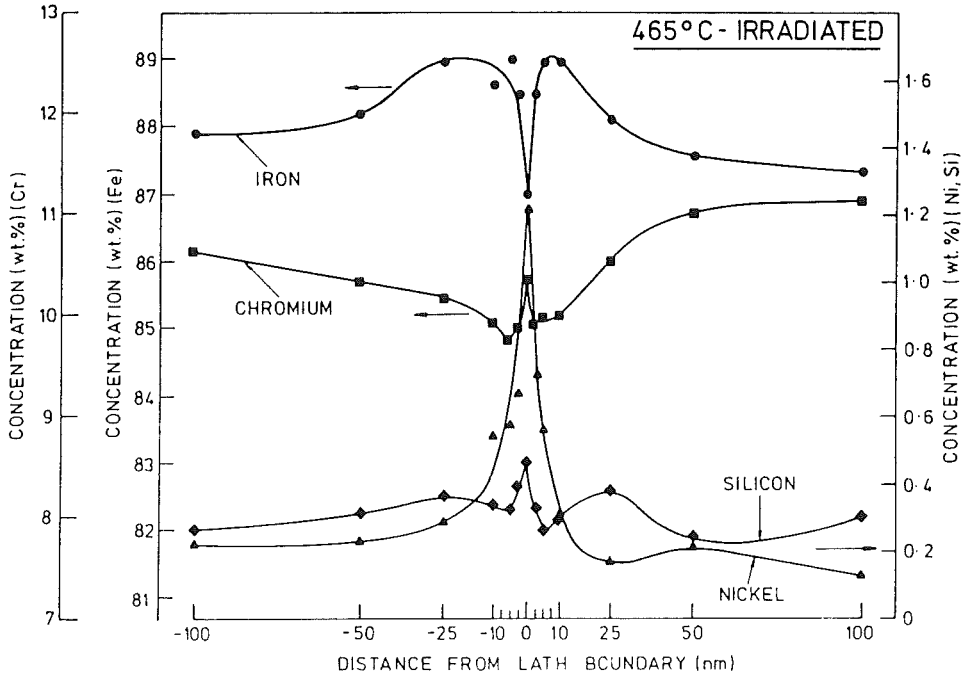


Fig. 1: Typical concentration gradients for Cr, Ni, Si and Fe on either side of a martensite lath boundary in FV448 steel irradiated at 465°C to 46 dpa [14].

*References*

1. H. Rauh, AERE Harwell Report R 13735.
2. C.A. Hippsley, H. Rauh and R. Bullough, Acta Met., 32 (1984) 1381.
3. H. Rauh, C.A. Hippsley and R. Bullough, ibid, 37 (1989) 269.
4. T.M. Williams, A.M. Stoneham and D.R. Harries, Met. Sci., 10 (1976) 14.
5. D.R. Harries and A.D. Marwick, Phil. Trans. Roy. Soc., A295 (1980) 197.
6. R.G. Faulkner et al, J.Nucl. Mater., 155 - 157 (1988) 612.
7. T.R. Anthony, "Diffusion in Solids: Recent Developments", A.S. Nowick and J.J. Burton, Eds., Academic Press (Mat. Sci. Series), 1975, p.365.
8. A.D. Marwick, J. Phys. F. Metal Physics, 8 (1978) 1849.
9. A.D. Marwick, R.C. Piller and M.E. Horton, AERE Report R 10895, 1983.

10. H. Wiedersich and N.Q. Lam, "Phase Transformations during Irradiation", F.V. Nolfi, Ed., Applied Sci. Pub., 1983, p.1.

11. C.A. English, S.M. Murphy and J.M. Perks, J. Chem. Soc. Faraday Trans., 86 (1990) 1263.

12. E.A. Little, J. Nucl. Mater., 206 (1993) 324.

13. R.E. Clausing et al, ibid, 141-143 (1986) 978.

14. T.S. Morgan et al, ASTM Special Technical Pubn. 1125, 1992, p.633.

15. T.S. Morgan et al, ASTM Special Technical Pubn. 1175, 1993.

16. P. Jung and H. Klein, J. Nucl. Mater., 182 (1991) 1.

17. G.J. Mahon et al, Proc. Symp. on "Radiation - Induced Sensitisation of Stainless Steels", Berkeley Nucl. Labs., September 1986, D.I.R. Norris, Ed., CEGB, p.99.

18. P.R. Okamoto and L.E. Rehn, J. Nucl. Mater. 83 (1979) 2.

## 2.6 Compatibilities with coolant, breeding and neutron multiplier materials

### 2.6.1 Aqueous corrosion and stress corrosion cracking susceptibility

(i) UKAEA

Specimens in the form of discs, approximately 19 mm diameter and 0.5 mm thick, were machined from ~20 mm diameter bars of FV448 (0.15C; 11.3Cr; 0.66Mo; 0.25V; 0.30Nb; 0.75Ni) and reduced activation [LA7Ta (0.15C; 11.4Cr; 0.25V; 2.9W; 0.12Ta; 0.073N), LA12Ta (0.16C; 9.8Cr; 0.27V; 0.85W; 0.10Ta; 0.042N) and LA12TaLC (0.09C; 8.90Cr; 0.39V; 0.76W; 0.09Ta; 0.19N)] martensitic steels and exposed for 500 and 1000 hours in high temperature (300°C) - high pressure (16 MPa) water in static stainless steel autoclaves, the water chemistry conditions being representative of PWR primary circuit coolant [1].

The weight changes during the tests were measured and the surface oxide films characterised by SEM/EDX examinations. The weight changes resulted from two processes: (a) loss of iron into the water by corrosion (weight loss) and the formation of an Fe-Cr spinel oxide (inner layer), the thickness of which corresponds to the thickness of metal consumed; and (b) deposition (weight gain) of magnetite onto the surface (outer oxide layer). The depths of the corrosion and the corro-

sion rates were determined from the weight losses after removal of the outer and inner oxide layers by sequential descaling treatments.

The aqueous corrosion of steels at high temperatures generally follows a parabolic rate law, with the thickness of the metal consumed being proportional to (time)$^{0.5}$; the weight gains during the tests and the depths of the corrosion are therefore shown as a function of $t^{0.5}$, where t is the exposure time, in Fig. 1 (a) and (b). The results of these restricted tests on the commercial (FV448) and reduced activation steels indicated no undue sensitivity to aqueous corrosion, the lower corrosion of the LA7Ta steel being tentatively attributed to its higher tungsten content compared to the other steels.

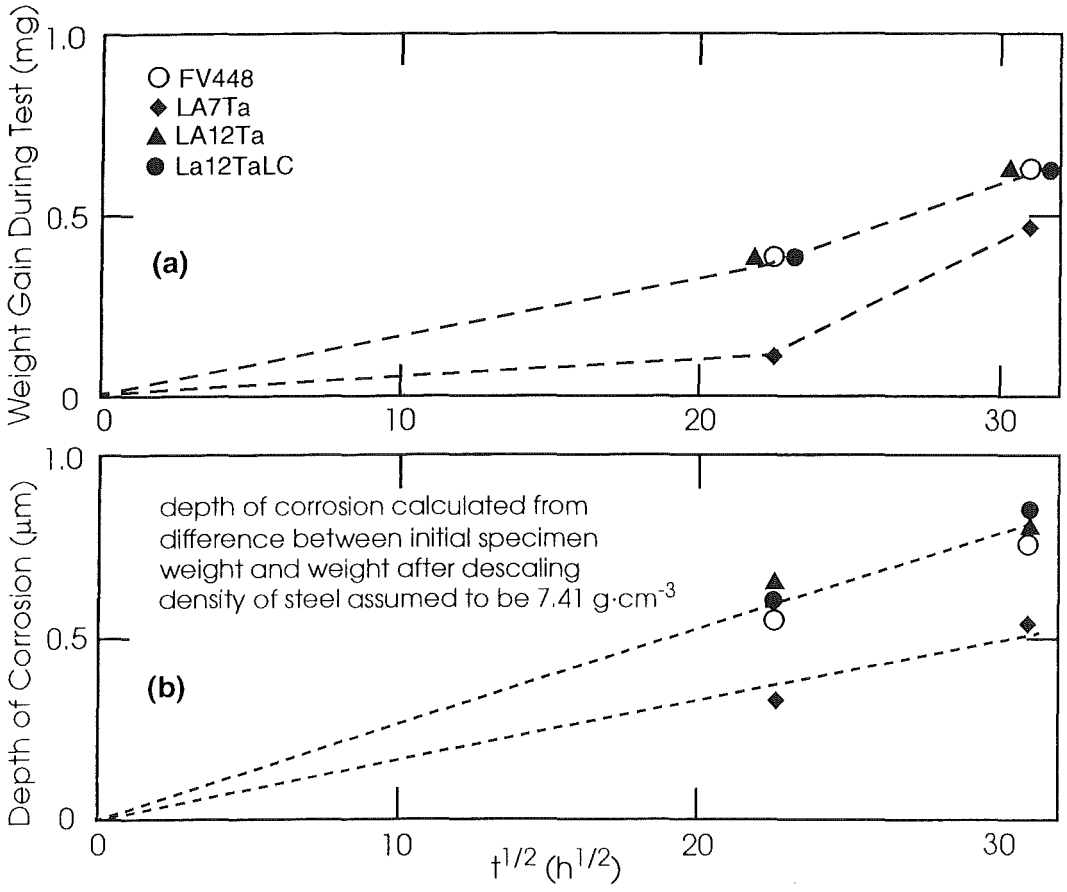


Fig. 1: Corrosion of FV448 and reduced activation martensitic steels in high temperature (330°C), high pressure (16 MPa) water; static autoclave tests.

(ii) NFR

FV448, 1.4914 [plate (0.13C; 10.6Cr; 0.77Mo; 0.22V; 0.16Nb; 0.87Ni; 0.02N), electron beam and laser welds) and the reduced activation LA7Ta, LA12Ta and LA12TaLC martensitic steels have also been exposed for times up to about 5000 hours in the high temperature (275°C) - high pressure (9 MPa) hydrogenated water austenitic stainless steel loop in the Studsvik R2 reactor [2]. The steel coupons were located in the core, above core and out - of - core regions of the loop and samples were removed for examinations after 300, 1460 and 4947 hours (time at reactor power of ≥30 MW; the respective displacement doses for the core region samples were approximately 0.12, 0.60 and 2.30 dpa. The corrosion was evaluated by weighing the coupons before and after exposure, after ultrasonic cleaning to remove loose crud deposits and after descaling.

The magnitudes of the corrosion of the steels exposed in the out - of - core region of the loop followed a $t^{0.4}$ relationship (Fig. 2), consistent with other observations on steels tested in high temperature water [3]. The values of the constant C in the relation $\Delta W = Ct^{0.4}$, where $\Delta W$ is the weight loss in mg/cm$^2$ and t is the exposure time in hours, for the ultra- sonically cleaned and descaled reduced activation and commercial steels are listed in Table I.

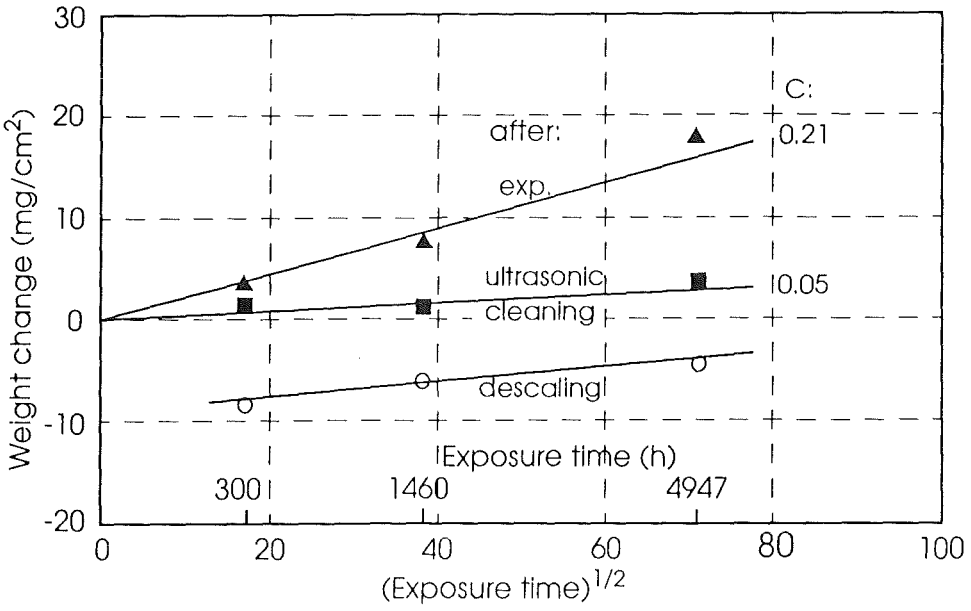


Fig. 2: Weight changes for the 1.4914 and FV448 martensitic steels exposed in the core, above core and out-of-core regions of the high temperature (275°C), high pressure (9 MPa) water loop in the R2 reactor.

**Table 1: Corrosion of Reduced Activation and Commercial Steels in High Temperature Water Loop [2]**

| Steel | Loop Region | C | Valid for exposure time (h) of: |
|---|---|---|---|
| Reduced activation | | | |
| LA7Ta, LA12Ta and LA12TaLC | Out-of-core<br>Above core<br>Core | 0.06*<br>0.19 - 0.49"<br>0.52 - 0.84" | 4.947<br>300<br>1.460 |
| | | | |
| Commercial | | | |
| 1.4914; FV448<br>1.4914<br>1.4914<br>FV448 | Out-of-core<br>Above core<br>Core<br>Core | 0.08*<br>0.18 - 0.33"<br>0.69 - 0.90"<br>0.44" | 4.947<br>4.947<br>300<br>300 |

* Ultrasonically cleaned "Descaled

The corrosion was a maximum for the reduced activation and commercial steels exposed in the core region, intermediate for the above core samples and a minimum for the coupons tested in the out - of - core region of the loop; this behaviour was consistent with the increased radiolytic decomposition of the water in the core compared with that in the above core region, and virtually negligible dissociation in the out - of - core position. In addition, the steel coupons exposed in the core may have been sensitised to corrosion as a consequence of neutron irradiation - induced interfacial segregation of chromium, leading to the precipitation of $\alpha'$ (Cr - rich ferrite) and depletion of the chromium contents of the matrices [4 - 6].

The scatter in the data was such that no clear distinction could be made between the corrosion behaviour of the commercial and reduced activation martensitic steels exposed in the respective regions of the loop.The corrosion weight losses of the FV448 and reduced activation steels tested for 500 and 1000 hours in the static autoclaves [1] were considerably lower (C = 0.035 for the FV448, LA12Ta and LA12TaLC and 0.023 for the LA7Ta steel) than for the same steels exposed in the out - of - core region of the high temperature water loop (C = 0.06 - 0.08); furthermore, the superior corrosion resistance of the LA7Ta steel in the static autoclave tests was not apparent following exposure in the high temperature water

loop. The differences may be attributed to the effects of the water flow on the corrosion kinetics.

Tensile and stress corrosion cracking tests were carried out on the 1.4914, FV448 and LA12TaLC martensitic steels previously exposed for 1460 and 4947 hours (time at a reactor power of $\geq$30 MW) in the core ($\sim$ 0.60 and 2.30 dpa respectively), above core and out - of - core regions of the high temperature water loop in the R2 reactor [7].

Irradiation assisted stress corrosion cracking (IASCC) was not detected in any of the steel samples stressed to 95% of the yield strengths in three point bend and autoclave tested for times up to 1500 hours at 250°C in air - saturated high purity water. It is well established that Type 316L and other austenitic steels were prone to failure by IASCC under comparable test conditions [8][9]; this has been attributed to irradiation - induced non - equilibrium segregation resulting in interfacial microchemical compositional changes [10]. It may well be that the high Cr martensitic steels have superior resistance to IASCC because they may not have been sensitised by the irradiation in a similar manner or to the same extent as the austenitic steels.

### 2.6.2 Lithium - lead (Pb-17Li)

Corrosion tests of MANET steel in liquid Pb-17Li alloy have been performed for long periods of time (several thousand hours) in the pumped loop PICOLO, the hot leg of which was constructed of ferritic steel [11]. Cylindrical bars of MANET steel were exposed in the flowing eutectic melt at 450 to 550°C, the flow velocity at the surfaces of specimens of 0.3 m/s (Re = 21000), provided turbulent flow conditions in the test section. The lowest temperature in the loop was $\approx$ 300°C, a magnetic trap was installed in the region of lowest temperatures. Magnetic corrosion products were precipitated in the cooling device and collected within this trap. The appearance of the deposited crystals indicated, that crystal growth may also contribute to the corrosion product collection in this trapping device. The corrosion tests were interrupted for determinations of material losses, kinetic data were gained in this way. The MANET specimens were examined by means of metallographic and chemical methods, mass losses were determined by measurement of the diameters.

The evaluation of long term corrosion tests of MANET steel in flowing liquid Pb-17 Li eutectic alloy at 450, 500 and 550°C in the PICOLO loop showed that the material did not suffer internal corrosion effects like the formation of depleted

zones. Mass losses of MANET steel due to corrosion in flowing Pb-17Li eutectic at 550°C were comparable to mass losses of 316L(N) steel at 500°C, the corrosion was temporarily reduced during the initial period of contact with the liquid alloy [12]. The result of corrosion tests indicate that the reduced corrosion during the initial period of up to 2500 h might be related to the removal of the passivation layers of the steel.

These material losses were analysed on the basis of a hydraulic model of dissolution and diffusion processes in the turbulent flowing liquid metal. The results showed that the corrosion in flowing Pb-17Li is due to a material dissolution mechanism [13].

The corrosion *dr* as loss of wall thickness can be expressed by the equation valid for the parameters in the test section, i.e. turbulent flow of the liquid alloy:

$$\log dr = 12.3384 - 10960/T \qquad (1)$$

This equation results in conservative values of the material losses, since it is valid for a downstream position near zero, the position of highest material losses. The annual material loss at 450°C and a flow velocity of 0.3 m/s is in the order of a layer of 13 µm thickness as calculated from the equation. The mass losses are not proportional to the flow velocity, they depend on the Reynolds number at less than linearity.

The influence of typical parameters of the fusion reactor blanket, the strong magnetic field and the irradiation with high energy neutrons has to be considered. Since the magnetic field may suppress the turbulence of the flow of the liquid alloy, corrosion may be less than in the experimental facility. Irradiation may enhance the diffusion rates in the solid material, faster diffusion may lead to higher corrosion rates. However, the system MANET steel/liquid alloy is not characterised by solid state diffusion, the corrosion is mainly a process of the solid/liquid interface. It can, therefore, be expected that the irradiation does not significantly increase the liquid metal corrosion of MANET steel. The irradiation causes the formation of activation products, thus the liquid alloy dissolves certain amounts of activated material which may be precipitated in peripheral parts of the cooling system.

These phenomena and data of the corrosion of MANET steel through the liquid alloy Pb-17Li are in good agreement with the results of tests in a similar loop in France. The mass loss data are within a scatter band, the absence of any internal corrosion layers was also observed in this work [14]. The martensitic steel is considerably more stable against corrosion in Pb-17Li liquid alloy than austenitic

steels like AISI 316L. For a given loss of material, MANET allows a service about 50 K higher than for the austenitic steel AISI 316L. The austenite suffers additionally from the formation of a spongy, ferritic sub-surface layer due to the selective leaching of nickel and other alloying elements [15], which has to be added to the mass losses.

The creep-rupture properties of MANET steel under corrosive Pb-17Li conditions were measured at temperatures up to 600°C in static capsules which were connected with creep machines. A series of about 30 tests was performed. The creep and creep-rupture data were not influenced by the presence of the eutectic Pb-17Li alloy [16], the bulk properties of the martensitic steel are not sensitive to the action of the molten alloy. However, the material loss due to corrosion has an influence on the creep data and must be considered in the design rules.

Some fatigue tests in a similar type of capsules in which the liquid alloy was at temperatures up to 600°C did not reveal any influence of the liquid alloy on the fatigue life of MANET specimens [17].

The necessity to coat the MANET steel with an insulating surface layer further reduces the corrosion problem in the self-cooled liquid metal blanket, since such a coating has a protective effect against liquid metal corrosion. It has been shown that under such conditions the corrosion rate was drastically reduced below the detection limit [18]. The insulating layer is based on $Al_2O_3$ formed by oxidation on an aluminide layer. The aluminizing was successfully performed by hot-dipping MANET steel samples into molten aluminum at 800°C for some minutes and subsequent oxidation at 950°C in a weakly oxidising atmosphere. The insulting layers were stable in the liquid alloy at 450°C for up to 10 000 hours, the layers prevented any material dissolution through liquid metal corrosion [18].

The compatibility of MANET steel with the liquid Pb-17Li-alloy does not reduce the functionality, feasibility and reliability of blanket components which are in contact with the flowing liquid alloy. It limits, however, the temperature of operation to about 450°C. Its composition is favourable for the use in contact with the liquid alloy. The only open point is the experimental proof of the corrosion rates under higher flow velocities of the liquid metal coolant.

### 2.6.3 Solid ceramic breeding materials

The reaction rates of powder-compacted lithium based oxide compounds LiO, LiSiO (metasilicate), LiSiO (orthosilicate) and LiZrO with the MANET and Type 316 steels (in the form of sheets) have been determined in argon at temperatures in

the range 500 - 900 C and for times up to 1000 hours [19]. The results of these studies and those obtained previously in capsule annealing tests have shown that the extents of the interaction depended not only on the temperature and time but also on the partial pressure of the water in the argon (varied between 1 and 100 Pa). The compatibility of the LiO with the steels was superior to that of the other oxides; the reaction rates of all the other oxides were very similar. Furthermore, the martensitic steel was more compatible with all the oxides than the Type 316 steel at temperatures up to 800°C. The ceramic - MANET steel compatibility in a neutron environment is being investigated as part of the SIBELIUS experiment in the SILOE reactor in France [20].

### 2.6.4 Beryllium neutron multiplier

Laboratory investigations have shown that 316L austenitic steel reacts with beryllium above 580°C, the depths of the attack being 25 and 50 μm after exposure for 1000 and 2000 hours respectively; however, noticeable interaction between beryllium and the MANET steel occurred only above 600°C.

The effects of irradiation on the beryllium - MANET steel compatibility at 550°C has also been examined as part of the SIBELIUS experiment [21]. The results showed only slight reaction at the interfaces of the beryllium - MANET steel (and Be - 316 steel) couples after exposure for 1690 hours [9 x $10^{17}$ (thermal), 9 x $10^{17}$ ($>$ 1 MeV) $n.m^{-2}s^{-1}$]. However, the beryllium surface was covered with a grey oxide layer 5 m thick and a discontinuous oxide layer of the same thickness was also observed on the surfaces of the MANET steel specimens.

*References*

1. C.B. Ashmore and N.R. Large, AEA Fusion Report 102.
2. R. Kallstrom, Studsvik Report M-93/106, March 1994.
3. L. Tomlinson et al, Corosion, 41 (1985) 257.
4. E.A. Little and L.P. Stoter, ASTM Special Technical Publication 782 (1982) 207.
5. R.E. Clausing et al, J. Nucl. Mater., 141 - 143 (1986) 978.
6. E.A. Little, ibid 206 (1993) 324.
7. A.-C. Nystrand, Studsvik Report M-94/18, February 1994.

8. K. Pettersson and A.-C. Nystrand, Studsvik Report NS-91/7, 1991.

9. Framatome Report EE/S, DC 288, September 1991.

10. D.I.R. Norris, Ed., Proc. Symp. on Radiation - Induced Sensitisation of Stainless Steels, Berkeley Nuclear Laboratories, September 1986.

11. G. Frees, G. Drechsler and Z. Peric, "Dynamische Korrosionsuntersuchungen in der eutektischen Blei-Lithium-Schmelze Pb-17Li", Werkstoffe und Korrosion 40 (1989) 593.

12. H.U. Borgstedt and H.D. Röhrig, "Recent results on corrosion behaviour of MANET structural steel in flowing Pb-17Li eutectic", J. Nucl. Mater., 179-181 (1991) 596.

13. M. Grundmann, H.U. Borgstedt and M. Schirra, "The creep-rupture behaviour of the martensitic steel X18 CrMoVNb 12 1 (Werkstoff-Nr. 1914) in liquid Pb-17Li at 550 and 600°C", 4th Internat. Conf. on Liquid Metal Engineering and Technology, Avignon, France, Oct. 17-21,1988; Proc. Vol 2, paper 510).

14. J. Sannier, T. Flament, and A. Terlain, "Corrosion of martensitic steels in flowing Pb-17Li", Proc. 16th Symp. on Fusion Technology (SOFT), London, September 1990, North-Holland, 1990, p. 901-905.

15. H.U. Borgstedt, G. Frees, and Z. Peric, "Material compatibility tests with flowing Pb-17Li eutectic", Fusion Engng. and Design, 17 (1991) 179.

16. H.U. Borgstedt, G. Frees, M. Grundmann and Z. Peric, "Corrosion and mechanical properties of the martensitic steel X18 CrMoVNb 12 1 in flowing Pb-17Li", Fusion Engng. and Design, 14 (1991) 329.

17. M. Grundmann, "Strukturmechanische Untersuchungen am 12% Cr-Stahl X18 CrMoVNb 12 1 (1.4914) im flüssigen Pb-17Li-Eutektikum", Bericht KfK 4703, Karlsruhe 1990.

18. H.U. Borgstedt, H. Glasbrenner and Z. Peric, "Corrosion of insulating layers on MANET steel in flowing Pb-17Li", J. Nucl. Mater. 212-215 (1994) 1501-03.

19. P. Hofmann and W. Dienst, Proc, 17th. SOFT, Rome, September 1992, p. 1374

20. N. Roux et al, J. Nucl. Mater., 179 - 181 (1991) 827.

21. N. Roux et al, ibid, 191 - 194 (1992) 168.

## 2.7 Hydrogen isotope effects

There are several potential sources of hydrogen isotope formation in fusion reactor First Wall and breeder structural materials [1][2]: (i) Neutral and charged hydrogen (tritium and deuterium) atoms with energies ranging from ~0.2 eV to $\leq$ 10 keV injected into the plasma facing components, (ii) Hydrogen formed by (n,p) transmutation reactions, (iii) Tritium generated in the breeding blanket, (iv) Hydrogen produced by corrosion at steel - water coolant interfaces, (v) Radiolysis of the water coolant, (vi) Hydrogen added to the water coolant to inhibit radiolytic decomposition, and (vii) Hydrogen absorbed from helium coolant (hydrogen added to inhibit oxidation and aqueous vapour corrosion).

The low energy near surface implantation of hydrogen atoms from the plasma can lead to sputtering, super-permeation [3], etc. However, there are no data on the blistering and sputtering of the 9 - 12% Cr steels under hydrogen bombardment and no information on the retention of the low energy implanted hydrogen in these steels. These effects form part of the important field of plasma - wall interactions and the available data on other materials have been reviewed periodically [4][5]. Nevertheless, it has been predicted [2] that the tritium and deuterium implanted from the plasma into an unprotected first wall could probably lead to high hydrogen concentrations and a wide range of damage effects but the present uncertainties in the expected magnitude of the ion flux do not permit reliable predictions of the likely hydrogen isotope concentrations. However, direct implantation from the plasma may not be a problem with a protected first wall under normal operating conditions although it may be important in the event of localised failure of the protective coatings or tiles.

The high chromium martensitic steels, in common with the bcc irons, carbon- and low alloy steels, are susceptible to hydrogen - induced changes in mechanical properties and fracture behaviour [1][6 - 9]. The hydrogen introduced electrolytically, by exposure to high pressure gas and by corrosion is in the uncombined state but recombination to form molecules can occur at discontinuities resulting in the development of high pressures and surface blistering. However, the nascent hydrogen may induce physical embrittlement, the principal characteristics of which are as follows: (a) The magnitude of the embrittlement, manifested as reductions in ductility and the true fracture stress in tensile tests, increases with increasing hydrogen partial pressure and concentration, (b) The effects are normally restricted to temperatures below 200°C and are reversible, (c) The embrittlement generally decreases with increasing deformation rate, (d) Delayed (brittle) fracture can occur in higher strength steels, (e) The fractures are gener-

ally transcrystalline, and (f) Temper embrittled steels are particularly prone to the embrittlement; thus, phosphorus segregation and the presence of Laves ($Fe_2Mo$) phase at the prior austenite and martensite lath boundaries accentuate the embrittlement.

Chemical embrittlement can occur at temperatures in excess of 200°C due to the reaction of hydrogen with the carbon in solution in the steels, resulting in the formation of methane:

$$C + 4H \leftrightarrow CH_4$$

This reaction only occurs at very high temperatures at normal pressures but attack starts at progressively lower temperatures with increasing hydrogen partial pressure. Small pockets of methane gas are formed at discontinuities, particularly grain boundaries, resulting in the formation of cracks and low ductility brittle failures and marked reductions in impact strengths. Increased alloying increases the resistance to this type of attack due to the decrease in carbon activity, with steels containing $\geq 6\%$ Cr being generally immune to chemical hydrogen embrittlement.

It has also been concluded [2] that bulk hydrogen up - take from the other fusion reactor sources listed above are unlikely to lead to the threshold concentrations at which effects such as surface blistering and physical and chemical embrittlement occur in the steels. These estimates, however, did not take into account the tritium generated in the blanket and the possible effects of irradiation on the solubility, diffusion and permeation of hydrogen in steels. There is some evidence that the irradiation - induced point defects and/or helium act as traps for the hydrogen, thereby reducing diffusivity and permeability [10].

There is a paucity of data on the effects of hydrogen in the MANET steels but the limited information available has been surveyed [7]. Thus, the fatigue lives of 1.4914 (MANET) steel at ambient temperature in vacuum were reduced when the testing was carried out in air and even more so in hydrogen at an external pressure of 1.5 bar (Fig. 1) [11][12]; the adverse effect of the hydrogen was enhanced at the lower frequency and hold times introduced during the fatigue test produced additional reductions in the endurances. Microstructural examinations showed that the hydrogen caused modifications of the surfaces of the test samples, particularly those tested at the lower frequencies, thereby influencing the crack initiation and/or propagation.

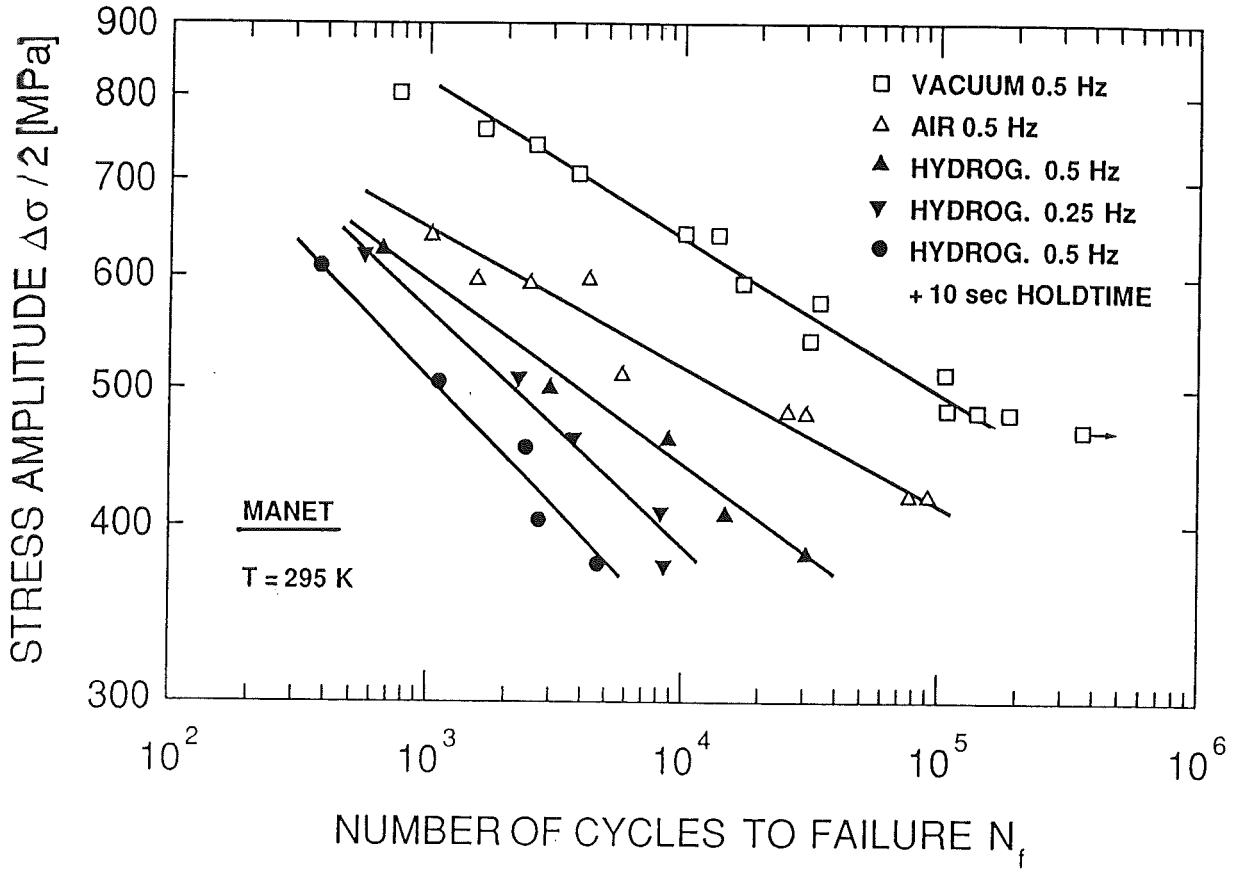


Fig. 1: Fatigue lives of 1.4914 (MANET) steel at ambient temperature in load controlled tests in vacuum, air and 1.5 bar hydrogen [11][12].

As already mentioned in section 2.4.1, studies of the effects of irradiation at 80 and 500°C with degraded beams of 104 MeV α - particles and/or 30 MeV protons in the Dual Beam facility at KfK showed that implantation with 500 appm hydrogen, with or without 500 appm helium and a displacement dose of about 0.3 dpa, produced little or no influence on the tensile strengths and ductilities of the MANET I steel at temperatures above 100°C [13]; this was probably due to the rapid loss of the hydrogen by diffusion from the small section thickness test specimens. However, synergistic detrimental effects of hydrogen charging and irradiation on the mechanical properties have been reported elsewhere [14].

The results of charged particle simulation irradiations have also demonstrated that the void swelling of various 9 - 12% Cr steels, including the MANET type, irradiated to $\leq$100 dpa was not enhanced by the sequential implantation of 1300 appm helium and 5200 appm hydrogen in the Harwell Variable Energy Cyclotron, the swelling being $<$ 0.2% [15].

*References*

1. D.R. Harries, Radiation Effects, 101 (1986) 3.
2. R. Boler, C.A.B. Forty and G.J. Butterworth, AEA FUS 164, February 1992.
3. F. Waelbroeck et al, J. Nucl. Mater., 85 and 86 (1979) 345.
4. See Proc. of International Conference on Plasma - Surface Interactions in Controlled Fusion Devices, J. Nucl. Mat. 196-198 (1992).
5. S.M. Myers et al, J. Nucl. Mater., 165 (1989) 9.
6. D.R. Harries, Proc. Topical Conf. on Ferritic Alloys for use in Nuclear Energy Technologies, Snowbird, 1983, J.W. Davis and D.J. Michel, Eds., Met. Soc. AIME, 1984, p.141.
7. P. Jung, Subtask MAN - 801 - D, Literature Survey on Hydrogen Effects in 9 - 12% Cr Steels, December 1992.
8. C.A. Hippsley and N.P. Haworth, Materials Sci. and Tech., 4 (1988) 791.
9. G. Sund, Studsvik Report STUDSVIK / M - 92 / 15.
10. K. Fukushima and K. Ebisawa, J. Nucl. Mater., 127 (1985) 109.
11. H. Ullmaier and W. Schmitz, ibid, 169 (1989) 233.
12. J.I. Shakib et al, ibid, 212 - 215 (1994) 579.
13. K.K. Bae, K. Ehrlich and A. Möslang, ibid, 191 - 194 (1992) 905.
14. A. Kimura et al, ibid, 179 -181 (1991) 737.
15. D. J. Mazey et al, ibid, 155 - 157 (1988) 891.

## 2.8 Recent (world wide) developments on 9 - 12% Cr steels

A comprehensive survey of recent developments on 9 - 12% chromium steels has covered the following items [1]:

(i) Physical metallurgy.

(ii) Microstructure and precipitation reactions.

(iii) Mechanical properties (tensile, impact, creep and fatigue) and microstructural correlation.

(iv) Temper and hydrogen embrittlement.

(v) Microstructural evolution under irradiation.

(vi) Irradiation effects on dimensional stability (swelling) and mechanical properties (tensile, impact and irradiation creep).

The relevant aspects have been noted and discussed in other sections of this report.

The development of new steels for applications in conventional "ultra - supercritical" power plants has been actively pursued in Japan where there is considerable interest in steam cycles with temperatures up to 650 or 700°C so as to achieve high thermal efficiency from imported coal. The associated R. & D. have in the last few years led to the development of the following high chromium martensitic steels (compositions in wt.%) which have high creep - rupture strengths and good toughness [2][3]:

Boiler tubes

TB9 (NF616): 0.10 C, 9 Cr, 0.4 Ni, 0.2 V, 0.05 Nb, 2 W, 0.05 N, 0.003 B.

TB12: 0.08 C, 12 Cr, 0.1 Ni, 0.5 Mo, other elements as for TB9.

Steam turbine rotors

TR1200: 0.12 C, 11 Cr, 0.8 Ni, 0.3 Mo, 0.2 V, 0.05 Nb, 1.8 W, 0.06 N.

HR1200: 0.12 C, 11.5 Cr, 0.6 Ni, 0.2 Mo, 0.2 V, 0.08 Nb, 2.5 W, 3 Co, 0.017 N, 0.015 B.

Large diameter steam pipes

HCM12A: 0.12 C, 10.6 Cr, 0.32 Ni, 0.4 Mo, 0.2 V, 0.05 Nb, 1.85 W, 0.85 Cu, 0.06 N.

The TB12 and TR1200 steels have the highest creep - rupture strengths at temperatures up to 650°C of all the commercial 9 - 12% Cr martensitic steels, including the modified 9% Cr - 1MoVNb (T91) steel developed in the U.S.A.

The development of 9 - 12% Cr martensitic steels with $10^5$ h creep - rupture strengths of about 100 MPa at 600 C for rotor forgings has been undertaken in Europe as part of the COST 501 programme. Recent work has led to the identification and characterisation of experimental heats of the following two steels (approximate compositions in wt.%) suitable for rotors operating at advanced steam conditions with temperatures up to 600 C [4]:

"E": 0.12 C, 10 Cr, 0.7 Ni, 1.0 Mo, 1.0 W, 0.05 Nb.

"F": 0.11 C, 10 Cr, 0.6 Ni, 1.5 Mo, 0.05 Nb.

U.S. data on the radiation hardening and embrittlement of commercial 9 and 12% Cr martensitic steels and reduced activation alloys with chromium contents ranging from 2.25 to 12% have shown that the least changes are produced in the steels and alloys containing 7-9% Cr after exposure to displacement doses up to 14 dpa (max.) at 365°C in FFTF [5][6]; in particular, a 9% Cr- 2WVTa steel exhibited little or no embrittlement. The superior radiation hardening resistance of the 7-9% Cr reduced activation steels was also manifested in the results of Japanese tests on disc bend specimens at ambient temperature after irradiation to $\leq$35 dpa at ~400 C in FFTF, with an 8% Cr steel showing negligible hardening [5].

*References*

1. L. Pilloni, "Review of Development of 9 - 12Cr Steels", ENEA Report (Unnumbered), 1993.
2. T. Fujita, Advanced Materials and Processes, 4/92, p.42.
3. A. Iseda et al, Proc. 5th. Int. Conf. on Creep of Materials, May 1992, Lake Buena Vista, Florida, ASM International, p.389.
4. C. Berger and R.W. Vanstone, "Development of High Strength 9 - 12% CrMoV Steels for High Temperature Rotor Forgings - A Collaborative Effort in COST 501/II", Unreferenced Report.
5. Proc. IEA Workshop on Ferritic/Martensitic Steels, Tokyo, Japan, October 1992.
6. R.L. Klueh and D.J. Alexander, Fusion Reactor Materials Semiannual Progress Report for the Period Ending September 30, 1993, USDOE/ER - 0313/15, February 1994, p.148.

# 3. 7 - 11% Cr-WVTa Reduced Activation Steels

## 3.1 Criteria for low or reduced activation materials

The issues involved in defining specific radiological criteria for low or reduced activation materials selection, in terms of radioactive emissions in routine and off - normal conditions, maintenance operations after a shut - down, waste management / disposal and recycling are complex [1]. For example, there are several areas, such as routine reactor maintenance, where the lack of design detail and operational experience has hindered progress. In addition, the absence of international consensus on radiological criteria for particular circumstances, such as

accidental releases of radioactivity and the disposal of radioactive wastes [Shallow Land Burial (SLB) versus Deep Geological Repository (DGR)] has necessitated the adoption of simplified objectives at the present time.

Thus, radiological criteria for a range of scenarios have been suggested and element - by - element activation data for use in comparing materials in non - design - specific ways described [2 - 4]. Some relevant parameters and proposed criteria are given in Table I [5].

Several investigations [15][16] have indicated, however, that all representative fusion reactor structural material wastes could be safely disposed in a fully engineered DGR. Thus, whilst low or reduced activation materials may offer little or no post - disposal safety advantages relative to conventional materials in DGRs, their reduced shielding requirements may make operations cheaper and / or safer. Moreover, the optimisation of the material compositions may substantially reduce the amounts of material requiring management as radioactive waste, as well as the quantities requiring disposal in DGRs as opposed to SLB.

It has been suggested, assuming the classification given in Table I for LLW, MLW and HLW and the neutron fluences to which the materials would be exposed during service, that an ideal but realistic configuration of a low activation fusion reactor should lead to the following distribution of its waste [6][11]:

| | |
|---|---|
| First wall and divertor materials : | MLW (geological disposal). |
| Blanket materials: | LLW (recycling). |
| Other materials (e.g. shield, magnets): | LLW (recycling, possibly "hands - on"). |

**Table I: Relevant Parameters and Some Proposed Criteria for Low Activation Materials**

| | Relevant Parameters | Proposed Criteria |
|---|---|---|
| Maintenance | Short-term contact dose rate at the surfaces of components to be handled or at various distances, subject to varying degrees of shielding. | Remote maintenance: Dose rate inside plasma chamber below $1x10^4$ Gy.h$^{-1}$ after 1 day cooling, or integrated dose below $1x10^7$ Gy, based on tolerable doses to electronic components [6]. |
| Safety | Decay heat power density (governs the maximum temperature that may be reached and whether or not oxidation, evaporation or melting will occur). Activity per unit mass or volume (source term), combined with the appropriate volatilisation rates. | Avoid any release that would necessitate off-site emergency action, interpreted as: Prompt dose at site boundary due to 100% release of inventory $< 2$ Sv [7]. Early dose at 1 km associated with accidental release of 100 kg of activated materials $< 50$ mSv [6]. Maximum early dose 100 mSv [ITER]. Limitations of off-site releases to $10^{14}$ Bq [2] |
| Recycling | Contact dose rate, activity per unit volume or mass and volumetric decay heat. | "Hands-on" contact dose rate limit: 25 $\rightarrow$ 10 µSvh after 100 y cooling [6][8][9]. Remote recycling limit (ability to remelt and refabricate remotely): $< 10$ mSvh$^{-1}$ after 50 y cooling [10]. Dose rate $< 2$ mSvh$^{-1}$ and decay heat $< 1$ W.m$^{-3}$ after 50 y interim storage [11]. For unrestricted release, residual activity should be $< 10^3$ Bq.kg$^{-1}$ . Less strict limits for reuse in fusion cycle. |
| Waste disposal | Amounts of particular long-lived radionuclides per unit quantity of waste (source term), combined with release rates from deep or near-surface land repositories and the transport and accumulation of the nuclides in soil, water and other media relevant to human radiation exposure.<br><br>Contact dose rate and volumetric decay heat.<br>LLW - Low level waste.<br>MLW - Medium level waste.<br>HLW - High level waste. | Maximum doses to inadvertent intruders and members of the public for near-surface- burial of 5 and 0.25 mSv.y$^{-1}$ (10CFR61, USA) [12][13][14].<br><br>Maximum annual individual risk for a single facility of $10^{-6}$ (Authorising Departments, UK), equivalent to a health risk associated with a dose of 0.1 mSv.<br><br>Dose rate mSvh$^{-1}$ / Decay heat W.m$^{-3}$<br>LLW: $< 2$ / $< 1$<br>MLW: $< 20$ / $< 10$<br>HLW: $> 20$ / $> 10$<br><br>after 50 y interim storage [11]. |

*References*

1. G.J. Butterworth, J. Nucl. Mater., 179 - 181 (1991) 135.
2. G.M. Smith and D. Charles, AEA FUS Report 122, July 1991.
3. G.M. Smith and G.J. Butterworth, J. Nucl. Mater., 191 - 194 (1992) 1455.
4. G.M. Smith and D. Charles, AEA FUS Report 165, January 1992.
5. D.R. Harries et al, J. Nucl. Mater., 191 - 194 (1992) 92.
6. P. Rocco and M. Zucchetti, Fus. Eng. Des., 15 (1992) 235.
7. S.J. Piet et al, Fus. Technol., 19 (1991) 146.
8. G.J. Butterworth and L. Giancarli, Proc 14th. Symp. on Fus. Technol., Avignon, September 1986, Pergamon Press, Oxford, 1986, p. 1343.
9. G.J. Butterworth, Fus. Eng. Des., 11 (1989) 231.
10. C.R. Gomer et al, ibid, 11 (1990) 423.
11. P. Rocco and M. Zucchetti, J. Fus. Energy, 12 (1993) 201.
12. Final Environmental Impact Statement, NUREG - 0945, U.S. Regulatory Commission, November 1982.
13. J.S. Herring and S. Fetter, J. Nucl. Mater., 155 - 157 (1988) 597.
14. D.G. Doran, ibid, 191 - 194 (1992) 1439.
15. M.G. Sowerby and R.A. Forrest, AERE Report R13708, March 1990.
16. R. Atkinson and P.J. Summer, AEA FUS Report 127, June 1991.

## 3.2 Nuclear data base

The development of fusion activation codes and libraries in Europe in the period up to 1992 has been reviewed previously [1]; in addition, the inventory codes and cross section and decay libraries developed in Europe, the U.S.A. and Japan for predicting the radionuclide inventories of materials irradiated in fusion reactors and the further work required to assemble a complete nuclear data base have been summarised [2].

FISPACT [3 - 6] is the most advanced inventory code, being able to treat correctly the multiple reaction pathways for fusion activation calculations, and is available as part of the European Activation System (EASY) [7]; the latter also includes activation (EAF 1, 2 [8][9], 3 [10 - 12] and 3.1[13]) and decay (UKDECAY 3 and 4) li-

braries, a subsidiary library of biological hazard data, and five reference fusion reactor neutron spectra (first wall, blanket, shield, and two magnetic coils) and therefore provides a comprehensive package for activation calculations.

It has also been recognised that sequential charged particle reactions [ A (n,x) B → A (x,n) C where x is a charged particle such as p, d, α, t, etc.] may contribute significantly to the residual activities, dose rates and decay heats in some circumstances [14], but these reactions have not been included in the activation codes hitherto. However, work at KfK [15 - 19] has led to (i) the creation of extended cross - section libraries KFKSPEC, KFKXN and KFKSTOP for all kinematically possible charged particle sequential reactions: (p,n), (d,n), (t,n), ($He^3$,n), (α,n), (d,2n) and (t,2n); (ii) the development and improvement of the code PCROSS for the production of pseudo - cross sections which can be used in conjunction with FISPACT for the computation of the induced radioactivity, surface dose rates, decay heats and biological hazards for irradiated steels and other alloys; and (iii) the experimental verification of the sequential cross sections for neutron irradiated V, Cr and Fe using the Karlsruhe Isochronous Cyclotron (KIZ).

With the implementation of the above libraries into the new version FISPACT 4.0/01 (June 1994) multistep reaction-chains including (x,n) sequential reactions are also available in the meantime for any metallurgically interesting combination of elements.

*References*

1. D.R. Harries, Long Term Fusion Technology Programme, Low Activation Materials, Review of Progress in 1989-91 and Summary of 1992-94 Programme, September 1992.
2. D.R. Harries et al, J. Nucl. Mater., 191 - 194 (1992) 92.
3. R.A. Forrest and D.A.J. Endacott, AERE Report M 3654 (Rev.), 1990.
4. R.A. Forrest, AEA FUS 153, May 1991.
5. R.A. Forrest and J.-Ch. Sublet, AEA FUS 227, 1993.
6. R.A. Forrest, Int. Conf. Nuc. Data for Sci. and Tech., Gatlinberg, J.K. Dickens, Ed., 1994, p. 845.
7. R.A. Forrest and J. Kopecky, The European Activation System (EASY), IAEA Advisory Group Meeting on FENDL-2, Vienna, November 1991.
8. J. Kopecky et al, ECN Report C - 91 - 073, 1991.

9. J. Kopecky and D. Nierop, ECN Report I - 91 - 053, 1991.

10. J. Kopecky and D. Nierop, ECN Report I - 92 - 023, 1992.

11. J. Kopecky et al, ECN Report C - 92 - 051.

12. J. Kopecky et al, ECN Report C - 92 - 058.

13. J. Kopecky, D. Nierop and R.A. Forrest, ECN Report I - 94 - 015.

14. S. Cierjacks and J. Hino, J. Nucl. Mater., 170 (1990) 134.

15. S. Cierjacks, P. Oblozinsky and B. Rzehorz, KfK Report 4867, July 1991.

16. S. Ravandal et al, KfK Report 4873, August 1991.

17. S.Kelzenberg et al, Proc. Topical Conf. on Nuclear Data for Fusion Reactors, Karlsruhe, October 1991.

18. S. Cierjacks et al, Report NEA/NSC/DOC (93) 17, July 1993.

19. S. Cierjacks et al, Fus. Tech., 4 (1993) 277.

## 3.3 Steel development and characterisation

The universal approach adopted in the development of reduced activation martensitic steels for fusion applications has entailed modifying the compositions of the conventional steels (FV448, 1.4914 and T91) by replacing the strengthening elements Mo and Nb, which promote long term activation, by "acceptable" elements such as W, V, Ta and / or Ti and maintaining a low concentration of Ni which is also radioactively undesirable.

The iron base provides the best achievable target and so the effects of individual alloying additions on the contact dose rate, induced activity and decay heat, relative to the contributions from the iron, have been calculated as a function of time after reactor shut down [1]; the inventory code FISPACT and the cross section library EAF-3 were used for the computations and the conditions assumed were those corresponding to the first wall of a fusion power reactor (2.5 y with a neutron wall loading of 2 MW/m$^2$). The results confirmed that Cr (any concentration), V ($\leq$8%), Mn ($\leq$1%), Ta (~1%) and Si ($<$0.4%) were acceptable alloying additions whilst Mo ($>$ 100 ppm), Nb ($>$ 1 ppb) and Ni ($>$ 50 ppm) were detrimental; C, B and Ti, at the concentrations normally encountered in the steels of this type, did not adversely influence the activation parameters of the iron base. Moreover, the data showed that the dose rate after 100 y with 1% W exceeded that for the iron, ultimately by two orders of magnitude. It has also been established [2 - 4]

that significant transmutations of Ta (mainly to W together with a smaller proportion of Hf) and W (to Os and Re) can occur during exposure to fusion neutrons. It follows, therefore, that W may not be the ideal substitute for Mo in these steels.

The allowable concentrations of other impurity elements in these reduced activation steels also have to be restricted, particularly in respect of the long term dose rate. The results of calculations have shown that, based on an individual element dose rate contribution of 25μ $Svh^{-1}$ at 100 y, the maximum concentations of thirteen or so elements (Pd, Sm, Gd, Dy, Yb, Lu, Hf, Ir, Bi, Ag, Eu, Tb and Ho) in addition to the Nb will have to be limited to levels below 1 ppm, with especially stringent restrictions applying to Ag, Eu, Tb, Ho, Nb and Bi [5].

The introduction of sequential (x,n) reactions into the inventory code FISPACT has shown [6], that in 17 from 81 investigated elements at least one of the calculated radiological quantities is increased by more than one order of magnitude (Table 1). Vanadium, chromium and manganese as base metals or major alloying elements as well as nitrogen as interstitial element and yttrium as desoxidation element belong to this category. Impurity or tramp elements like silver, bismuth and rare earth metals which were already earlier identified as critical elements [7] are not affected by sequential reactions.

**Table 1: Effect of sequential (x,n) reactions in single element inventory calculations of three radiological quantities.**

| Element | Activity | | γ-Dose Rate | | Decay Heat | |
|---|---|---|---|---|---|---|
| | Factor of Increase | Radio-isotope | Factor of Increase | Radio-isotope | Factor of Increase | Radio-isotope |
| Li | only (x,n) | $^{10}$Be | only (x,n) | $^{10}$Be | only (x,n) | $^{10}$Be |
| B | 1.2 | $^{14}C$ | — | | — | |
| N | — | | $5.5 * 10^3$ | $^{18}$F | — | |
| O | — | | 41 | $^{18}$F $^{22}$Na | — | |
| F | — | | $1.8 * 10^{11}$ | $^{22}$Na | 1.1 | $^{22}$Na |
| Ne | — | | 14 | $^{22}$Na $^{26}$Al | 2.3 | $^{22}$Na |
| Na | $6.6 * 10^4$ | $^{26}$Al | $1.5 * 10^9$ | $^{26}$Al | $8.2 * 10^5$ | $^{26}$Al |
| Mg | 29 | $^{26}$Al | 29 | $^{26}$Al | 29 | $^{26}$Al |
| V | $1.9 * 10^5$ | $^{53}$Mn | $1.8 * 10^3$ | $^{54}$Mn | $2.5 * 10^4$ | $^{53}$Mn |
| Cr | 89 | $^{53}$Mn | 1.1 | $^{54}$Mn | 89 | $^{53}$Mn |
| Mn | — | | 16 | $^{60}$Fe/$^{60}$Co | — | |
| As | — | | $1.9 * 10^2$ | $^{81}$Kr | — | |
| Y | $9.7 * 10^2$ | $^{92}$Nb $^{93}$Mo | $4.6 * 10^4$ | $^{92}$Nb $^{94}$Nb | $1.0 * 10^3$ | $^{92}$Nb $^{94}$Nb |
| Zr | — | | 6.6 | $^{92}$Nb | — | |
| Rh | — | | 1.1 | $^{108m}$Ag | — | |
| Xe | — | | 24 | $^{138}$La | — | |
| Cs | — | | $1.5 * 10^3$ | $^{138}$La | — | |
| Pr | — | | 1.9 | $^{146}$Pm | — | |
| Nd | — | | 1.3 | $^{166m}$Ho | 1.2 | $^{166m}$Ho |
| Sm | 1.2 | $^{166m}$Ho | 1.2 | $^{166m}$Ho | 1.2 | $^{166m}$Ho |
| Eu | 1.1 | $^{166m}$Ho | 1.8 | $^{166m}$Ho $^{176}$Lu | 1.9 | $^{166m}$Ho $^{176}$Lu |
| Gd | — | | 1.3 | $^{176}$Lu | 1.3 | $^{176}$Lu |
| Tb | 1.1 | $^{176}$Lu | 1.3 | $^{176}$Lu | 1.3 | $^{176}$Lu |
| Dy | — | | 1.1 | $^{176}$Lu | 1.1 | $^{176}$Lu |
| Ho | 1.1 | $^{176}$Lu | 1.1 | $^{176}$Lu | 1.1 | $^{176}$Lu |
| Re | 1.1 | $^{193}$Pt | — | | — | |
| Pt | 3.2 | $^{202}$Pb/$^{202}$Tl | $4.3 * 10^4$ | $^{202}$Tl | 18 | $^{202}$Tl |
| Au | $3.2 * 10^4$ | $^{202}$Pb/$^{202}$Tl | $1.3 * 10^6$ | $^{202}$Tl | $6.0 * 10^5$ | $^{202}$Tl |
| Hg | 1.1 | $^{202}$Pb/$^{202}$Tl | 1.3 | $^{202}$Tl | 1.3 | $^{202}$Tl |
| Tl | — | | 17 | $^{202}$Tl $^{207}$Bi | 1.4 | $^{207}$Bi |

The most dramatical effect of sequential (x,n) reactions is found for the element fluorine. The increase in γ-dose rate due to the contribution of sequential reactions reaches as much as 11 orders of magnitude. In the case of vanadium the effect in activity and dose rate results from the production of different radioisotopes and occurs in different time regions. Gold shows that sequential (x,n) reactions affect not only light and medium, but also heavy elements.

*References*

1. J-Ch. Sublet and G.J. Butterworth, J. Nucl. Mater., 212 - 215 (1994) 695.

2. C.A.B. Forty et al, AEA FUS Report 180, 1992.

3. C.A.B. Forty et al, AEA FUS report 232, 1993.

4. C.A.B. Forty et al, J. Nucl. Mater., 212 - 215 (1994) 640.

5. R.A. Forrest, M.G. Sowerby and D.A.J. Endacott, Proc. 16th Symp. on Fus. Tech., September 1990, London, (1991).

6. K. Ehrlich, S. Cierjacks, S. Kelzenberg and A. Möslang, Proceedings: Symposium on Effect of Rad. on Materials; D.S. Gelles, Ed.; ASTM STP 1270 (1996) 1109.

7. D. Murphy and G. Butterworth, Journ. of Nucl. Mater. 191-194, p. 1444-1449 (1992).

### 3.3.1 LA steels

UKAEA

The development of elementally tailored reduced activation martensitic steels in Europe was first pursued by the UKAEA, Government Division - Fusion (formerly AEA Technology, Culham) in collaboration with the British Steel Company and other U.K. industries and organisations. About 14 steels, based on the standard FV448 (11% Cr-Mo -V- Nb) specification and having the following compositions (wt.-%) in terms of the austenite and ferrite stabilising elements, were melted and fabricated on an experimental scale:

Austenite stabilisers: 0.09 - 0.18 C; 0.004 - 0.076 N; 0.70 - 1.00 Mn.

Ferrite stabilisers: 8.9 - 11.7 Cr; 0.65 - 2.96 W; 0.22 - 0.39 V; ~0.10 Ta; 0.02 - 0.45 Si.

No attempt was made to achieve very low concentrations of impurities in the steels as the principal objectives were (a) to produce a fully martensitic structure with no - ferrite or retained austenite after rapid cooling from the austenitisation temperature, and (b) to examine the effects of variations in the concentrations of the major elements within the above ranges on the structures and properties.

Studies were undertaken of the effects of quenching and tempering temperatures and times and long - term thermal ageing on the microstructures and mechanical (hardness, room and elevated temperature tensile, creep and rupture

and impact toughness) properties [1 - 5]. The results demonstrated that 9 and 11% Cr - W - V - Ta steels could be developed with stable microstructures and strength and toughness characteristics comparable to those of commercial martensitc steels by balancing the composition, grain refinement and optimisation of the tempering treatments. The best combination of properties was exhibited by a steel, designated LA12TaLC, containing (wt. %): 0.09 C; 0.03 Si; 1.00 Mn; 8.9 Cr; 0.39 V; 0.76 W; 0.019 N and 0.10 Ta.

Some of the reduced activation 9 and 12% Cr steels were irradiated with 52 MeV Cr ions to a displacement dose of 20 dpa, with and without 260 appm helium pre - implantation, at 475°C in the Harwell Variable Energy Cyclotron [6]; transmission electron microscope examinations showed negligible void formation and swelling but there was some evidence of irradiation - induced phase instabilities.

Tensile tests have been performed in vacuum and in liquid LiPb at 250 and 400°C at an initial strain rate of $1.1 \times 10^{-4}$ $s^{-1}$ on the LA12TaLC and the following reduced activation steels [7]:

LA7TaLN - 0.18 C; 11.1 Cr; 0.24 V; 2.95 W; 0.10 Ta and 0.005 N.

LA12TaLN - 0.17 C; 9.1 Cr; 0.25 V; 0.77 W; 0.10 Ta and 0.004 N.

LA13Ta - 0.18 C; 9.0 Cr; 0.25 V; 2.96 W; 0.11 Ta and 0.045 N.

None of the steels exhibited liquid metal embrittlement (LME) when tested in the fully tempered condition. However, all the steels given a simulated weld - heat affected zone (HAZ) treatment (1300°C / 3 min. and water quenched) showed LME in the tests at 250°C; recovery of the ductilities occurred at 400°C except for the LA13Ta steel which was still embrittled when tested in the liquid metal. The properties could be partially or completely recovered by tempering the steels at 750°C for 1 h after the simulated HAZ treatment.

The aqueous corrosion behaviour of these LA steels is described and their propensities to Type IV weld cracking and hydrogen attack are discussed in other sections of this report.

CEA

Investigations of the isothermal and anisothermal phase transformations [8][9] and microstructural evolution have recently been carried out by CEA on six of the UKAEA reduced activation steels in an attempt to optimise further the initial heat treatments and to improve our understanding of the composition - structure - mechanical property relationships.

The $Ac_{1b}$ and $Ac_{1e}$ temperatures, corresponding to the start and end of the martensite to austenite transformation respectively, during heating are listed in Table I. The critical minimal ($R_m$) rate for full transformation of the austenite to martensite and maximal ($R_f$) rate to produce a complete transformation of the austenite to ferrite during cooling of the steels ranged from 45 - 200 and 10 - 80°C $h^{-1}$ respectively.

**Table I: Transformation Temperatures for LA Steels during Heating**

| Heating rate C / h. | $Ac_{1b}$ C. | $Ac_{1e}$ C. |
|---|---|---|
| 360 | 825 - 855 | 899 -950 |
| 50 | 804 - 821 | 860 - 940 |

Isothermal transformations of the austenite to the ferrite phase was studied in the range 625 - 775°C after austenitisation at 1050 and 1150°C for 0.5 h. The TTT diagram displayed typical "C" curve behaviour with the nose of the curve being at 700 - 725°C. The apparent activation energies for the growth of the ferrite phase at 625 - 725°C were generally consistent with those for bulk diffusion of Cr and / or Fe in the high Cr martensitic steels. Increasing the initial austenitisation temperature slowed down the rate of the isothermal transformation.
Metallographic and SEM examinations showed that the ferrite and precipitated carbide microstructure was strongly dependent on the transformation temperature. At temperatures above the nose of the TTT curve random precipitation of coarse carbides occurred within the ferrite matrix which exhibited low hardness values (150 HV); the ferrite appeared to be nucleated preferentially at the junctions of the austenite grain boundaries. However, the nucleation of the ferrite occurred simultaneously with extensive precipitation of "interphase" carbides on all the prior austenite grain boundaries at temperatures below the nose of the TTT curve; this structure was characterised by higher hardness values (~210 HV after transformation at 625 - 650°C).

Investigations of samples partially transformed at 650 and 750°C and the formation of martensite during the final cooling to ambient temperature have been made. The evolution of the corresponding M temperature, the hardness of the martensite and the thermoelectric power values were interpreted in terms of the rapid reductions in the C and N contents within the untransformed austenite during the isothermal transformation.

*References*

1. D. Dulieu, K.W. Tupholme and G.J. Butterworth, J. Nucl. Mater., 141 - 143 (1986) 1097.
2. K.W. Tupholme, D. Dulieu and G.J. Butterworth, ibid, 155 - 157 (1988) 650.
3. K.W. Tupholme, D. Dulieu and G.J. Butterworth, ibid, 179 - 181 (1991) 684.
4. idem, AEA FUS Report 109, May 1991.
5. idem, AEA FUS Report 110, May 1991.
6. D.J. Mazey et al, AERE Report R 13604, January 1990.
7. T. Sample, H. Kolbe and L. Orecchia, Proc. SOFT , (1992?)
8. A. Alamo et al, CEA Progress Report CEA/CR SRMA 93.1419, June 1993.
9. A. Alamo et al, CEA Progress Report CEA/NT SRMA 94-2052, December 1993.

### 3.3.2 BATMAN steels

A series of potential reduced activation martensitic steels, termed "BATMAN", with compositions based on the specification of the high strength T91 (modified 9% Cr - 1Mo) steel [1] but with substitution of the Mo and Nb by W and Ti respectively and an increased Mn content to ensure a fully martensitic structure, has been evaluated by ENEA [2][3][4]. Initially, four - 240 Kg heats of the steels were produced in the form of thick walled, centrifugally cast tubes which were split and processed to thinner sections by routes involving hot and cold working and thermal treatments. The steel compositions (wt.%) were within the following ranges:

0.08 - 0.105 C; 8.90 - 9.27 Cr; 0.96 - 1.53 W; 0.01 - 0.29 Ti; 0.21 - 0.32 V; 3.10 - 3.81 Mn; 0.027 - 0.034 N.

Investigations aimed at optimising the compositions and thermo - mechanical treatments in respect of the optical and electron microstructures, especially the prior austenite grain size, hardness, tensile (ambient to 700°C) and stress - rupture (500 and 600°C, $\geq 6 \times 10^3$ h) strengths and ductilities, and impact (sub - size Charpy) toughness have been implemented [5]. The results demonstrated that:

(a) Titanium was effective in stabilising the prior austenite grain size as a result of the formation of TiN or Ti(C,N) particles which remained out of solution during austenitisation and pinned the boundaries; however, the tempering resistance was reduced due to the removal of nitrogen from solution by the titanium.

(b) Nitrogen enhanced the precipitation of preferentially oriented, "blocky" carbo - nitride particles and thus promoted large differences in the longitudinal and transverse toughness values.

(c) The $Ac_{1b}$ temperature was reduced to about 700°C, presumably as a consequence of the high manganese content, thereby restricting the maximum temperature at which tempering could be carried out.

(d) The Ti - bearing steels (austenitised at 1050°C / 1 h, air cooled, tempered at 650 C / 4 h and air cooled) possessed adequate tensile strengths and high ductilities at ambient and elevated temperatures, relatively low rupture strengths and high rupture ductilities, and impact toughness comparable to that of the MANET I steel; however, the DBTT could be significantly reduced and the USEs increased by a thermo - mechanical treatment involving single or double austenitisation, tempering, cold working 30% and ageing at 700°C for 8 h [Fig. 1].

A second series (seven heats) of the steels with the following compositions (wt.%) have been produced [6]:

0.08 - 0.14 C; 7.55 - 8.67 Cr; ~1.4 W; 0.07 - 0.12 Ti; ~0.2 V;

0.48 - 1.48 Mn; 0.002 - 0.007 N.

Reductions in the Ti and N contents, relative to those of the first series of the 9 Cr - WVMnTi steels, were effected primarily to limit or avoid the formation of the large carbo - nitride particles; the Mn was decreased so as to increase the Ac and thereby facilitate tempering at a high temperature to maximise the toughness. The thermo - mechanical treatments of these steels have been optimised and preliminary results showed that the toughness was far superior (lower DBTTs and higher USEs in Charpy V - notch impact tests) to that of the first series of BATMAN steels [7].

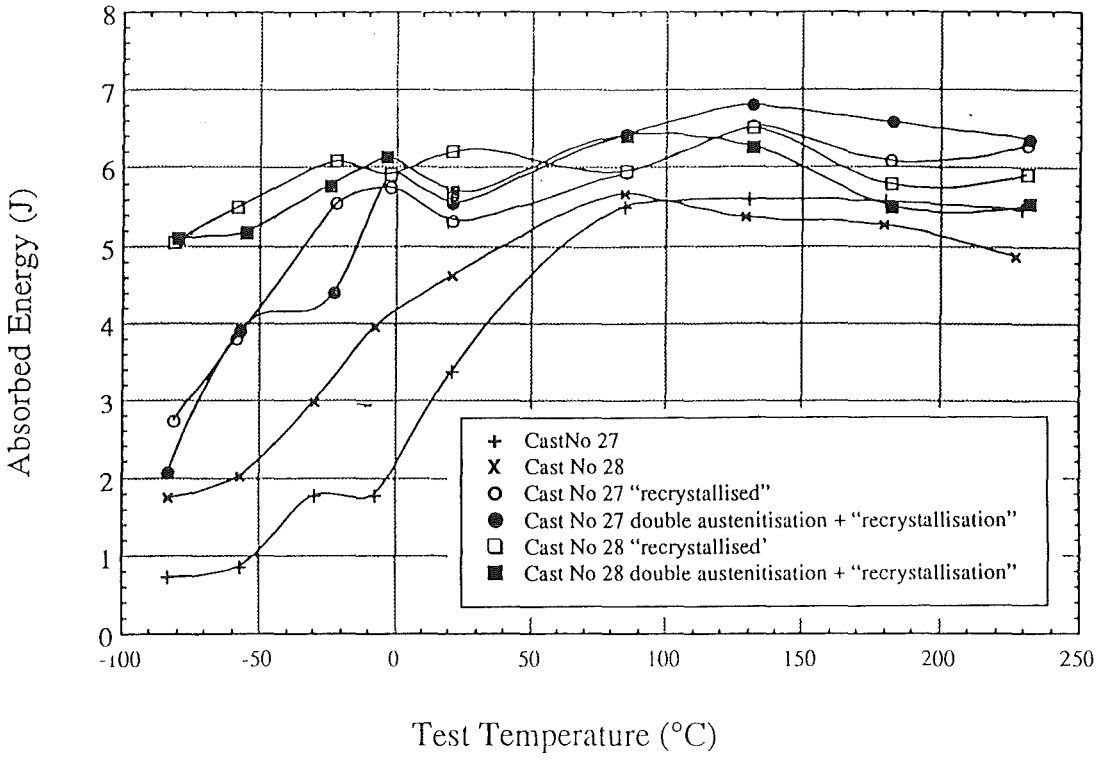


Fig. 1: Effects of thermo - mechanical treatments on the sub - size Charpy V - notch impact DBTTs of the BATMAN steels.
Cast 27 - 0.1% C; 8.9% Cr; 1.45% W; 0.20% Ti; 0.21% V; 3.1% Mn; 0.034% N.
Cast 28 - 0.09% C; 8.94% Cr; 1.51% W; 0.01% Ti; 0.24% V; 3.51% Mn; 0.034% N.

***References***

1. V.K. Sikka, Proc Topical Conf. on Ferritic Alloys for Use in Nuclear Energy Technologies, Snowbird, June 1983, J.W. Davis and D.J. Michel, Eds., Met. Soc. AIME, 1984, p.317.

2. L. Pilloni, G. Filacchioni and A. Calza-Bini, Proc. IEA Workshop on Low Activation Materials, Culham, U.K., April 1991, EUR FU BRU/XII - 6/91-MATIA 16, Vol. II.

3. G. Filacchioni, L. Pilloni and F. Attura, Proc. IEA Workshop on Ferritic/Martensitic Steels, October 1992, JAERI, Tokyo, Japan, Vol. II, March 1993, p.164.

4. L. Pilloni, F. Attura and G. de Santis, ENEA Report RT - INN (94) 4.

5. G. Filacchioni et al, paper submitted for publication in J. Nucl. Mater.

6. L. Pilloni, A. Calza-Bini and G. Filacchioni, ENEA Report C-S-01-92 (1992).

7. G. Filacchioni et al, ENEA Report (1995), to be published.

### 3.3.3 OPTIMAX steels

Two variants (high Mn / low N and low Mn / high N) of the reduced activation martensitic steels based on the 9% Cr - WVTa composition have been investigated by CRPP - FTM in collaboration with Sulzer Innotec with the primary objective of elucidating the factors controlling the toughness [1]. The alloys were double vacuum melted using high purity alloying ingredients and cast into 40 kg ingots which were subsequently hot rolled at 950°C to 10 - 15 mm thick plates. The analyses of the steels are given in Table I.

**Table I: Analyses (wt.%) of Steels**

| Steel | C | Mn | Cr | W | V | Ta | Mo | Al | N | Ce |
|---|---|---|---|---|---|---|---|---|---|---|
| A | 0 | 0 | 9 | 0 | 0 | 0 | 0 | <0.02 | 0 | 0 |
| B | 0 | 0 | 9 | 0 | 0 | 0 | 0 | <0.02 | 0 | 0 |

Optimised heat treatments (Steels A and B - austenitised at 960 and 980°C respectively and tempered at 750°C) were selected, based on the results of studies of the effects of austenitisation temperature on the prior austenite grain sizes and the "as - quenched" hardness and of the hardness as a function of tempering temperature. Both steels were fully martensitic and the respective prior austenite grain sizes were 18 and 16 m.

Steel B was slightly stronger and less ductile than steel A in tensile tests at temperatures in the range ambient to 500°C. In addition, both steels in the respective optimised heat treatment conditions exhibited lower DBTTs and higher USEs compared with those of the MANET II steel (austenitised at 1075°C / 0.5 h and tempered at 750°C / 2 h) in sub - size Charpy V - notch impact tests (see Table II). Two types of carbides or carbo-nitrides, nucleated on the prior austenite and/or martensite lath boundaries, were identified in the tempered A and B steels by EDX and PEELS: coarse (20 - 250 µm) $M_{23}C_6$ type [M analysis (at.%): 50 - 70 Cr; 25 - 35 Fe; ~3W; ~1V] and small, spherical (10 - 20 nm diameter) TaVFe based carbo - nitrides [typical analysis (at.%): 60 - 70 Ta; 14 - 18 V; 2 - 6 Fe]. The slightly greater tensile strength of steel B was attributed to a larger density of the fine precipi-

tates formed as a result of its higher nitrogen content, whilst the superior toughness of steel A was due to its lower strength and lower nitrogen content coupled with the low concentrations of residual impurities.

In common with other observations on high Cr martensitic steels, softening occurred during low cycle, strain controlled fatigue tests in air at ambient temperature; the endurances of steel A were comparable to those of steel B and superior to those of the MANET II steel.

**Table II: Ductile-Brittle Transition Temperatures and Upper Shelf Energies**

| Steel | DBTT. C. | USE. J. |
|---|---|---|
| A | ~ - 90 | 200 |
| B | ~ - 40 | 100 |
| MANET II | - 10 | 90 |

*Reference*

1. M. Victoria et al, Proc. Symp. on Effects of Radiation on Materials, D.S. Gelles, Ed. ASTM STP 1270 (1996), 721.

### 3.3.4 CeTa and OPTIFER steels

The development of 9 - 10% Cr-WVTa martensitic steels with reduced long - term activation has also been pursued by FZK in collaboration with SAARSTAHL GmbH. The specifications of the steels were based on the results of computations of the neutron - induced activation, including the contributions of sequential reactions with charged particles [1]. Fig. 1 demonstrates the status of a common development of the Institute of Materials Research at FZK and the steel company Saarstahl GmbH, showing a comparison of the γ-dose rate for the conventional 9-10% CrMoVNb steel MANET II with two laboratory melts of 9-10 CrWVTa alloys CETA and OPTIFER-real on the basis of the actual chemical compositions. While the long-term dose rate of MANET II is governed by the radioisotope $^{94}$Nb with a half life time of about 20 000 years, tungsten controls the long term activation of the alloys OPTIFER-reference. OPTIFER-reference represents the lowest achievable dose rate if impurity elements could be reduced to a certain limit. 30 kg heats of the steels were produced by vacuum induction melting followed by vacu-

um arc refining, with cerium or yttrium being used for deoxidation, and the cast ingots forged to 22 mm square bars. The designations of the steels and the analyses (wt. %) of the principal alloying elements are given in Table I.

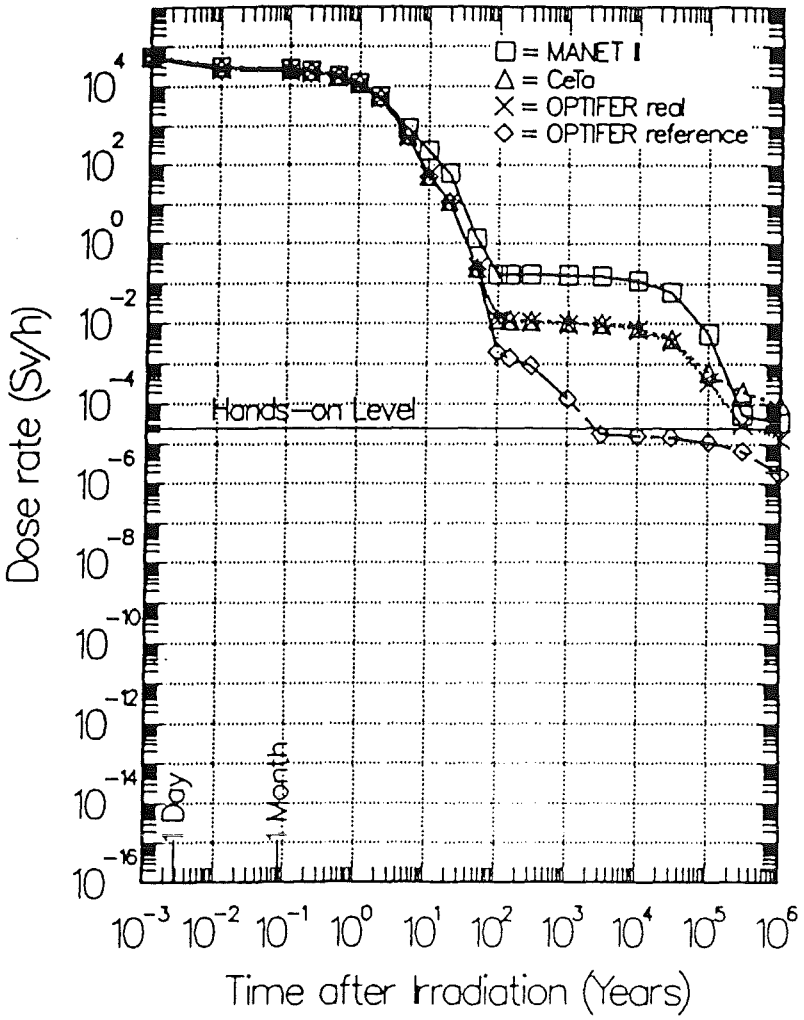


Fig. 1: γ-dose decay after irradiation with First Wall neutrons to an integrated wall loading of 12.5 MWy/m² for MANET II, CeTa and OPTIFER steels.

Several aspects of the physical metallurgy of these steels, including the hardenability, transformation behaviour, tempering characteristics and optical and electron microstructures, have been investigated [1 - 5].

The results of the studies have demonstrated that the Ta is effective in stabilising relatively fine prior austenite grain sizes during austenitisation at temperatures in the range 950 to 1150°C as a result of pinning of the boundaries by primary TaC or Ta(C,N) particles and in this respect behaves similarly to Nb.

**Table 1: Analyses (wt.%) of CeTa and OPTIFER-Steels**

| Steel | C | Mn | Cr | W | V | Ta | Al | N | Ce | Y |
|---|---|---|---|---|---|---|---|---|---|---|
| CeTa | 0.175 | 1.35 | 9.6 | 0.81 | 0.59 | 0.48 | 0.085 | 0.015 | 0.13 | - |
| OPTIFER Ia | 0.1 | 0.5 | 9.3 | 0.97 | 0.26 | 0.066 | 0.008 | 0.016 | <0.001 | - |
| OPTIFER Ib | 0.12 | 0.49 | 9.53 | 0.98 | 0.235 | 0.163 | 0.015 | 0.0062 | 0.041 | <0.001 |
| OPTIFER III | 0.12 | 0.5 | 9.32 | 0.024 | 0.248 | 1.6 | 0.01 | 0.0177 | <0.001 | - |
| OPTIFER IV | 0.1 | 0.62 | 8.45 | 1.17 | 0.24 | 0.1 | | 0.06 | | - |

The continuous cooling time - temperature - transformation (TTT) diagrams showed that the CeTa and OPTIFER 1a and 1b steels had high hardenability, guaranteeing fully martensitic structures in thick sections with cooling rates from the austenitisation temperature in excess of 5 C/min; the quenched steels exhibited similar martensite lath structures to the MANET II steel, with all the prior austenite grain boundaries being decorated with Cr - rich $M_{23}(C,N)_6$ type precipitates. However, the W - free, high Ta OPTIFER III steel had lower hardenability, attributed to the observed formation of a large volume fraction of the coarse Ta(C,N) particles which were insoluble at the austenitisation temperature and the consequent reduction in the carbon in solution in the austenite. The transformation temperatures for the CeTa and OPTIFER steels are compared with those of the MANET I and II steels in Table II. The $Ac_{1b}$ temperatures of the former are 30 - 50°C higher than those of the MANET steels as a result of the elimination of Ni; this facilitates an increase in the tempering temperature with a consequent improvement in the fracture toughness. The $M_s$ and $M_f$ temperatures are consistent with the observation of fully martensitic structures with no retained austenite being produced on quenching to ambient temperature.

**Table II: Transformation Temperatures for MANET, CeTa and OPTIFER Steels**

| Steel | $Ac_{1b}$ | $Ac_{1e}$ | $M_s$ | $M_f$ |
|---|---|---|---|---|
| MANET I | 790 | 870 | 310 | 153 |
| MANET II | 775.00 | 890 | 340 | 155 |
| CeTa | 830 | 930 | 335 | 60 |
| OPTIFER | 820 - 830 | 900 - 930 | 395 - 442 | 172 - 260 |

Secondary hardening occurred during tempering of the CeTa and MANET II steel at 500 - 550°C. The hardness decreased rapidly on increasing the tempering temperature above 550°C, due primarily to the recovery of the martensite lath dislocations, dissolution of $M_2X$ precipitates and the formation of massive $M_{23}C_6$ particles at the lath boundaries; the initial observations on the OPTIFER steels were consistent with this behaviour.

The tensile (ambient temperature to 650°C), stress - rupture (450 - 650°C) and Charpy V - notch impact properties of the CeTa and OPTIFER steels have been investigated by KfK, with some of the testing of the latter steels being carried out in collaboration with CIEMAT [6].

The tensile strengths of the CeTa steel were about 100 MPA lower but the ductilities were equivalent or marginally higher than those for the MANET I and II steels when tested in the 1075°C / 0.5 h + 750°C / 2 h reference heat treatment condition; the OPTIFER steels were significantly stronger but somewhat less ductile than the CeTa alloy in the tensile tests at temperatures above 500°C. The stress - rupture lives of the OPTIFER steels were also superior to those of the CeTa alloy and comparable to those of the MANET II steel at 450 - 650°C and applied stresses in the range 40 - 500 MPa.

The Charpy V - notch impact DBTTs and USEs were similar for the reference heat treated CeTa and MANET II steel; however, the OPTIFER 1a and 1b steels exhibited considerably lower DBTTs and higher USEs (Fig. 2) but the CrVTa steel (OPTIFER III) possessed inferior toughness and has been excluded from further considerations. It has also been demonstrated, in agreement with the trends shown by the MANET steels, that the tensile strengths, DBTTs and USEs of the OPTIFER 1a and IV steels were sensitively dependent on the initial austenitising and tempering temperatures (Fig. 3), with a 0.2% proof stress value at 500°C of approximately 460 MPA, a DBTT of about - 100°C and an USE in the region of 250 J being shown by the OPTIFER IV steel after austenitising at 900°C and tempering at 700°C. These observations have thus confirmed previous data [7][8] in showing that the DBTTs of the high Cr martensitic steels can be significantly reduced at the expense of the tensile and creep - rupture strengths by control of the initial austenitisation and tempering treatments. The superior fracture toughness behaviour of the W - containing OPTIFER 1a and IV steels may also be attributed in part to the deoxidation and desulphurisation of the original melts by the cerium.

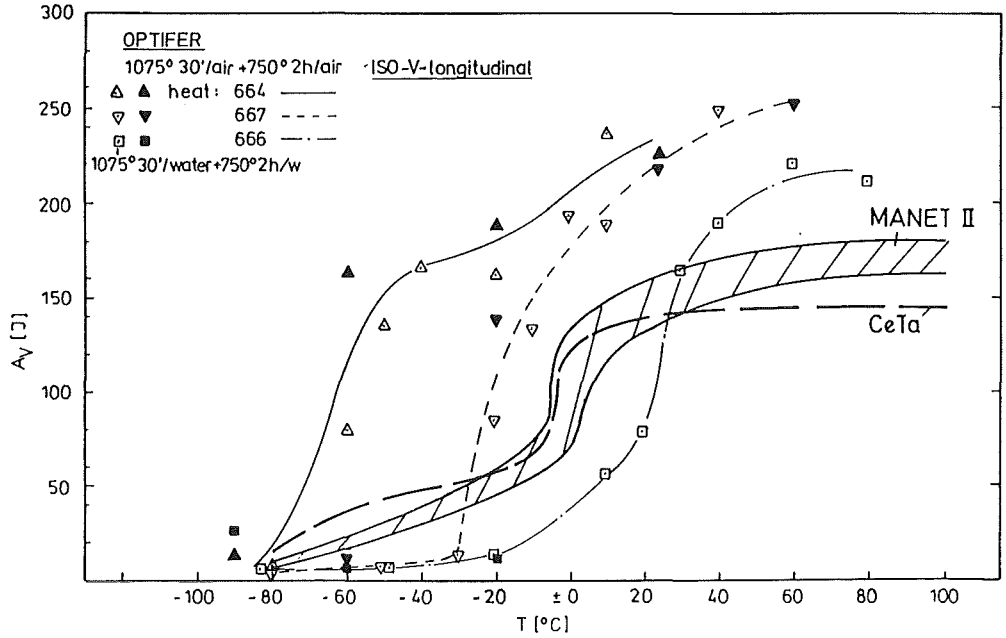


Fig. 2: Impact energies versus test temperatures for MANET II, CeTa and OPTIFER Ia, Ib and III steels.

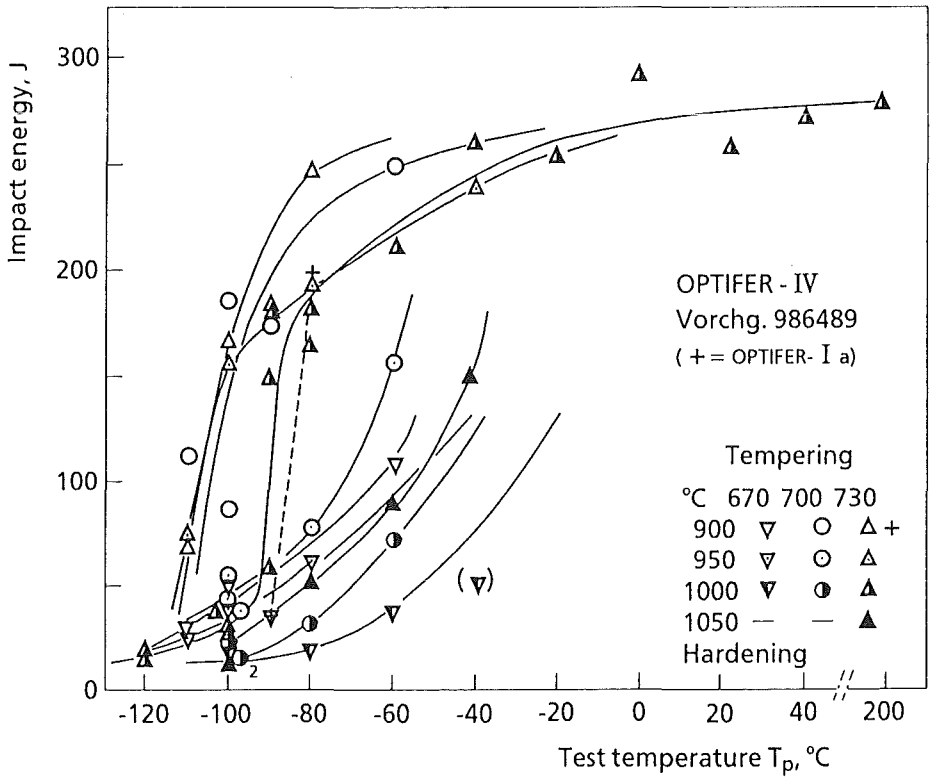


Fig. 3: Effects of initial thermal treatment on the DBTTs and impact energies of the OPTIFER IV steels.

The results of these studies have therefore confirmed that the basic physical metallurgy of the 9 - 12% Cr martensitic steels are not significantly modified by the substitution of the Mo, Ni and Nb by W and Ta and that the CrWVTa reduced activation steels possess better fracture toughness for comparable tensile and stress - rupture properties than the more conventional CrMoVNb (MANET) steels.

*References*

1. K. Ehrlich et al, J. Nucl. Mater., 212 - 215 (1994) 678.
2. K. Anderko et al, KfK Report 5060, 1993.
3. K. Ehrlich and M. Schirra, Vortragsveranstaltung der Arbeitsgemeinschaften fur warmfeste Stahle und Hochtemperaturwerkstoffe, Düsseldorf, November 1992, p. 64.
4. L. Schäfer and H. Kempe, KfK Report 5353, 1994.
5. E. Materna - Morris, FZK Report to be published.
6. J. Lapena, CIEMAT report to be issued.
7. E.A. Little et al, Metals Tech., 4 (1977) 205.
8. F. Abe, IEA Workshop on Low Activation Materials, Cullham, April 1991, EUR FU BRU / XII - 6 / 91 - MATIA 16.

### 3.3.5 F82H-mod

As a consequence of the above recorded calculations, observations and associated discussions, an international collaborative test programme on reduced-activation ferritic/martensitic steels for fusion has been launched under the auspices of the IEA Executive Committee for the Implementing Agreement on Fusion Materials. At the IEA workshop on ferritic/martensitic steels in Tokyo, October 26-28, 1992, the Japanese offered to purchase two large heats of reduced activation steel. In the meantime a 5 t heat of a modified (high purity) F82H fully martensitic steel [composition (wt.%) - 0.09 C, 0.11 Si, 0.16 Mn, 0.002 S, 0.002 P, 7.70 Cr, 0.02 Ni, 0.003 Mo, 1.95 W, 0.16 V, 0.0001 Nb, 0.002 Ta, 0.01 Cu, 0.005 Co, 0.01 Ti, 0.003 sol. Al, 0.007 total N, 0.0002 B] has been procuded by JAERI/NKK Corporation Japan and 7.7 and 15 mm thick plates supplied for a series of coordinated tasks to be implemented within the European Fusion Association Laboratories, in Japan and the USA. In addition, a second 5 t heat of the same steel was melted and rolled to 15 and 25 mm thick plates and for the production of TIG and electron beam welds

in the 15 mm thick sections. Finally, a 1 t heat of JLF-1 [nominal composition (wt.%) - 0.07 C, 0.1 Si, 0.30 Mn, 9 Cr, 2 W, 0.2 V, 0.08 Ta, 0.025 N, 0.0020 B] martensitic steel and several 150 Kg heats of the steel with variations in the manganese and boron contents have been produced by MONBUSHO/Nippon Steel Corporation and are also being provided for the IEA coordinated programme.

The objective of the combined test programme on the heat F82H mod is to have a reference for improved reduced activation steel developments, and to show the feasibility of using ferritic/martensitic steels for fusion by developing a comprehensive data base.

## 3.4 Applications of reduced activation martensitic steels

The results of calculations have clearly demonstrated that the neutron - induced radioactivity in the 1.4914 (MANET type) steel when used for the first wall in a fusion power reactor with a neutron loading of 5 MW/m$^2$ for 2.5 y did not satisfy any of the criteria proposed for safety, maintenance, medium and low level waste and (hands - on) recycling (see section 3.1.) [1 - 3].

The effects of fusion neutron flux, irradiation time and fluence on the activation of conventional (FV448) and reduced activation (LA12TaLC) martensitic steels (neglecting the impurity element concentrations) have been compared [4][5]. The reduced activation steel was slightly inferior to the conventional steel in respect of the induced activity, contact dose rate and heat output for periods up to about 1 y after reactor exposure for 2.5 y with a neutron wall loading of 1 MW/m$^2$. However, the parameters for the reduced activation steel were two to four orders of magnitude lower after a cooling period of 100 y or so and, under these conditions, satisfied the residual activity, dose rate and decay heat criteria for recycling and the dose rate and decay heat criteria for the proposed classification of low level waste. The computations for the LA12TaLC steel containing (wt.%) 0.019 N and 0.76 W showed that the long term ($>$ 100 y) specific activity was determined by the $C^{14}$ produced from the N whilst the W addition dominated the$\gamma$ - dose rate [6]; the N content of the steel would have to be kept below 0.005 wt.% to avoid the activity increases associated with the $C^{14}$.

The computed dose rates for the CeTa and OPTIFER developmental alloys shown in Chapter 3.3.4 were about an order of magnitude lower than that of the MANET II steel after about 100 y cooling following exposure for 2.5 y with a neutron wall loading of 5 MW/m$^2$ but remained in excess of the "hands - on" recycling limit of 25x10$^{-6}$ Svh$^{-1}$ [7]. The long term radioactivity in these alloys was domi-

nated by the elements Fe, W and Ta and the Nb impurity; the additional contributions of sequential reactions for Cr, V, Mn and N were second order effects and, hence, could be neglected.

Whilst an attempt was made to achieve low concentrations of the radioactively undesirable elements in the production of the OPTIFER steels, it is evident from the comparison of the analyses of some of the elements with the maximum allowable concentrations to satisfy the long - term (hands - on) dose rate criterion (Fig. 1) that this objective was not realised in many instances [9]. This conclusion also applies to the other experimental reduced activation steels under investigation and whose elemental compositions are included in Fig. 1. The projected target for a "pure" 9 - 10% Cr WVTa martensitic steel is shown in Fig. 1; this target would only be achieved if the Nb content and the concentrations of the other undesirable elements could be maintained at the required low values.

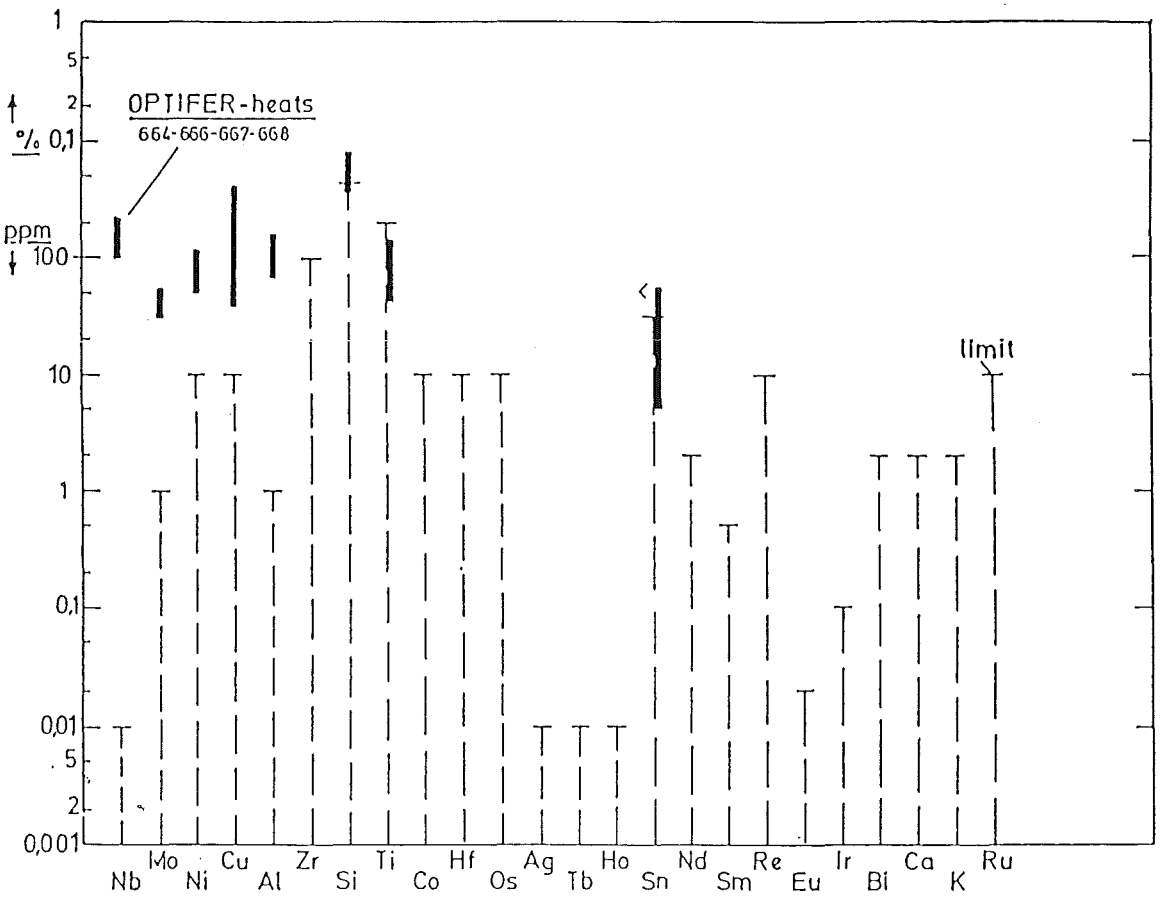


Fig. 1: Concentrations of undesirable impurity elements in the experimental reduced activation steels.

An initial survey has indicated that the production of steels with the required low concentrations of the undesirable residual elements can probably be achieved by the selection of high purity raw materials, the use of vacuum melting and vacuum arc refining techniques and the avoidance of impurity pick - up during processing [8]. It was also concluded that analytical techniques, such as glow discharge mass spectrometry (GDMS), offered sufficient sensitivity for the quantification of the lowest level trace elements in the reduced activation steels. It remains to be demonstrated, however, that the required degree of purity can be routinely guaranteed in practice.

Another important feature of reduced activation steels are the significantly improved fracture toughness properties before and after irradiation. While in conventional CrNiMoV(Nb) ferritic/martensitic alloys neutron irradiation to high damage doses practically does not influence mechanical properties above about 400°C, significant embrittlement has been observed in a variety of conventional steels below that irradiation temperature (chapter 2.3).

A recently performed benchmark experiment [10] with instrumented Charpy impact specimens on commercial 10-11% Cr-NiMoVNb steels (MANET-I and -II, OPTIMAR and 1.4914-K-heat) and reduced activation materials (OPTIFER-heats (FZK), F82H (JAERI, Japan), 9Cr-2WVTa (ORNL, USA) and GA3X (Battelle, USA)) confirmed the general consensus of already published data, that some of the reduced activation alloys have significantly improved impact properties (Fig. 2): The upper shelf energies show generally higher values than the Cr-NiMoVNb steels. Another finding was, that before irradiation some of the reduced activation steels have DBTT values below -60°C. Without deterioration of other properties these DBTT data can be further improved to values well below -100°C by adjusting the thermal treatment [11].

After neutron irradiation at 365°C to 7 and 13-14 dpa some of these reduced activation steels still show very good impact toughness properties: the DBTT of a 9Cr-2WV steel increased by 59°C; this same composition with an addition of 0.07 % Ta developed an increase in DBTT of only 34°C [12]. These investigations verify together with initial results on various other alloys [13] the excellent irradiation resistance of some reduced activation alloys even after higher damage dose. Although the available low temperature irradiation data does not yet allow to draw final conclusions, it can be stated, that all examined reduced activation materials provide clearly better mechanical properties than the corresponding commercial steels (MANET type). Especially the 9Cr-2WVTa steel shows excellent promise for use in a fusion reactor.

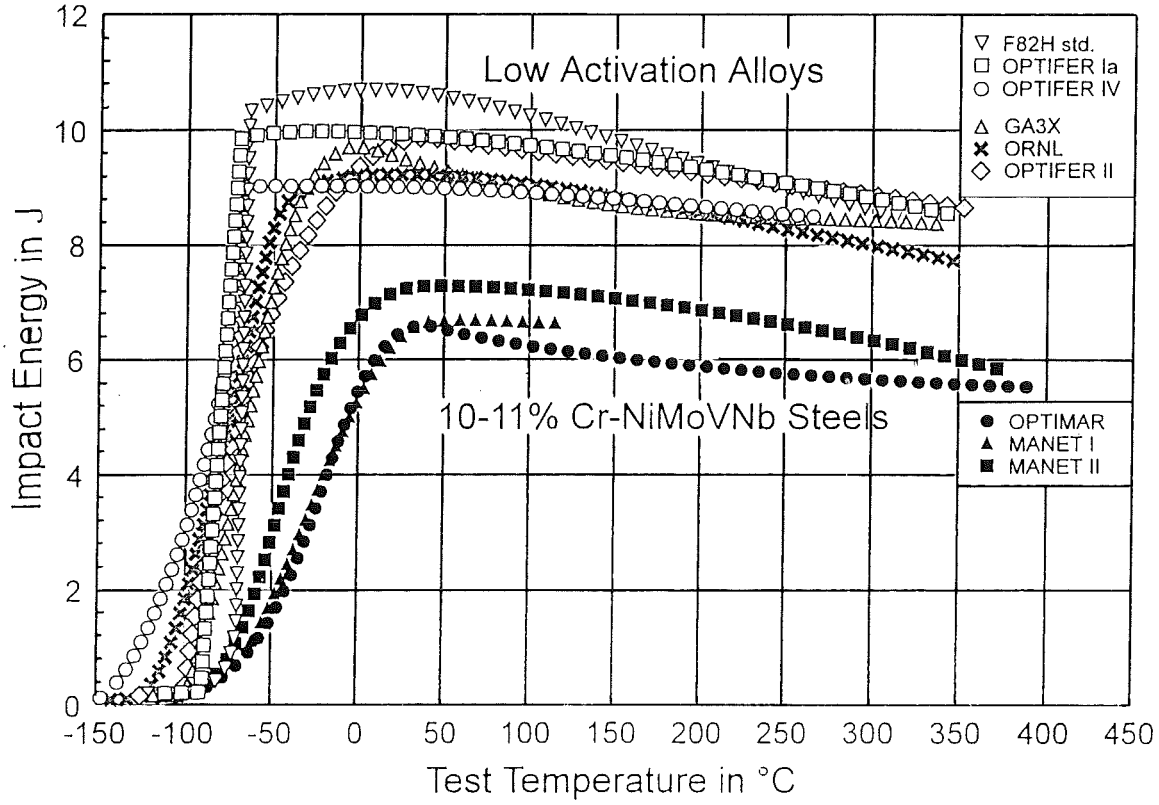


Fig. 2: Impact energy vs. test temperature curves of various reduced activation alloys prior to irradiation. All KLST specimens were manufactured and tested under the same conditions.

***References***

1. P.Rocco and M. Zucchetti, Fusion Engrg. and Des., 15 (1992) 235.
2. P. Rocco and M. Zucchetti, J. Fus. Energy, 12 (1993) 201.
3. P. Rocco and M. Zucchetti, J. Nucl. Mater., 212 - 215 (1994) 649.
4. J-Ch. Sublet and G.J. Butterworth, AEA FUS Report 201, August 1992.
5. J-Ch. Sublet and G.J. Butterworth, Proc. 17th Symp. on Fusion Technology, Rome, September 1992.
6. J-Ch. Sublet and G.J. Butterworth, J. Nucl. Mater., 212 - 215 (1994) 695.
7. K. Ehrlich et al, ibid, p. 678.
8. G.J. Butterworth and S.R. Keown, J. Nucl. Mater., 186 (1992) 283.

9. M. Schirra, K. Ehrlich, S. Heger, M.T. Hernández, J. Lapeña, FZKA-Report 5624 (1995).

# 4. Assessment of Present Status

In this report the available data of the 10-12% CrMoVNb steels MANET I and II investigated in the European Fusion Technology Programme have been summarized. They include informations on the physical metallurgy, the transformation- and hardening/tempering behaviour as well as data on tensile-, creep/creep-rupture-, isothermal- and thermal fatigue and fracture toughness properties. Also the effects of neutron- and ion irradiations on microstructure, radiation hardening and embrittlement have been investigated in the relevant temperature region between RT up to 500°C and up to fluence levels of $\leq$ 15 dpa. Compatibility studies of the structural materials with coolant-, breeding and neutron multiplier materials are also included.

In comparison with conventional 9-12% CrMoVNb steels of Types FV548, DIN 1.4914 and T91 the MANET II alloy has a better thermal creep and creep-rupture behaviour and improved fracture toughness data when compared with unstabilized versions of the 9CrMoV-ferritic-martensitic steels like EM 10. Other mechanical properties lie within a broader scatter band of the conventional alloys.

One apparent drawback of the MANET-type steels is the observed strong shift in the DBTT after irradiation below 400°C even after very low neutron fluences of $\leq$ 5 dpa. This seems to limit the lower operational temperature of this material to about 250-300°C. Though there is experimental evidence that a reduction in the Cr-content reduces the irradiation-induced $\Delta$DBTT, the real reasons for this different behaviour is not known and has to be studied more intensively.

More recent studies on the influence of variation of the austenitisation temperature on fracture toughness properties indicate that a reduction of the presently used very high hardening temperatures ($\sim$ 1050°C) down to about 950°C could have a beneficial effect. Whether or not this measure will help to overcome the strong effect of irradiation on the fracture toughness data is unclear.

Several irradiation experiments in which the high He/dpa- and H/dpa-values typical for fusion neutron irradiations have been simulated by light-ion (protons and $\alpha$-particles) irradiations have confirmed that the MANET-steels are not sensitive to high He-or H-contents. In tensile tests the observed radiation hardening below 400°C can be scaled with the displacement damage rather than with the implanted He- or H-concentration. Also the effect of relatively high He-

concentrations on in-situ fatigue- and creep-properties is moderate and can again be explained by radiation hardening rather than a He-effect.

In general the irradiation behaviour of MANET steels is in the very relevant temperature region RT - 400°C and up to few dpa much better studied than in any other commercial 9-12% Cr steel. And the irradiation induced limitations are induced by the radiation hardening and embrittlement.

The European approach on 7-11% CrWV(Ta,Ti) alloys with reduced activation is broad and combines the variation of GB-stabilizing elements like Ta or Ti with changes of elements which act as matrix hardeners (W,Ge), Mn-additions and others. From the results presented so far it seems that the general physical metallurgy, the transformation- and hardening behaviour of the new alloys is not negatively influenced and has led to a general improvement of the fracture toughness properties. If tendencies of first irradiation experiments at low fluence levels which show a reduced increase of radiation hardening and embrittlement in some alloys can be confirmed, a reasonable selection of few alloys will be possible.

The high chromium martensitic steels can be effectively joined by conventional (for example, TIG) and advanced (electron beam and laser) welding techniques. The mechanical properties of the welds produced by these processes are generally comparable to those of the base steel in the unirradiated condition; also, the properties of the electron beam welds do not appear to be inferior to those of the base steel after irradiation, but there are insufficient data on the effects of irradiation on the welds produced by the other techniques. Furthermore, the susceptibility of the MANET and other high chromium martensitic steel weldments to Type IV cracking still has to be investigated.

Preliminary studies have shown that diffusion bonding is an attractive process for joining martensitic steel thick sections but additional work is required to fully characterise the joints with respect to their metallographic structures and mechanical properties in the unirradiated and irradiated conditions. Other work has demonstrated that hot isostatic pressing is also a feasible process for the fabrication and joining of similar and dissimilar materials and the applicability of this process for bonding the high chromium martensitic steels should also be established.

The results of static autoclave and dynamic loops tests of the aqueous corrosion of the MANET and reduced activation martensitic steels have not revealed any unusual or unexpected behaviour. However, the general corrosion is accelerated under irradiation as a consequence of the radiolysis of the water and/or

sensitisation of the steel due to a precipitation but initial observations after low fluence irradiation suggest that these steels are not susceptible to stress corrosion cracking as a result of radiation-induced segregation (RIS) processes; additional work following exposure to higher neutron fluences is necessary to further clarify these issues.

The corrosion of the martensitic steels in liquid $Li_{17}Pb_{83}$ is determined, following an incubation period, by the more or less uniform dissolution of iron and chromium at a rate significantly lower than that for nickel in austenitic steels. The upper temperature limit for the martensitic steel in the flowing liquid metal is concluded to be 450°C, about 50°C higher than that for Type 316L austenitic steel. Additional work, however, is required to establish the corrosion rates for the high chromium martensitic steels in the liquid metal at high flow velocities.

The information available on the effects of hydrogen on the structure and properties is totally inadequate for assessing its significance with respect to the performance and endurance of martensitic steel components in fusion devices. Extensive, well controlled and quantitative investigations are required on the simultaneous effects of hydrogen uptake, temperature, irradiation and stress on the magnitude of the (hydrogen-induced) physical and chemical embrittlement.

One of the principal limitations of the MANET and similar composition martensitic steels is their rapid loss of strength at temperatures above 500-550°C. However, the present design and/or compatibility considerations may well dictate that the use of these types of steels in fusion devices has to be restricted to temperatures below these limits. Nevertheless, based on recent developments of steels of this type for advanced thermal power plant applications and also on powder metallurgy-mechanical alloying approaches, there is potentially considerable scope for modifying the compositions and enhancing the thermal creep strengths such that their use at temperatures up to 600 or even 650°C can be contemplated. It must be pointed out, however, that the compositions of these steels do not comply with reduced activation specifications; also, no irradiation data have been generated on these advanced steels to date but some results should be forthcoming within the next 2-3 years following irradiation in HFR.

It remains to be established that the production of reduced activation martensitic steels with the required low concentrations of radioactively undesirable residual elements is possible by the use of high purity raw materials, vacuum melting and refining techniques and "clean" processing conditions. This demonstration is urgently required to guide the future development and application of reduced activation martensitic steels. However, the compositional modifications effected to

date on an industrial scale, whilst not having met all the required objectives, have at least shown that considerable benefits are already possible in terms of reducing the long-term radioactivity and, hence, the volume of fusion reactor waste requiring disposal in deep geological sites.